

# PERFORMANCE OF PLATE FIN HEAT EXCHANGER AT CRYOGENIC TEMPERATURE

*Dissertation submitted in partial fulfillment*

*of the requirements of the degree of*

***Doctor of Philosophy***

*in*

***Mechanical Engineering***

*by*

***Ajay Kumar Gupta***

(Roll Number: 511ME127)

*based on research carried out*

*under the supervision of*

***Prof. Ranjit Kumar Sahoo***

*and*

***Prof. Sunil Kumar Sarangi***



October, 2018

Department of Mechanical Engineering  
**National Institute of Technology Rourkela**



October 10, 2018

## Certificate of Examination

Roll Number: *511ME127*

Name: *Ajay Kumar Gupta*

Title of Dissertation: *PERFORMANCE OF PLATE FIN HEAT EXCHANGER AT CRYOGENIC TEMPERATURE*

We the below signed, after checking the dissertation mentioned above and the official record book (s) of the student, hereby state our approval of the dissertation submitted in partial fulfillment of the requirements of the degree of *Doctor of Philosophy* in *Mechanical Engineering* at *National Institute of Technology Rourkela*. We are satisfied with the volume, quality, correctness, and originality of the work.

---

Sunil Kumar Sarangi  
Co-Supervisor

---

Ranjit Kumar Sahoo  
Principal Supervisor

---

Ashok Kumar Satpathy  
Member, DSC

---

Krishna Pramanik  
Member, DSC

---

Alok Satpathy  
Member, DSC

---

External Examiner

---

D.R.Parhi  
Chairperson, DSC

---

D.R.Parhi  
Head of the Department



**Prof. Ranjit Kumar Sahoo**

Professor

**Prof. Sunil Kumar Sarangi**

Professor

October 10, 2018

## **Supervisors' Certificate**

This is to certify that the work presented in the dissertation entitled *Guidelines for Formatting Dissertation* submitted by *Ajay Kumar Gupta*, Roll Number 511Me127, is a record of original research carried out by him under our supervision and guidance in partial fulfilment of the requirements of the degree of *Doctor of Philosophy in Mechanical Engineering*. Neither this dissertation nor any part of it has been submitted earlier for any degree or diploma to any institute or university in India or abroad.

---

Sunil Kumar Sarangi  
Professor

---

Ranjit Kumar Sahoo  
Professor

# **Dedicated**

*To my father, who unfortunately didn't stay in this world  
long enough to see his son become a doctor.*

*Signature*

# Declaration of Originality

I, *Ajay Kumar Gupta*, Roll Number 511ME127 hereby declare that this dissertation entitled *Guidelines for Formatting Dissertation* presents my original work carried out as a doctoral student of NIT Rourkela and, to the best of my knowledge, contains no material previously published or written by another person, nor any material presented by me for the award of any degree or diploma of NIT Rourkela or any other institution. Any contribution made to this research by others, with whom I have worked at NIT Rourkela or elsewhere, is explicitly acknowledged in the dissertation. Works of other authors cited in this dissertation have been duly acknowledged under the sections “Reference” or “Bibliography”. I have also submitted my original research records to the scrutiny committee for evaluation of my dissertation.

I am fully aware that in case of any non-compliance detected in future, the Senate of NIT Rourkela may withdraw the degree awarded to me on the basis of the present dissertation.

October 10, 2018

NIT Rourkela

*Ajay Kumar Gupta*

# Acknowledgment

My long tenure in the fields of Mechanical Engineering and Thermal science since 2002 as Pd.D. undergraduate and graduate student have been enriched by the help of many people. Here I would like to take this opportunity to thank the people who have in no small way made the research in this thesis possible.

First and foremost, I would like to thank my advisor, Prof. Ranjit Kumar Sahoo. I thank him for introducing me to the wonders and frustrations of scientific research. I thank him for his guidance, encouragement and support during the development of this work. He has been teaching me all about self-discipline in laboratory work and in written scientific communication. I have profoundly benefited from my association with him over the past 5 years. I deeply thank him for the unprecedented freedom he offered to explore my intellectual curiosity in our experiments, and for fostering my capacity critically as an independent researcher. His advice and encouragement were always important guiding lights towards my personal and professional development.

I am especially thankful to Prof. Sunil Kumar Sarangi, I can say he is my co-supervisor with high respect and deep sense of appreciation for his expert and active involvement in each, experiment explaining clearly, providing all necessary things to carry out research at NIT, Rourkela

Besides my guide, I am grateful to my Doctoral Advisory Committee (DSC) members Prof. Ashok Satpathy and Prof. Krishna Pramanik for their encouragement, critical and insightful reviews and comments. A special thanks to Prof. Dibya Prakash Jena, for giving valuable guidance and precious time to my research out of your busy schedule. You have helped me to accomplish my goal of doing a good research.

A very special thanks to a very special friend of mine, Pankaj Kumar. You have been with me through thick and thin, understood me, put-up with my mood swings and tantrums, listened to my worries and excitements. You have made my journey much Simpler. Thank you. I am also grateful to my co-researchers Dr. Balaji Choudhury, Dr. Sachindra Kumar

Rout, Mr. Arvind Yadav, Mr. Animesh Kumar, and Mr. Manoj Kumar Gupta. It was great being around such inspiring people. Thank you for all the love and support.

I am indebted to the staff members of my department: Mr. Jnana Ranjan Nayak, Mr. Narendra Bisoi and Mr. Somnath for the fabrication of the heat exchanger test rig. They have provided, physical and mental support and suggestions in accomplishing the research work.

In the beginning of 2016, Sudhananda Pani joined our lab. Simply put, he is a hardworking genius and an exceptionally talented colleague! Upon his arrival, Pani and I spent days and nights in the lab. I am very proud of the experiment that resulted from this collaboration. Pani pursued a number of Experiment with me in this thesis, and often times I was moved by his aspiring character of diligence and modesty. I thank him for his super hard work with excellence and for sharing all the excitements with me in the lab.

I want to express sincere gratitude to my presently working Institute Chairperson Mr. Ajay verma for facilitating the facility of permission and Dr. C.S.Sharma of same Institute for expediting in my thesis writing.

Finally, I would like to express my eternal gratitude to my parents and family for their everlasting love and support. I acknowledge that the empirical research of my thesis is due to the cooperation of my family.

October 10, 2018  
NIT Rourkela

*Ajay Kumar Gupta*  
Roll Number: 511ME127

# Abstract

The objective of this study is to provide experimental data that could be used to predict the effectiveness and performance of a plate fin heat exchange for low temperature conditions. In this study, plate fin heat exchangers are tested with a variation of the mass flow rate.

Plate fin heat exchangers are widely used in cryogenic liquefaction. Such heat exchangers have high fin density and offer narrow passages for the fluid flow which often leads to significant pressure drop. The stringent requirement of high effectiveness and excessive pressure drop occurring in plate fin heat exchanger makes it necessary to test the heat exchanger before using in any system. An experimental setup is made in the laboratory to test the plate fin heat exchanger at cryogenic temperature. In this setup compressed nitrogen gas will be passed through the plate fin heat exchanger as hot stream. The hot stream gas will be passed through a liquid nitrogen coil heat exchanger to cool the high pressure gas. The cold gas is then passed as a reverse stream of the plate fin heat exchanger. The experimental setup is mounted to the measurement instrument like RTDs, Pressure gauge, Differential pressure gauge, Orifice plate flow meter etc. The effectiveness of heat exchange will be calculated from the measured temperatures directly from the experiment. Also the pressure drop will be obtained from the experiments. The effectiveness and pressure drop data is simulated with Aspen software and also compared with other correlations to confirm the accuracy of the experiment.



# List of Content

## Contents

Abstract .....	viii
List of Content .....	ix
List of Figures .....	xii
List of Table .....	xiv
1 INTRODUCTION .....	1
1.1. Heat exchanger .....	1
1.2. Practical applications .....	2
1.3. Classification of heat exchanger .....	3
1.3.1. Compact Heat Exchanger .....	4
1.4. Plate Fin Heat Exchanger .....	5
1.4.1 Crossflow .....	5
1.4.2 Counter flow .....	6
1.4.3 Cross-Counter flow .....	6
1.4.4 Geometrical Structures of Fin Surfaces .....	8
1.5. Heat transfer and flow friction characteristics .....	9
1.6. Experimental Methods .....	9
1.7. Objectives of the Present Investigation .....	10
1.8. Organization of the Thesis .....	10
2 LITERATURE REVIEW .....	11
2.1 Plate fin heat exchanger .....	12
2.2 Contraction and manufacturing process of PFHX .....	13
2.3 Geometry of Plate Fin Heat Exchanger .....	15
2.3.1 Plain Fins .....	17
2.3.2 Interrupted Fins .....	17
2.3.3 Louvered Fins .....	17
2.3.4 Offset Strip Plate Fin Heat Exchanger .....	18
2.4 Experimental studies of offset strip fins .....	18
2.4.1 Liquid cooled modules .....	21
2.4.2 Visualization technique .....	22
2.5 Numerical and analytical .....	24
2.5.1 Optimization Technique .....	27

2.6.	Heat Transfer and Friction Factor characteristics .....	28
2.6.1	Heat Transfer and Friction Factor Correlations .....	29
2.7.	Deviations from Idealized Condition .....	34
2.7.1	Consequence of Axial and Longitudinal Heat Conduction. ....	34
2.7.2	Effect of Heat Transfer To The Ambient.....	35
2.7.3	Effect of Flow Maldistribution .....	36
2.7.4	The effect of variable fluid properties .....	36
3	DESIGN SPECIFICATION OF PLATE FIN HEAT EXCHANGER.....	38
3.1	Brief Outline of Design Method.....	38
3.2	Specification of Fin Geometry and Input Parameters .....	47
3.3	Design Correlations of Heat Exchanger.....	49
3.4	Simulation Software for Design of Heat Exchanger .....	52
3.5	Specification of Heat Exchanger Dimensions.....	52
4	RATING OF PLATE FIN HEAT EXCHANGER.....	54
4.1	Specified Heat Exchanger and Input Parameter.....	55
4.2	Rating of Specified Heat Exchanger Through Different Correlations.....	56
4.2.1	Performance Evaluation Using the Correlation of Maiti And Sarangi.....	57
4.2.2.	Performance evaluation using the correlation of Manglik and Bergles.....	64
4.2.3.	Performance evaluation using the correlation of Joshi and Webb.....	65
4.3	Rating based on simulation software .....	66
4.4	Effect of heat leak to surroundings .....	68
5.	THE EXPERIMENTAL STUDIES .....	69
5.1	Experimental setup and procedure .....	69
5.1.1	Simple representation of Fluid Flow Facility of Experimental setup .....	73
5.2.	Description of associated equipment and instruments .....	73
5.2.1.	Storage tank .....	74
5.2.2.	Vaporizers .....	74
5.2.3.	Plate Fin Heat Exchanger.....	75
5.2.4.	Chiller unit .....	78
5.4	Instrumentation.....	87
5.4.1	Temperature measurement.....	87
5.4.2	Orifice mass flow meter.....	92
5.5.	Estimation of heat exchanger Performance.....	96
5.6.	Effect of heat leaks surrounding.....	96
5.7.	Experimental error analysis.....	97

6	PERFORMANCE ANALYSIS .....	102
6.1.	Experimental results of cold and hot tests.....	102
6.1.1.	Effectiveness of Plate –Fin Heat Exchanger at different mass flow rate.....	104
6.2	Comparison of effectiveness of cold and hot tests .....	108
6.3	Effect of heat transfer to surrounding .....	108
6.4	Validation of effectiveness obtained with and without heat loss with cold tests....	110
6.5	Uncertainty assessment in experimental results.....	110
6.6	Heat transfer and friction factor of Heat Exchanger .....	111
6.7	Effect of pressure drops with mass flow rate .....	114
6.8	Results and Discussion.....	119
7	CONCLUSIONS .....	121
7.1	Conclusion.....	121
7.2	Future work .....	123
	REFERENCES .....	125

## List of Figures

Figure 1.1 Classification of heat exchangers .....	3
Figure 1.2 Classification of Plate exchangers .....	4
Figure 1.3 Cross flow arrangement.....	6
Figure 1.4 Counter flow arrangement.....	6
Figure 1.5 Cross-Counter flow arrangement .....	7
Figure 1.6 Geometrical Structures of Fin Surfaces.....	9
Figure 3.1 Flow diagram for optimizing a Plate fin heat exchanger .....	46
Figure 3.2 Counter flow offset plate fin heat exchanger strip .....	47
Figure 3.3 Geometrical of strip fin .....	47
Figure 3.4 Dimensions of Plate fin heat exchanger using Simulation software .....	52
Figure 4.1 Temperature with respect to the longitudinal distance Aspen Muse <sup>®</sup> .....	67
Figure 4.2 Pressure with respect to the longitudinal distance Aspen Muse <sup>®</sup> .....	67
Figure 5.1 Process Flow & Instrumentation diagram of the experimental test rig .....	71
Figure 5.2 Photograph during commissioning .....	72
Figure 5.3 Image of Final Experimental setup.....	72
Figure 5.4 Schematic Fluid Flow diagram of Experimental setup .....	73
Figure 5.5 Sketch of Plate Fin Heat Exchanger .....	77
Figure 5.6 Design Model of Chiller Heat Exchanger .....	78
Figure 5.7 temperature profile w.r.t length .....	79
Figure 5.8 Design Sketch of Chiller Heat Exchanger.....	84
Figure 5.9 Temperature contour of Heat Exchanger of Chiller .....	85
Figure 5.10 Temperature Vs Mass flow rate variation .....	86
Figure 5.11 Effectiveness Vs Mass flow rate variation .....	87
Figure 5.12 RTD calibrations Setup with PT100.....	89
Figure 5.13 RTD calibrations graph .....	90
Figure 5.14 ADAM View Connections .....	91
Figure 5.15 Photograph of ADAM View .....	91
Figure 5.16 Display of ADAM View S/W .....	92
Figure 5.17 Photograph of Orifice .....	92
Figure 5.18 Sketch of Orifice.....	93
Figure 5.19 Mass flow rates of Devices.....	95
Figure 6.1 Variation of effectiveness with mass flow rate .....	106
Figure 6.2 Variation of effectiveness with mass flow rate .....	106
Figure 6.3 Variation of effectiveness with mass flow rate .....	107
Figure 6.4 Variation of effectiveness with mass flow rate .....	107
Figure 6.5 Comparison of effectiveness with cold and hot tests .....	108
Figure 6.6 Variation of effectiveness with mass flow rate .....	110
Figure 6.7 Variation of effectiveness with mass flow rate .....	110
Figure 6.8 Variation of Colburn factor with Reynolds No. ....	112

Figure 6.9 Variation of Colburn factor with Reynolds No. ....	113
Figure 6.10 Variation of Friction factor with Reynolds No.....	113
Figure 6.11 Variation of Friction factor with Reynolds No.....	114
Figure 6.12 Pressure drop across the channel of both side .....	115
Figure 6.13 Variation of Friction factor with mass flow rate at 107K (Hot Side).....	115
Figure 6.14 Variation of Friction factor with mass flow rate at 107 (cold Side).....	116
Figure 6.15 Variation of Friction factor with mass flow rate at 111 K (Hot side) .....	116
Figure 6.16 Variation of Friction factor with mass flow rate at 111 K (Cold side).....	117
Figure 6.17 Variation of Friction factor with mass flow rate at 118 K (Hot side) .....	117
Figure 6.18 Variation of Friction factor with mass flow rate at 118 K (Cold side).....	118
Figure 6.19 Variation of Friction factor with mass flow rate at 122 K (Hot side) .....	118
Figure 6.20 Variation of Friction factor with mass flow rate at 122 K (Cold side).....	119

# List of Table

Table 2.1 Range of the plate fin heat exchanger .....	14
Table 2.2 Application of brazed PFHX .....	14
Table 2.3 Manufacture List.....	15
Table 2.4 Heat Transfer and Friction Factor Correlations .....	30
Table 3.1 Joshi and Webb correlation.....	42
Table 3.2 Manglik and Bergles correlation.....	43
Table 3.3 Maiti and Sarangi correlation.....	43
Table 3.4 Fin geometry used in heat exchanger.....	48
Table 3.5 Specified Input Data for Plate Fin Heat Exchanger used for LN2 plant.....	48
Table 3.6 Effective properties at mean temperature .....	49
Table 3.7 Flow configurations for both sides of counter flow .....	49
Table 3.8 Design parameters based on correlations.....	51
Table 3.9 Interior and total size of the plate fin heat exchanger .....	53
Table 4.1 Rating Process.....	55
Table 4.2 Design Process .....	55
Table 4.3 Size of the offset Plate Fin Heat Exchanger interior.....	55
Table 4.4 Core size of a Plate Fin Heat Exchanger.....	56
Table 4.5 Dimensions of Fin Geometry .....	56
Table 4.6 Input values of Plate Fin Heat Exchanger.....	57
Table 4.7 Fluid properties of hot and cold gas.....	58
Table 4.8 Fluid flow Parameter of hot and cold gas .....	60
Table 4.9 Heat transfer area ( $m^2$ ) .....	60
Table 4.10 Maiti and Sarangi correlation.....	61
Table 4.11 Heat transfer coefficient and effectiveness .....	62
Table 4.12 Heat transfer coefficient and effectiveness .....	64
Table 4.13 Evaluated values of friction factor and pressure drop.....	64
Table 4.14 Manglik and Bergles correlation.....	65
Table 4.15 Joshi and Webb correlation.....	65
Table 4.16 Effectiveness at mass flow rate.....	67
Table 4.17 Pressure drop (Hot End) at mass flow rate .....	68
Table 4.18 Pressure Drop (Cold End) at mass flow rate .....	68
Table 5.1 Basic Technical Specifications of Storage Tank.....	74
Table 5.2 Technical Specification of Star Fin Vaporizer.....	75
Table 5.3 Flow arrangement of the heat exchanger .....	75
Table 5.4 Core size of the heat exchanger .....	75
Table 5.5 Fin Geometry of the heat exchanger .....	76
Table 5.6 Flow parameters of the heat exchanger.....	76
Table 5.7 Outlet Temperature as a function of mass flow rate .....	86
Table 5.8 Temperature at different T100 .....	90
Table 5.9 Gas mass flow rate ( $Q_{mass}$ ) at various pressure differences $\Delta P$ .....	94
Table 5.10 Gas mass flow rate ( $Q_{mass}$ ) at various .....	94
Table 5.11 Error Differences in between Orifice and Rotameter .....	95
Table 6.1 Test Data for a range of Mass Flow Rate at cold inlet temperature of 107K.....	102
Table 6.2 Test Data for a range of Mass Flow Rate at cold inlet temperature of 111K.....	103

Table 6.3 Test Data for a range of Mass Flow Rate at cold inlet temperature of 117K.....	103
Table 6.4 Test Data for a range of Mass Flow Rate at cold inlet temperature of 122K.....	103
Table 6.5 Error percentage when the inlet temperature is 107K.....	105
Table 6.6 Uncertainty assessment in the effectiveness in different mass flow rate at 107K .....	111
Table 6.7 Colburn factor at 107K on hot side of PFHX .....	111
Table 6.8 Colburn factor at 107K on Cold side of PFHX.....	112
Table 6.9 Friction factor at 107K on Hot side of PFHX.....	113
Table 6.10 Friction factor at 107K on Cold side of PFHX .....	113
Table 6.11 Percentage of error.....	120

## Nomenclature

$A$	Heat transfer area of the heat exchanger with subscripts h or c denoting hot and cold fluid, m <sup>2</sup>
$A_{ff}$	Free flow area available for hot or cold fluid with subscripts h or c respectively, m <sup>2</sup>
$A_{fr}$	Frontal area available for hot or cold fluid with subscripts h or c respectively, m <sup>2</sup>
$A_w$	Total wall area for transverse heat conduction from the hot fluid to cold fluid, m <sup>2</sup>
$a$	Plate thickness, m
$a_f$	Fin surface area, m <sup>2</sup>
$a_{ff}$	Free flow area/fin, m <sup>2</sup>
$a_{fr}$	Frontal area/fin, m <sup>2</sup>
$a_s$	Heat transfer area/fin, m <sup>2</sup>
$a_w$	Total wall cross sectional area for longitudinal conduction, m <sup>2</sup>
$C$	Flow stream heat capacity rate with subscript h or c for hot and cold fluids, W/K.
$C_d$	Coefficient of discharge, dimensionless
$C_{min}$	Minimum of c C or h C, W/K
$C_p$	Specific heat at constant pressure, J/kg-K
$C_r$	Heat capacity rate ratio, dimensionless
$D_e$	Equivalent diameter of the flow passage, m
$f$	Fin frequency, Number of fins per meter length, fins/m
$f$	Fanning friction factor, dimensionless
$G$	Core mass velocity, kg/m <sup>2</sup> s
$H$	No flow height (stack height) of the heat exchanger core, m
$h$	Height of fins, m
$h$	Convective heat transfer coefficient, W/m <sup>2</sup> K
$j$	The Colburn factor, non-dimensional heat transfer characteristic
$K_c$	K Contraction coefficient, no units
$K_e$	e K Expansion coefficient, no units
$K_f$	f K Conductivity of the fin material, W/m- K
$K_w$	w K Conductivity of the wall material, W/m- K
$L$	Fluid flow (core) length on one side of the heat exchanger, m
$l$	Fin flow length on one side of a heat exchanger, m
$l_e$	Effective fin length for efficiency determination with subscripts h and c denoting hot and cold fluids, m
$m$	Mass flow rate, kg/sec.
$N$	Total number of layers or total number of fluid passages
$N_{tu}$	Number of heat transfer units, UA/C <sub>min</sub> , dimensionless
$n_{tuc}$	Number of heat transfer units based on cold fluid side
$n_{tuh}$	Number of heat transfer units based on the hot fluid side
$P_f$	Fin pitch, 1/ f, m
$Pr$	Prandtl number of the fluid
$Q$	Heat load, W
$Re$	Reynolds number, dimensionless
$Re^*$	Critical Reynolds number with subscripts j or f for heat transfer and pressure drop



	considerations
s	Spacing between adjacent fins,
T	Temperature of the fluid (with subscripts c, h or i, o)
t	Thickness of fin, m
$U_o$	Overall heat transfer coefficient. W/m <sup>2</sup> K
W	Width of the core, m

## **Chapter I**

# **INTRODUCTION**

### **1.1. Heat exchanger**

The heat exchanger is a device used for transferring heat from one medium to another medium either from fluid to solid or from fluid to fluid. Energy transfer occurs when the fluids are at a different temperature. Heat transfer in heat exchanger is based on laws of thermodynamics preferably the second law of thermodynamics i.e. heat flows from one object of higher temperature to another object at a lower temperature. The application of the heat exchangers is very vast and is widely used for the transfer of heat in industrial and in house hold equipment's such as in refrigeration and air conditioning, process and distribution plant, manufacturing industry, cryogenic and air separation plant etc.

However, especially in cryogenics, a wide range of heat exchangers is used. It is one of the most important equipment of any liquefaction process in the industry. The heat exchangers are relevant for liquefaction to storage, loading and transportation. The thermal energy is transferred by the fluid from one surface to another surface predominantly by the phenomena of conduction and convection.

The two ways of transferring energy are direct contact and indirect contact method leads to two types of heat exchangers called recuperative and the regenerative. In one of the such classes, the heat transfer surface separates fluids, and preferably they do not mix or leak such type of heat exchangers are mentioned as direct transfer type of heat exchanger, or simply recuperators. In contrast, the other class of heat exchanger transfers heat alternatively between the hot and cold fluids through stored heat energy in a matrix. This is known as an indirect transfer type of heat exchanger, or simply regenerators.

## 1.2. Practical applications

Specifically, the application of heat exchanger is to heat or cool the system as per the necessity. There is numerous application of heat exchanger. Some of the applications are given below.

- i. In industry heat exchangers are used for various purposes. The major units of industries which use different types of heat exchangers are:
  - Transformer oil coolers
  - Motor and generator coolers
  - Chemical plants
  - Food processing plant
  - Petroleum Processing
  - Mining
  - Textiles
- ii. Heat Exchanger are used in aircrafts mainly for keeping the engine cool. Highly inflammable fuel used in air crafts makes the use of heat exchanger very crucial.
  - Aerospace liquid cooling
  - Liquid cooling in an airplane
  - Duct heater for a military helicopter
- iii. In cryogenics the heat exchanger plays major role in the field of liquefaction of gases and also in the other equipment's such as given below.
  - Gas turbine power plant
  - Gas liquefaction
  - Chiller's
  - Cryo refrigerators
  - Biopharmaceutical
  - Cryogenic packaging and treatment equipment such as MRI
  - Cryogenic fuel lines
  - Superconducting magnets

iv. Automobiles too need heat exchanger technically the heat exchangers effectiveness required for automobile is comparatively low as compared to the heat exchanger used in cryogenics purpose.

- Radiator
- Oil coolers
- Exhaust gas recirculation coolers
- Air conditioning
- Unmanned aerial vehicles

### 1.3. Classification of heat exchanger

Depending on the nature heat exchanger can be classified on the basis of shapes, flow direction, functional process. The use of any particular type of heat exchanger is determined by the requirement are described by R.K.Shah [1]. But the heat exchangers are mainly divided into two parts ‘recuperative and regenerative type’ as shown in Figure 1.1. The focus of this research is on plate fin heat exchanger which comes under the recuperative type. The recuperative type is further subdivided into direct and indirect type. The plate fin heat exchanger is an indirect type of plate heat exchanger with serrated fins or offsets fins. The classification of plate heat exchanger is shown in Figure 1.2.

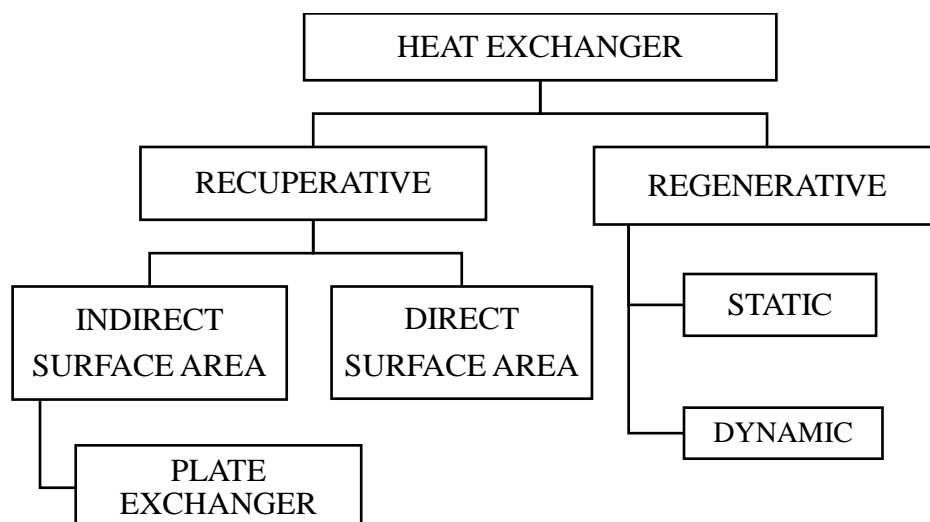


Figure 1.1 Classification of heat exchangers

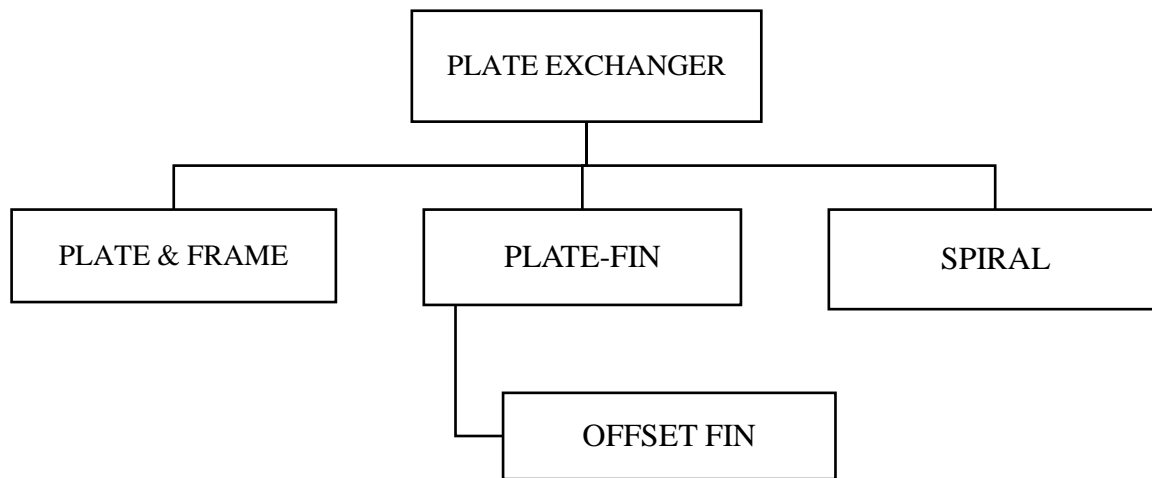


Figure 1.2 Classification of Plate exchangers

### 1.3.1. Compact Heat Exchanger

Heat exchanger is essential for the process industries and, therefore, the requirement of heat exchanger increases. Massively it is essential for a heat exchanger to be more efficient and acquire less space. As per the Newton's law of cooling it is either to increase the temperature difference or to extend the surface area. The demerit of increasing temperature difference in practical application is to do some extra work for cooling or heating the fluid. Secondly, thermal stress deformation may cause reduction of life of heat exchanger or its effectiveness. So it is better to extend the surface area. The overextended surface area is called the fin or secondary or indirect surface. If the surface area is to be extended, it requires space, material and support structure. So to overcome these problems without losing heat transfer rate, improved process engineering comes in the form of compact heat exchanger. It has a large heat transfer surface area per unit volume ( $\text{m}^2/\text{m}^3$  or  $\text{ft}^2/\text{ft}^3$ ), this means it acquires less space in a particular volume with high heat transfer rate.

The smallest heat exchanger called compact heat exchanger comprise with the gas to fluid stream have its surface area of about greater than  $700 \text{ m}^2/\text{m}^3$  and for liquid or for the two

phase flow it is more than  $400 \text{ m}^2/\text{m}^3$  of heat transfer area density. Therefore, it is essential in applications where the size and weight are important constraints.

Varieties of Compact Heat Exchanger [18] are,

- Plate heat exchanger (PHE)
- Plate fin heat exchanger (PFHE)
- Printed circuit heat exchanger (PCHE)
- The marbond heat exchanger
- Ceramic heat exchanger
- Spiral heat exchanger (SHE)

The compact heat exchangers are sorted by the measure of the amount of extended surface per unit volume. There are numerous sorts of fins that are embraced in a heat exchanger to expand the heat transfer rate. Among them, the plate fins are more desirable because of its simplicity in construction and potential for upgraded thermal hydraulic execution.

## **1.4. Plate Fin Heat Exchanger**

Plate Fin Heat Exchanger is a type of Compact heat exchanger. It comprises of alternating lining of interleaving grooved and wavy Fins (sheets), differentiated by separating sheets encased at the boundaries by sidebars to form a progression of finned cells. Fins and separating sheets are join together by vaccum technology using oven brazing technique which turn the unit into an independent structure in a flexible core. The core can be more than one and can effortlessly rearrange it adequately. It Permits the Plate Fin Heat exchanger to control it in flow arrangements such as parallel flow, crossflow, counter flow, cross-counter flow or co-current flow.

### **1.4.1 Crossflow**

The application or the example of utilization of cross flow heat exchanger is in a car radiator, and the evaporator coil of an air conditioner. The flow across in the cross flow heat exchanger is normal to each other. Its effectiveness is not more as compared to counter flow. The cross flow effectiveness lies between the counter flow and parallel flow. The problem with the cross flow heat exchanger is that there are only two streams took in cross flow arrangement, but the positive thing is that it is cheaper, simpler and easier in manufacturing as the header tanks placed on each side of entry and exits of flow pattern. So cross flow heat

exchanger is a better option when the effectiveness is required to be adjustable and flow of two fluids is required. Figure 1.3 illustrates an arrangement of Plate fin heat exchanger of cross flow type.

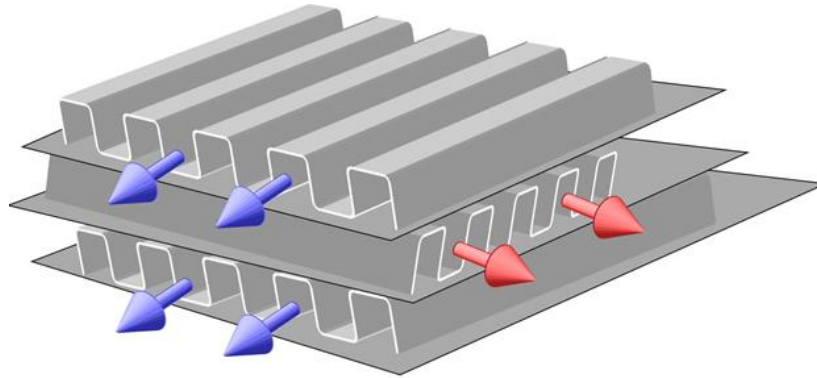


Figure 1.3 Cross flow arrangement

### 1.4.2 Counter flow

The most commercial application of counter flow heat exchanger is in cryogenics for refrigeration and the liquefaction process of gasses. The most promising heat exchanger is the counter flow heat exchanger. Its effectiveness is better as compared to other heat exchangers. It is the most capable flow technique, generating the maximum temperature change in respective fluid associated with any other two-fluid configuration for a given set of overall thermal conductivity ( $UA$ ), inlet temperatures and mass flow rates of fluid. However, the design process is complex because its header and distributor geometry is complicated. (Figure 1.4 illustrates a counter flow arrangement of Plate fin heat exchanger)

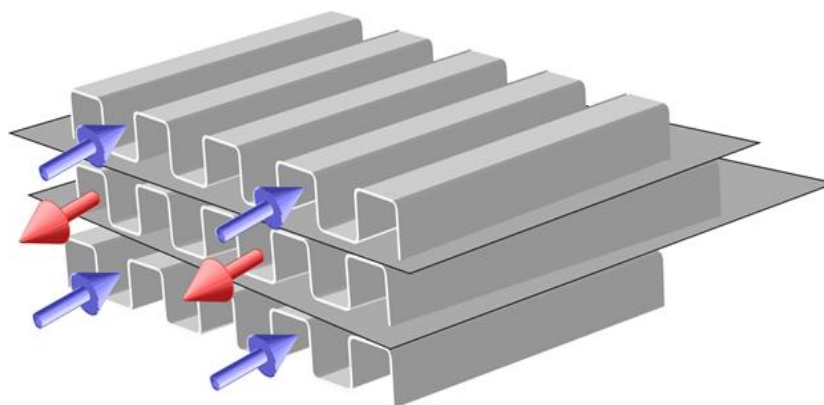


Figure 1.4 Counter flow arrangement

### 1.4.3 Cross-Counter flow

Adequately the utilization of Cross CounterflowPlate fin heat exchangers is similar to those of simple cross flow exchangers. The design procedure is much informal therefore its construction and assembly are also easier. Such heat exchangers are mainly fit for the uses in which the two fluids have extensively dissimilar mass flow rates or allow considerably change in drops of pressure. Consequently, it is a form of fusion structure of cross flow and counter-flow arrangements, with the quality of both the heat exchangers. It has a higher heat transfer rate of the cross flow configuration along with the better thermal effectiveness of counter-flow heat exchanger. In this configuration, primary fluid flows in a straight forward direction, whereas the secondary fluid follows a criss-cross direction normal to that of the primary fluid flow. Even though transferring along the zig-zag manner, the second fluid flow covers the duration of the heat exchanger in a manner reverse to that of the next move. Thus, the drift pattern may be assumed to be generally in counter-flow while closing locally in cross flow.

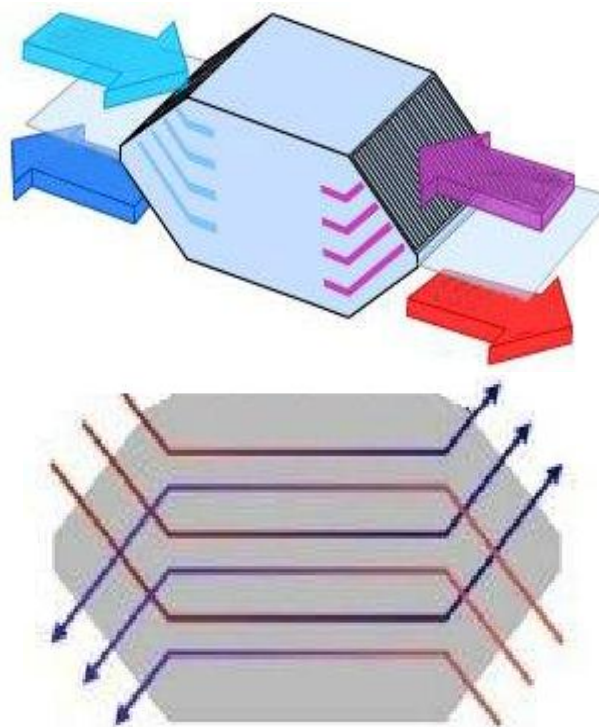


Figure 1.5 Cross-Counter flow arrangement

A basic cross-flow stream design is appropriate in a simple flow layout utilized widely for low and moderate duty and is compelling when it is low-pressure at one side. For high flow



rate obligation, the counter flow design regularly compromises an effective arrangement. The more elevated amounts of effectiveness accomplished by counter flow type of plate fin heat exchange are more applicable to low-temperature practices. Figure 1.5 illustrates the arrangement for a cross-counter flow type of heat exchanger.

#### 1.4.4 Geometrical Structures of Fin Surfaces

The requirement of fins in plate fin heat exchanger is to enhance the heat transfer by transferring energy from one fluid to another through a separated wall or plate via fins. The plate and the fins base straightforwardly brazed to the plate, which make it the perfect heat transfer surface and divide the individual stream sections for two and more fluids. Heat transfer surface range, obtain a low hydraulic diameter, decreases the thermal resistance and improves overall heat transfer area for the same temperature difference over the surfaces. Moreover, it also supports the configuration to resist the design pressure at the design temperature notably at the outline temperature as a fundamental part of a component in the structural design. So designer prefers both the prerequisites reply upon the application. Therefore, different sorts of fin geometry are subsequently created to meet the purpose by considering those factor. The structure of fins as shown in Figure 1.6 differentiated into various types such as Plain Fin, offset strip Fin, Wavy fin, perforated fin, Louvered-Fin, and Pin Fin, etc.

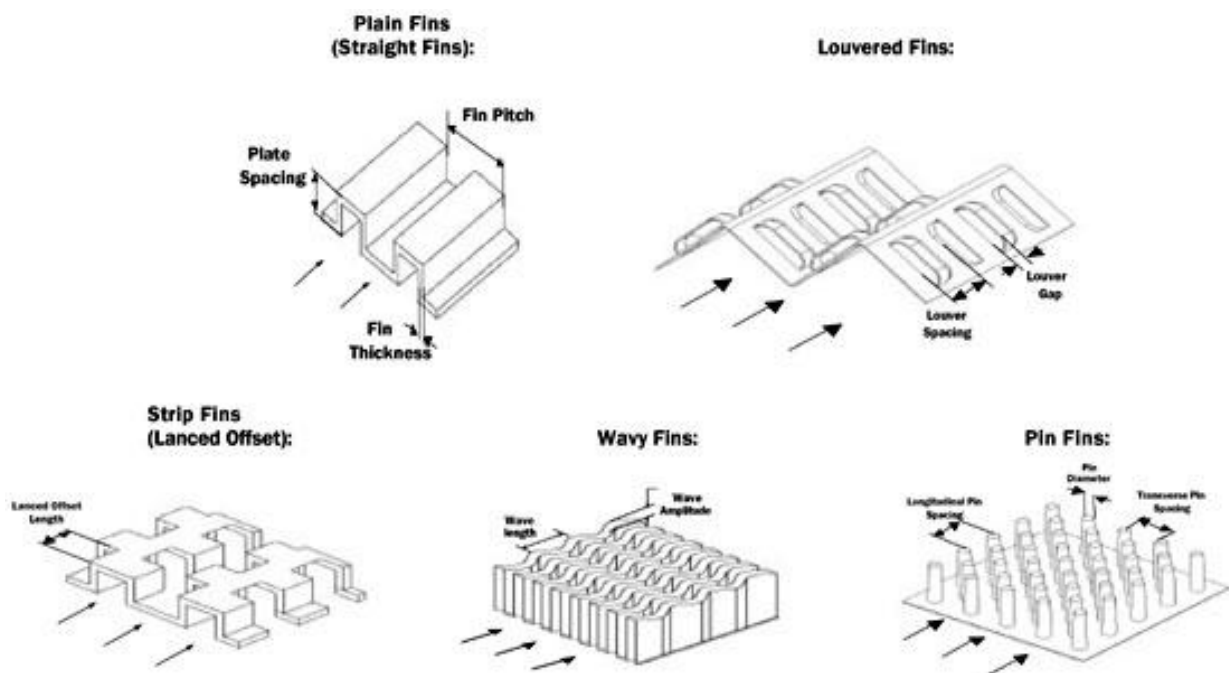


Figure 1.6 Geometrical Structures of Fin Surfaces [153].

## 1.5. Heat transfer and flow friction characteristics

Heat transfer and flow friction are the significant terms to find the performance of plate-fin heat exchanger. Most of the correlations are based on these factors. Heat transfer and flow frictions are the terms represented in a form of Colburn factor and Fanning friction factor.

$$j = \frac{h}{Gc_p} (\text{Pr})^{2/3}$$

$$\Delta p = \frac{4flG^2}{2D_h\rho}$$

Where

$h$  = heat transfer coefficient ( W / m<sup>2</sup> -K )

$G$  = Mass velocity ( kg / s-m<sup>2</sup> ) [for minimum free flow area]

$l$  = Flow passage Length (m)

$D_h$  = Hydraulic diameter (m)

$\rho$  = Fluid mean density (kg/m<sup>3</sup>)

## 1.6. Experimental Methods

The experiment is performed to obtain the heat exchanger performance of a specified heat exchanger under steady state condition. The complete description of experimental setup and procedures including cooling pure nitrogen to a uniform temperature (approximately 107K lower than the ambient temperature in this test rig) is described in Chapter 5. When subjected to the test rig, the heat transfer performance of plate-fin heat exchanger at a different mass flow rate of nitrogen is investigated at a fixed cold and hot inlet temperature. Subsequently, the same procedure is repeated for different temperature lower than ambient temperature in this test rig. The cryogenic temperature is achieved by plate fin heat exchanger at the inlet of the cold side due to another coil type heat exchanger which is dipped inside a nitrogen bath. The construction and geometrical detail are specified in chapter-5. The change

in temperature on the four sides of the heat exchanger is noted using ADAM module through RTD's. Manometers are used to observe the differences in the pressure between the high and low-pressure side and it is also used for calculating mass flow rate through the orifice plate. Required recorded data is simulated with Aspen software and also compared with other correlations to confirm the accuracy of the experiment.

## **1.7. Objectives of the Present Investigation**

The aim of this thesis is three folds.

1. To build an experimental setup for testing the Plate Fin Heat Exchangers at liquid nitrogen temperature
2. The response of heat exchanger in term of effectiveness is compared with 'ASPEN MUSE<sup>®</sup>' to confirm the validity of experimental data within an acceptable margin of experimental error. The effectiveness and pressure drop data is simulated with Aspen software and also compared with other correlations to confirm the accuracy of the experiment.
3. The third point is to compare data of cold test with hot test [151] for effectiveness and pressure drop. Since specific variation under the temperature range (hot to cold) is small, it may be possible to conduct an only hot test which is easier than a cold test to obtain the efficiency experimentally.

## **1.8 Organization of the Thesis**

Chapter 1 deals with the general introduction to Plate Fin Heat Exchanger (PFHX) with its classification and application. Chapter 2 presents the survey of literature related to various aspects of PFHX. Chapter 3 discusses the design aspect of low-temperature PFHX test facilities. Design Correlations and Simulation Software are presented in chapter 4. Experimental studies at low temperature (cold test) are presented in chapter 5. Chapter 6 deals with the comparison of the analytical and experimental values on the cold test. The hot test values are also compared in this chapter. Chapter 7 represents discussion on the results of PFHX.

## **Chapter 2**

# **LITERATURE REVIEW**

An extensive literature survey about the compact heat exchanger and the plate fin heat exchanger containing offset strip fins has been carried out. In this literature, most practical and common models are addressed which have been analytically, numerically and experimentally presented by various researchers. The complete information about the offset type of plate fin heat exchanger used by different researchers are also summarised in the study.

The review organized into several parts. The application of heat exchanger particularly compact type heat exchanger in the field of cryogenic are emphasised. The approaching part relates to the review of plate fin heat exchanger and its construction process. Consequently, the experimental, numerical and optimization of offset type of plate fin heat exchanger is reviewed and addressed. The deviation from the ideal condition of the heat exchanger and the various correlations proposed by the researchers are reviewed.

The heat exchangers are widely used in the various field such as aerospace, automobile, electronics cooling devices, etc. Shah [1] presented a classification of the heat exchangers taking in several aspects mainly divided into regenerative and recuperative. A contextual background including design and its application of regenerator that used mostly for small equipment like pulse tube cryocoolers in cryogenics are describe by Ackermann [2]. In a regenerator, fluid streams are passing through the heat exchanger surfaces one after the another by absorbing and releasing energy separately whereas in a recuperator energy is exchanged at the same time through a parting sheet.

In cryogenics, a variety of heat exchanger are used as explained in [3], since it requires highly efficient heat exchanger for liquefaction of gases. Many researchers [4-6] investigated its sensitiveness for the production of liquefaction of gases, Barron [6] reported that no liquefaction is obtained if the effectiveness of heat exchanger is lower than 85%. The study of the process of heat transfer in the heat exchanger and its design methods have been explained critically by various authors and scholars [7-14]. Based on design criteria on spacing or say compactness, the compact heat exchanger is one of the best types of heat exchanger.

A compact heat exchanger confirms greater than  $700 \text{ m}^2/\text{m}^3$  of heat transfer area density. Therefore, the size is an essential factor in a specific application where the size and weight is an important constraint which is defined by Shah [11, 14]. He also including characteristics and its classification in their reports. Hesselgreaves [15] stated the different forms of compact heat exchanger employed for industrial uses. A general idea of fins in the heat exchanger for an automobile as well as in air conditioning system developed by Cowell and Webb [16, 17]. Qi Li [18] reports the different types of compact heat exchanger like plate heat exchanger, printed circuit Heat exchanger, plate fin heat exchanger, spiral heat exchanger, Marbond heat exchanger, ceramic heat exchanger etc. However, for large equipment high compactness, multifluid flow plate fin heat exchanger provides the best result amongst other [19-21]. As it is a multi-streams, many streams can be accommodated within a one compact heat exchanger unit. Consequently a number of item is reduce or remove to reduce its weight and size [19].

The high-quality work on compact heat exchanger was reported by London [22]. He has also co-authored in a monograph with Kays [8] and Shah [23]. Earlier in 1940 Kays *et al.* [24] carried out experimental works on heat exchangers and explained the test method for heat transfer and fluid flow characteristics. The literary work of Kays *et al.* was adopted by various researchers. Even Kays *et al.* also followed their own developed data in their further studies on correlations and other related experiments.

## **2.1 Plate fin heat exchanger**

PFHX is one of the most important categorized heat exchanger among other compact heat exchangers. It comprises serrated fins sandwiched between parallel plates one after another and placed in a sequence to form a compact heat exchanger

PFHX was formerly used in the auto industry in 1910 gradually in 40's it comes to the aerospace industry for gas to gas heat exchanger application. In 1950 plate fin heat exchanger of aluminium is owned for liquefaction of gases, as aluminium have the desirable mechanical and thermal properties for low temperature. At present brazed aluminium plate fin is used to great extent such as in automobile plant, refrigeration, air conditioning, cryogenics etc [1].

## **2.2 Contraction and manufacturing process of PFHX**

Various authors have reflected on the design and development of PFHX by considering the material selection to shape, size, weight and surface design [1, 15, 25, 26]. Hesselgreaves [15] proposed one of the important procedure for selection, design and operational process. In 1961 Lenfestey [25] presented a review of the design method and the construction processes of the low-temperature heat exchanger. Later on, Lenfestey [26] in 1968, added up further details in a consequent publication and proposed advanced heat exchanger.

The material employed for plate fin heat exchanger depends according to the requirement for temperature, pressure, and spacing. The temperature ranging up to 50°C; paper is used (mainly for ventilation purpose), for higher temperature up to 840 °f metal is preferred, and for much higher temperature up to 1370 °f ceramic materials are used. The metallic material required for plate fin heat exchangers are aluminium, stainless steel, copper alloy, nickel alloy [1, 27]. Recently Seara *et al.* [28] presented PFHX made up of titanium brazed offset fins strip. Ceramates, [29] design a ceramic heat exchanger. According to Taylor,[30] aluminium is the desired material for cryogenics applications. Mass production of cryogenic equipment permitted makers to put resources into expensive aluminium brazing furnaces. The brazing of plate fin along with the parting sheets are done by employing two methods, one is salt bath brazing, and another is brazing in a vaccume furnace. In salt bath brazing the interface joints between fin and parting sheet is filled with aluminium shim and wet flux and then submerged into the liquid salt bath. The temperature of the bath is enough to melt the brazing alloy. As most of the alloy of aluminium losses their strength in slight above temperature than ambient temperature, therefore, this method is preferable for aluminium rather than vaccume furnace used for many metals but vaccume brazing gives highly clean

surface. The parting sheet, fins, edge-bars and top sheets are brazed together to form a block of PFHX and then the header and the nozzle are welded to the block.

Table-2.1 shows the minimum and maximum range of pressure, temperature and other geometrical factors that are affecting the effectiveness of the plate fin heat exchanger.

Table 2.1 Range of the plate fin heat exchanger

[1] [16] [26] [27] [28] [29]

Factors	Minimum range	Maximum range
Pressure	700 kPa	35000 kPa
Temperature	-269°C	1370°C
Compactness	700 m <sup>2</sup> /m <sup>3</sup>	5900 m <sup>2</sup> /m <sup>3</sup>
Fin density	120 (Fins/m)	2100 (Fins/m)
Thickness of the Fin	0.05 mm	0.25 mm
Height of the fin	2 mm	2.5 mm

Table 2.2 Application of brazed PFHX

[30]

Plant types	Industrial gas production	Natural gas processing	LNG	Petrochem	Refrigeration
Temperature	+65 to -200	+100 to -130	+65 to -200	+120 to -200	+100 to -269

---

range, °C

Pressure range, bar	1 to $\geq 100$	15 to $\geq 100$	5 to 100	1 to $\geq 100$	15 to 45
---------------------	-----------------	------------------	----------	-----------------	----------

(abs)

---

Table 2.3 Manufacture List

---

Manufacturer

---

Altec (USA)

IMI Marston (UK)

Kobe Steel (Japan)

Linde AG (Germany)

Nordon Cryogenic (France)

Surnitomo Precision (Japan)

ALPEMA

Apollo

---

## 2.3 Geometry of Plate Fin Heat Exchanger

The fins in a PFHX can be effortlessly organised in many ways. According to the flow direction or the flow arrangements, PFHX are categorised as parallel flow, crossflow, counter flow, cross-counter flow or co-current flow. The pattern of the flow affects the surface area of the heat exchanger. The application of cross flow heat exchanger vastly used in the air conditioner, evaporator coil and the car radiator. The flow across the cross flow heat exchanger is normal to each other, and its effectiveness is less as compared to counter flow type. The effectiveness of cross flow type lies in between the counter flow and parallel flow. The demerit is that only two streams flow occurs in cross flow arrangement at a time, but the



favourable thing is that it is cheaper, simpler and easier in manufacturing as the header tanks placed on each side of entry and exits of flow pattern. So where the requirement of effectiveness is not so predominant, and the two fluids streams are present, the cross flow heat exchanger are the better options. The most commercial application of counter flow heat exchanger is in cryogenics for refrigeration and the liquefaction of gases. The most promising heat exchanger is the counter flow heat exchanger in the form of better effectiveness as compared to other heat exchangers. It generates maximum variation in the temperature as compared to the other types of two-fluid configuration for a given fluid inlet temperature, mass flow rates, and overall thermal conductivity (UA) therefore its flow arrangement much capable than another. However, the design process is complex for the reason that its header and distributor geometry is complicated. Adequately the utilization of Cross Counterflow PFHXs is alike to those of simple cross flow exchangers. The design procedure is much informal are therefore its construction and assembly are also easier. They mainly fit for the uses where the mass flow rates of two streams have many variations or allow considerable drop in pressure. Consequently, it is a form of fusion structure of crossflow and counter flow arrangements, with the quality of both the heat exchangers. Cross-Counter flow type of heat exchanger has larger heat transfer rate as in cross flow configuration along with the better thermal effectiveness of counter-flow heat exchanger. In the configuration of this type heat exchanger one fluid have straight forward flow pathwhile the second fluid follows crosswise direction that is normal to the directionof the first fluid flow. Even though transferring along the zig-zag manner, the fluids cross each other in opposite direction. Hence, the fluid flow is supposed to be partially counter-flowing and up to some extent across theflow.

A basic cross-flow stream design is appropriate in a simple flow layout utilized widely for low and moderate duty and is particularly compelling when one side is a low-pressure gas. For heavier obligation, the counter flow design regularly offers an effective arrangement. Therefore, in low-temperature practices counter flow type of plate fin heat exchanger are more applicable since it accomplish delegated amounts of effectiveness.

#### **GEOMETRICAL STRUCTURE OF FIN SURFACES**

The fin enhances the surface area to the volume ratio of the heat exchanger [31] so that to increase the heat transfer rate and also for supporting the structure consequently it increases the heat transfer coefficient also with a total rate of heat transfer. To optimize, various

geometrical design is proposed and implemented according to their requirement by effectiveness, cost, weight, space and pressure drop. The different types of fins are [1].

### **2.3.1 Plain Fins**

- Triangular
- Rectangular
- Trapezoidal

### **2.3.2 Interrupted Fins**

- Offset Strip
- Louver
- Perforated
- Pin fins
- Wavy

Among above-designed fin geometries Plain, are perforated and offset strip fins preferable for the manufacturing. Also in same situation wavy fins are used. Perforated in controls the pressure variation developed due to the vaporization of fluid. It also makes available uniformity in the flow pattern through the sub passages [32]. Whereas the offset fin provides better heat transfer rate and also sustain high-pressure difference.

The innerstructures of plate fin surface extended and interrupted to provide better heat transfer coefficient. The structures divided into two groups one is continually interrupted i.e. wavy fins, and another is interrupted flow due to cuts provided in between i.e. louvered and offset.

### **2.3.3 Louvered Fins**

Louvered fins have found wide application in the aerospace industry. The flow phenomena were explained experimentally aligned with the louvered angle at high and low Reynolds number by Achaichia *et al.* [33]. In 1990 CFD work on louvered fins[34-36]was performed considering the data Achaichia *et al.* [33]. Achaichia [34] presented the arrangement of flow

regimes with different angle  $\alpha$  of mean flow formed due to the change in Reynolds number. Whereas Ha [36] have to predict Nusselt number and friction factor. Atkinson [35] developed the 2-D and 3-D models. The computational and experimental analysis together had been done by Springer *et al.* [37]. Tafti [38, 39] considered the time phenomena to solve the governing equations.

### **2.3.4 Offset Strip Plate Fin Heat Exchanger**

The Plate fin heat exchanger of offset strip is comparatively efficient, stable and adaptive to a suitable system. It is most demanding system among heat exchangers. A small cuboid duct shape serrated strip frame placed and brazed laterally parallel to the line slightly backward from the position of the previous strip accommodated plate to form an offset corrugated pallet so that flow can be interrupted. Offset plate fin heat exchanger have an enhanced interrupted surface that is required to raise the effective heat transfer surface area per volume periodically to form thermal boundary layer over the interrupted surface provides homogenized flow. The formation of the new boundary layer to every fourth interrupted surface serves as a primary effect on the effectiveness of the offset plate fins, but there is a drop in pressure because of the resistance offered by the plates and form drag due to the fins.

Due to this complex geometry of offset fin, the path of flow of fluid around the fins generates a complex model and its correlation. The analytical and numerical analysis construct their correlation with some assumptions by various researchers such as flow is incompressible, no radiation, property of fluid does not change with temperature, flow is steady and laminar. Besides these in the numerical analysis they considered laminar flow that disaffirms the experimental validation. Despite that one of the most common assumption was that they consider the thickness of the fin as zero although Patankar *et al.* [40] and Suzuki [41] consider the fin plate thickness even considering all those assumptions the analytical correlations are not suitable by the designers and researchers.

## **2.4 Experimental studies of offset strip fins**

In this section, experimental works are arranged according to temporal sequence. Starting earlier from 1942 Norris *et al.* [42] had reported the first experimental report on offset strip fin on which three type of offset fins were tested and has drawn out the effect of heat transfer coefficient by length, thickness and pitch of fins and also reduced the friction factor and Colburn modules. Joyner 1943 [43] put up an experimental research to measure total heat transfer and pressure drop of five serrated fins of different length to determine local heat-

transfer coefficient, Nusselt number, Reynolds number and friction factor and plotted graph between them. By above investigation Norris *et al.* [42] and Joyner 1943 [43] along with other three total five references prescribed by the Manson [44] to predict first empirical correlation on which one equation was for heat transfer over the entire range of conditions investigated. The friction data required separate correlation equations below and above the transition Reynolds number of 3500. However, the data base engaged comprised of different geometries such as louvered fins, finned flat tubes and offset strip fins. In 1950 'Kays and London' carried forward one of the primary support on experimental investigations for some offset fin geometry in two parts [45, 46]. In the first part, it gives the detailed descriptions of the experiment apparatus and method of test data analysis where as in the second part it gives the  $j$  and  $f$  factors for two different offset strip fins cores. The  $j$  and  $f$  design data of three offset plate fin was summarized later on 1955 Kays, [47]. Further in 1960, Kays [48] explore the research on analogous geometry along with six more heat transfer surfaces that was the first effort for calculating overall efficiency of finned passage. Briggs and London [49] presented design data of  $j$  and  $f$  for eleven compact plate-fin surfaces. Five surfaces are of the offset rectangular-fin type, and six are of the plain triangular-fin type. The cores are some of aluminium and rest of them are of an alloy of stainless steel and nickel that was suitable for high-temperature applications. Kays *et al.* [50] gathered  $j$  and  $f$  design data in 1964 from [47, 48, 50] in a book form relevant to compact heat exchangers. With the reference of Kays [47] report A. L. London and Shah [51] in 1968 extended the work on heat transfer and flow friction design data of nine offset rectangular plate-fin surfaces two of them was made up of stainless steel. They also analysed the mal-flow distribution through the test core and their effects. Voronin and Dubrovsky [52] advert an equation for friction factor and Nusselt number. They found that the flow separation due to interruption played a significant role. In 1975, A. R. Wieting [53] set up the statically relationship between the variable from earlier experimental heat transfer and flow friction data of an offset fin for plate fin heat exchanger. By using this statical relationship untested offset fin geometries can be predicted realistically and accurately within the parametric range. Mochizuki *et al.* [54] experimentally shows the optimized value of fin length and demonstrated the most desirable optimized value of the fin length for better performance of heat exchanger on seven aluminium fin cores. Sparrow *et al.* [55] 1980 demonstrated the uses of the naphthalene sublimation technique to achieve the heat transfer effects via the heat and mass transfer analogy on the flow over serrated offset strip fins. Webb and Joshi presented two papers [56, 57] one by one in the year 1982 and 1983. In 1982 experimental study on the friction data for the offset strip fin

matrix with no burred fin edge and suggested that the burrs have no such effect on the heat exchanger. Later they worked out on semi-empirical correlation with verification from data in [50, 51] to predict the friction factor by using eight test section. In 1984 Kays *et al.* [8] compile the previously reported data of twenty-one offset fin. Joshi *et al.* [58] developed an analytical model to correlate the  $j$  and  $f$  factors related to wake region in boundary layer separation of the fins. The offset fin arrays were used to anticipate the wake during the transition regions from laminar to turbulent flows. The equation of Reynolds number for the wake width, i.e. the transition Reynolds number, was formulated and then  $j$  and  $f$  factors correlations for the laminar and turbulent flow was given to visualize the flow patterns in the fin wake to analyse the stress on transition. In the same year, Mochizuki *et al.* [59] presented the graphical  $j$  and  $f$  data and its correlation for offset plate fin, and also it found that offset configuration provides a better result in comparison of slotted and plain straight fins. Dubrovsky *et al.* [60] determined the Nusselt number and coefficient of friction pressure losses Reynolds number and the fin geometrical parameter and their correlation experimentally for eleven interrupted surface. The Reynolds number was varied from 500 to 10000 during the process with air as working fluid. Brackmeier [61]. Purposed the best execution qualities by using vortex generator surface on permitting a decrease in heat transfer surface area of about 76% without altered its pumping power and heat capacity. It is beneficial to reduce obligatory heat transfer zone to dismiss the capital expenses. Dubrovsky [62, 63] innovated and analysed the result of precise exploratory examinations into the rational improvement of convective heat transfer in the passages of plate fin heat exchanger. In a laminar stream of Reynolds number 550–1100, which was done in this study surprisingly, made it conceivable to reach inferences that are imperative in a pragmatic admiration.

Manglik *et al.* [64] choose an experimental data of 18 offset plate fin surfaces from Kays *et al.* [8], London *et al.* [51] and Waiters [65]. To investigate the impact of the non-dimensional constraints on them they derived a correlation.

The proposal of utilizing plate fin heat exchanger of offset, rectangular fin in the solar air collector, was proposed by Youcef-Ali [66]. The enhanced the heat transfer between the fluid and the absorber plate, which evidently intensified the performance of solar collector thermally as compared to the conventional flat plate solar collector. Again in 2006 Youcef-Ali [67] analysed plate collector and predicted the results by developing a mathematical

model and done the comparison with the experimental results. Peng *et al.* [68] experimentally examined fins with the different air stream and a consistent vapour flow over a range of Reynolds number 500-5000. Dong [69] developed a correlation on the groundwork of experimental studies that were acquired by regression analysis. To find the thermal hydraulic performance of the offset strip fin NTU approach was used.

Dong in 2008 [70] provided a valuable design guidance for heat exchanger and plotted the graph between coefficient so heat transfer versus the pumping power per unit frontal area.

### **2.4.1 Liquid cooled modules**

Most of the research work performed using air as working fluid. But few works were performed using the liquid as coolants in offset Plate fin heat exchanger. The comparatively little investigation had done in the area of liquid cooled modules. For improved thermal management and heat transfer coefficients, liquid cooling is considered in this review. An experimental test performed by Robertson [71] using liquid nitrogen on offset fin at 80K with Prandtl number of 24. They added a relationship; that the boiling heat transfer coefficient works out as a function of local mass and the inlet Reynolds number. In 1980 Robertson [72] results are compared with the very similar boiling characteristics for the same test section, with Freon-11 as a test fluid under comparable flow conditions. At low Reynolds number in both water and air streams on the plate were tried by Roadman *et al.* [73]. Brinkmann [74] performed an experiment on heat transfer effect on four types of offset strip fin, using dielectric fluorocarbon with liquid coolant water. For that, the range of Prandtl number was selected in the range of 6 to 25. Whereas Hou [75] purposed the experimental study of 80 rows of fins for high Prandtl number ranges from 7 to 70 for Reynolds number between 30 to 2,700 in the fin array. The test results indicated that the Colburn and flow friction factors are different for different types of fluids. Marr [76] recommended that by adjusting the correlations of air-cooled, heat transfer to a single-phase the Prandtl numbers can be estimated. Fortunately, Marr does not present the validation between the model and experimental data. Whereas Tinaut [77] presented a validated correlation satisfactory to estimate the heat transfer and flow friction coefficients of a water cooled engine oil compact heat exchanger. LeVasseur [78] done the assessment of transferring maximum surface temperature using water flow through an SEM-E electronic module. This research reported the effect of Prandtl number on the heat exchanger, but the Prandtl number effect did not fully define because the restricted nature of the offset fin in the studies of its

performance. On taking this paper as reference Hu and Herold[79], shows the large effect of Prandtl number on the Nusselt number for liquid coolants (polyalphaole fin and water) on offset fins compact heat exchanger. They suggested a liquid coolant instead of using previous air cooled models in an experimental set up to evaluate heat transfer and pressure drop of offset fin heat exchanger. It shows that the liquid cooled apparatus Prandtl number has a large effect on Nusselt number, and numerical analysis examines the surface temperature distribution. Herold [80] identified the impact of high Prandtl number fluids. This paper demonstrates that the Colburn factor increased by increasing Prandtl number without much change in Fanning friction. Dejong [81] conducted the comparison of two different geometry offset strip and louvered fin by four methods including the investigation of mass transfer information. Peng and Ling [82, 83] have done a series of experimental studies of flow over offset strip fins implemented oil as functioning fluid at low Reynolds number.

Recently Seara *et al.* [28] represented an experimental set to show the significant heat transfer process, and pressure drop in between liquid-liquid plate-fin heat exchanger of titanium brazed offset strip fins. Correlation also developed to define the single-phase convection heat transfer coefficients to the Reynolds number as a function that validates with other experimental research.

## 2.4.2 Visualization technique

Some of the research involving distinctions based remark, expressing by the careful visual perception that involves various interactive technique for visualization like dye diffusion, smoke injection, and time exposure photography. They are the traditional methods further with the advanced technique flow visualization. The schlieren methods, hydrogen bubbles technique, stroboscopic illumination, laser sheet illumination and injection of tracers sensitive of fluid properties such as field measurement approach, temperature approach, etc are some of the methods. The first visual observation was expressed by Adarkar [84]. Loehrke [85] also emphasised on two collinear plate array in the direction of flow was visualized and trace the flow pattern using hydrogen bubbles technique. Dye employed as tracers the probe (hot-film anemometry) situated near the leading edge of the second plate whereas in [84]. Some of the effect was explained in the experiment done by CUR *et al.* [86]. With the reference of experiment of two collinear plates presented the mass transfer analogy with heat transfer in a form of a Nusselt - Reynolds - Prandtl instead of Sherwood – Reynolds – Schmidt on the basis of plate thickness and spacing between the plates and their effects on the Nusselt

number reliant on the Reynolds number. Mochizuki *et al.* [87] performed stream visualization tests for the varieties of stunned level plates and found that the stream gets to be turbulent from transient to laminar at the Reynolds number more than 50 on taking plate thickness. Loehrke *et al.* [88] watched the stream flow between interrupted plates on a channel over the arrays and the proof of this intermittent flow measured in the form of frequency and amplitude from the discharge noise of flow from a firmly stuffed array tried in the air and form a correlation. The critical velocity at the starting point at which periodic oscillation initially watched was resolved by Roadman *et al.* [73] and found that this velocity depends firmly on the thickness of the plates, plate length, and plate partition separation and pitifully on stream unsettling influence level. Zelenka *et al.* [89] measured heat transfer from two plates adjusted to the stream bearing in a wind passage. The impacts of driving edge, plate separating distance, and Reynolds number on the main and trailing plate normal warmth exchange rate were also concentrated.

Mullisenand *et al.* [90] purposed fluid flow phenomena utilizing Schlieren visualization technique with three particularly distinctive stream administrations found inside of the cores made out of in-line plates.

Although the research is on an interrupted plate, flow limited up to the low Reynolds number. Mochizuki *et al.* [91] conducted an experiment to visualise the turbulent flow intensity on the downstream region for high Reynolds number in the core and measured the pressure drop of that interrupted surfaces of three types of core plate which comprise plain straight fins, slotted fins and offset-strip fins with total 18 cores of different fin geometry. Even though the numerical investigation was performing very well the limitation or assumption due to the complexity of a compact heat exchanger made it complex. The mechanism of heat transfer of offset fins described earlier in various research papers, but the proper visualisation of isotherm using laser holographic interferometry technique shows that the offset arrangement enhances the heat transfer rate is absorber in the experiment done by Kurosaki *et al.* [92] on staggered louver arrays in 1988.

The visualization analysis, although it was not an offset fin array but compile the relation with offset fins flow visualization had been examined by Majumdar [93]. They placed thick collinear plates in the middle of a channel described streamwise precariousness that emerges in a thick boundary layer in the space between two progressive plates. Disregarding these broad accomplishments, again in 1993 Hagiwara [94] accomplished a premise investigation technique for flow visualization in a better way and the augmentation



of heat transfer leads to a higher possible Reynolds number of the drawing nearer stream to the second fin.

Brutz [95] introduced an oscillatory blades consilience forcing on the baseline to form the amplitude and frequency of the flow at the range of  $800 < Re < 1500$ . The prototype of offsetstrip fin array placed in the forepart of the oscillatory blades and visualized the flow pattern using Dye-in-water flow modules. The flow unsteadiness detected in the course of these experiments already reported to fundamentally documented to enhance heat transfer considerably (at higher Reynolds number) in unforced arrays.

## 2.5 Numerical and analytical

Kays 1972 [96] purposed an analytical model for purely laminar boundary layer flow over irregular plate surface. An investigation performed by Sparrow [97] for the laminar stream and heat transfer in channels whose dividers interfered intermittently along the streamwise heading and such diverts often utilized in superior smaller heat exchangers. These outcomes were acquired for a scope of Reynolds number and for estimations of a dimensionless geometrical parameter portraying the streamwise length  $L$  of the individual plate fragments that make up the intruded on dividers.

Sparrow *et al.* [98] anglicised and reported that for a constant fin surface area and heat transfer the effectiveness of corrugated plate is higher than in plate line channel for more circumstances whereas in the segmented schedule have a higher drop in pressure. So the paper serves the effectiveness  $\varepsilon = (T_{\Delta x} - T_i) / (T_w - T_i)$  and the pressure drop  $\Delta P / (1/2 \zeta u^2)$  by non-dimensional plate length, i.e.,  $(L/4H) / Re$  which comprises dimensions and flow rate both. Patankar [40] analysed on an interrupted plate passage on which flow pattern and heat exchanger developed by using finite difference method of heat conduction. Kays [50] suggested that the thick plate creates high-pressure drop even not increasing heat transfer ( $\varepsilon$ ) despite increasing surface area and increased mean velocity.

Susuki [99] conducted a numerical examination on the accessibility of a flat plate staggered array heat exchanger that used for extracting heat from waste heat. The performance

judgement of the heat exchanger flowfield and temperature calculated by the local Nusselt number investigated by integrating the governing differential equation of elliptic nature for superimposing convection in low Reynolds number on offset fin of zero thickness.

Heat transfer efficiency of the fin gets affected due to the presence of burrs on the edges of rear and front part of the fins that earlier correlations have not included in this part. Patankar *et al.* [40] predict the heat transfer and flow friction that occurs not accurately confirm with the experimental values due to the absence of exact information acquire by grating the information on scaled-up matrix geometries with the assumption of no burrs on the edges of fins. Whereas Webb *et al.* [56], reported the impact of burrs in the heat exchanger performance and presented the correlated results with precision.

Later on Webb *et al.* [57] predicted the friction factor on the analytical model. Moreover, on its correlation with zero thickness of offset fins they predicted the most of the data acceptably up to the accuracy of -10% at low Reynolds number and for high Reynolds numbers. Its error increases since of the formation of vortex or eddy in the wake that was not so promising in laminar flow.

K. Susuki [41] extended the work of Patankar *et al.*, which was quite a variance as its own earlier with zero thickness of fins [40] and present work which considered the thickness of fins in their results. Consequently, a test study was done along with the numerical study. Whereas Patankar *et al.* [40] compared the numerical with experimental done by Kays *et al.* [50] also with the Susuki [41] work. This accomplished for the entire heat transfer system of a two-dimension geometry of the offset-fin and established that the fin thickness is as low as possible according to the length, the shortest fin offset spacing create disturbance causing high-pressure drop but in the case of the larger draft heat exchanger it gives better performance.

Kelker [100] had done a computational examination of laminar stream and heat transfer through the channels. All the glow trade surfaces are thought to be at a uniform temperature. A parametric study made for diverse estimations of the perspective extent and the edge length parameter. Neighbourhood results were shown to give a conventional physical perception of the stream and warmth trade ponders. It also presented an examination of the numerical results with the open exploratory data.

Kelker [101] examined the fluidflow and heat transfer analysis in two dimension finned entries for steady state laminar stream. The two parallel plates shaped the entry to which blades gets connected in a corrugated manner. Both the plates are kept up at a consistent temperature. The fin geometry conductance parameter Reynolds number and the Prandtl number are the variables on which it found that the corrugated fin arrangement provides significantly heat transfer but pressure drop increases.

Joshi *et al.* [58] developed analytical models to correlate the  $j$  and  $f$  factors related to wake region in boundary layer separation of the fins. Offset fin arrays were used to anticipate the wake from transition region during the laminar to turbulent flows. Suzuki Evaluated a Numerical examination to show the illustrations of rapid eddy curves formation. Due to which velocity deformity and thermal sharing in the flow wake takes place by diverting the cold fluid with higher velocity into the wake from the mainstream, and diverting the more sweltering and lower speed liquid in the wake of the mainstream.

DeJong [102] investigated a comprehensive test and numerical results of an offset strip fin. Heat transfer and fluid flow analysis represent this complexity checks that a two-dimensional numerical recreation catches the vital components of the stream and warmth exchange for a scope of conditions. The outcomes demonstrate that the limit sheet advancement, stream detachment and reattachment, wake arrangement, and vortex shedding are exceedingly essential in this geometry.

Arash Saidi [103] considered in the middle range of Reynolds numbers at which the larger part of test examinations do not give relationships and compared the friction factor and Colburn factor with the effect of another numerical result using averaged time mean values. Secondly, heat transfer enhancement mechanism in a certain Reynolds number range is special and unique. Furthermore, it demonstrates the uniqueness among the two procedures of heat transfer and mass transfer in that scope of Reynolds numbers. Subsequently a finite volume method is utilized as a part of the computational examination.

There are some papers in the literature regarding computational fluid dynamics method presented for offset fins of plate fin heat exchanger. Subramanian [104] construct a compact heat exchanger of offset strip fin type made of a composite material of ceramic matrix to stain high temperature. The operating fluid was helium gas and liquid salt. Finite volume method is

used to yield the numerical results in the form of fluid flow and heat transfer studied in three-dimensions.

Despite all of the work in the field of offset stripfin, no work has been reported that covers the effects of height, gap, and rounded fin edges all of the previous works have only covered rectangular-fin edges and displayed the effects of channel height in dimensionless. Chen [69] explain the heat transfer and fluid flow effects of height, gap, and rounded fin edges.

Zhu *et al.* [105] established assessments of  $j$  and  $f$  factors between the four essential fins of plate fin heat exchanger namely rectangular plain fin, perforated fin, wavy fin and offset strip fin. For numerical analysis at laminar flow regime on the fluid flow and heat transfer they considered fin thickness, thermal entry effect and end effect as three-dimension. They Presented three-dimensional computational flow analysis at low Reynolds number at 132.3–1323 range and established confirmation with the experimental and analytical results. Peng *et al.* [106] conducted a sequence of experimental analyses of flow over offset strip fins by experiment and established a numerical validation for different Reynolds number and different fin geometry in various research. Ismail [107] investigated the impact of stream maldistribution on the heat exchanger execution. The alignment of inlet and outlet headers plays a major role in characterization for the same, and its computational analysis was conducted using fluent. Wang *et al.* [108], evaluated and offered a simpler numerical models of heat exchangers for serrated fin and plain fin at low Reynolds numbers via CFD code FLUENT. It assesses the  $j$  and  $f$  factors along with the heat transfer performance and pump power consumption in the two ducts. Kim [109] established simple correlations that can realistically provide  $j$  and  $f$  factors for different fluids and various geometries of offset strip fin. The existing correlation revised since earlier correlations are appropriate to a purpose of air as the working fluid; the obtained revision considered some more working fluids, specifically, air, water and diesel fuel. Additionally, the the optimal geometry of the offset strip fins is suggested based on optimization.

The recent preference work on CFD by Saad [110, 111] provided a numerical model to examine the phases and pressure drop distribution in offset stripfin units whereas the most recent work on CFD was presented by Aliabadi *et al.* [68, 112]

### **2.5.1 Optimization Technique**

Recently the work was concentrated on the prediction and optimization technique to simulate the performance of heat exchangers. Reneaume [113] used an optimisation technique to simulate the design problem of plate fin heat exchanger. The problem was a Mixed Integer Non-Linear Programming (MINLP) having different variables to solve distinctive solution approaches. The objective function such as manufacturing cost expenses reduction is greater than 10 % using Successive Quadratic Programming (SQP) algorithm techniques. Another example is the solution of the original MINLP problem using Simulated Annealing (SA) or Branch and Bound (BB) algorithms. Manish [114] in 2004 presented genetic algorithm optimization technique to optimise the multilayer type of plate fin heat exchangers. Another conventional technique solved graphically as well as through gradient search technique that compared with the genetic algorithm and found near about same results. The plan decides ideal estimations of length and width of the heat exchanger, which minimize aggregate yearly cost. The work on offset fin of plate fin heat exchanger based on genetic algorithm also performed by Xie [115] in which the objective was to reduce the volume of the heat exchanger at the rate of total annual cost. In this one more optimization was done i.e. moderate the pressure drop. As there were more than two objectives, therefore it is considered as a multi-objective problem that has elevated by considering with pressure drop and without with pressure drop. Peng *et al.* [116] utilized artificial neural networks (ANNs) to predict Colburn factor  $j$  and friction factor  $f$  with a small range of experimental data through. This predicts the thermal attributes of other fins characteristics in PFHEs under different working conditions. A single objective genetic algorithm based optimisation by Mishra [117] have applied for optimizing offset-strip of plate fin heat exchangers.

Besides, work aimed at multi-objective optimization using a genetic algorithm for offset strip developed by Sanaye [118] to obtain the maximum effectiveness and the minimum total annual cost as two objective functions and employing ANN analysis for six decision variables with acceptable precision. Amongst other evolutionary algorithms, the work on the multi-objective optimizations such as particle swarm optimization (PSO), teaching-learning-based optimization (TLBO), imperialist competitive algorithm (ICA) algorithms were used by Rao [119, 120] and Yousefi [121]. There are still numerous issues to examine for the betterment of the offset type of heat exchanger.

## **2.6. Heat Transfer and Friction Factor characteristics**

The heat transfer rate at which energy is transferring depends upon on some factors.

- Heat transfer surface area
- Volume of heat transfer material (i.e. heat capacity)
- Thermal conductivity of a material
- Temperature difference between the system and the surrounding

The heat transfer rate increases with increasing the temperature difference between the system and the surrounding but the demerit of increasing temperature difference in practical application are to do some extra work for cooling and heating of the fluid and also due to thermal stress deformation takes place that causes reduction of life of heat exchanger. If volume increases, the mass of the system increases which is not preferable. In some cases, it is desirable where the heat capacity is an essential factor, for example, regenerators. Whereas the thermal conductivity of various material do not vary. So the only substitute is to extend the surface area. On the other hand, on extending the surface area, the coefficient of friction will act on the surface and also the formation of drag force due to the finite thickness of the surfaces obstacles which is perpendicular to the direction of flow. Therefore, the enhancement of the surfaces increases both the quantities, heat transfer rate and the pressure drop due to the friction. To increase the heat transfer and to decrease the pressure drop in a plate fin type of heat exchanger fins are arranged set apart (fin spacing) in a proper manner according to their size (fin thickness, length, and height).

Correlations are developed analytically and experimentally between Friction Factor and Heat Transfer to find out the required geometrical features for the desirable flow rate of the fluid.

### **2.6.1 Heat Transfer and Friction Factor Correlations**

The performance representation of plate-fin heat exchanger is in the form of flow friction and heat transfer. Heat transfer and flow friction usually define in the form of Colburn factor  $j$  and Fanning friction factor  $f$  vs. the Reynolds number  $Re$ . While for enhanced surface  $j$  and  $f$  factor is high as compared to the plain surface. Various correlations represented the dramatical change in those factors due to the dimension and mass flow rate. The Correlations established by the researchers using analytical or experimental model are listed ahead in tabular form (Table: 2.4).

Table 2.4 Heat Transfer and Friction Factor Correlations

For  
Offset Strip Fin

Investigator(s) / Year	Reynolds No.	Correlation		Hydraulic Dia.	Base on Reference s
		Heat transfer	flow friction		
Manson [44] 1987	$\text{Re} \leq 3500$	$j = \begin{cases} 0.6(l/D_h)^{0.5} \text{Re}^{0.5}, & l/D_h \leq 3.5 \\ 0.321 \text{Re}^{0.5}, & l/D_h > 3.5 \end{cases}$	$f = \begin{cases} 11.8(l/D_h) \text{Re}^{0.24}, & l/D_h \leq 3.5 \\ 3.371 \text{Re}^{0.67}, & l/D_h > 3.5 \end{cases}$	$D_h = \frac{2sh}{s+h}$	[42, 43, 122]
	$\text{Re} > 3500$		$f = \begin{cases} 0.38(l/D_h) \text{Re}^{0.24}, & l/D_h \leq 3.5 \\ 0.1086 \text{Re}^{0.24}, & l/D_h > 3.5 \end{cases}$		
Kays [96] 1988	For Laminar boundary layer	$j = 0.665 \text{Re}^{-0.5} l$	$f = 0.44(t/l) + 1.328 \text{Re}^{-0.5} l$	$D_h = \frac{2sh}{s+h}$	Analytical model
Wieting [53] 1975	$\text{Re} \leq 1000$	$j = 0.483(l/D_h)^{-0.162} \alpha^{-0.184} \text{Re}^{-0.536}$	$f = 7.661(l/D_h)^{-0.384} \alpha^{-0.092} \text{Re}^{-0.712}$	$D_h = \frac{2sh}{s+h}$	[50, 51, 65, 122]
	$\text{Re} \geq 2000$	$j = 0.242(l/D_h)^{-0.322} (t/D_h)^{0.089} \text{Re}^{-0.368}$	$f = 1.136(l/D_h)^{-0.781} (t/D_h)^{0.534} \text{Re}^{-0.198}$		

Investigator(s) / Year	Reynolds No.	Correlation		Hydraulic Dia.	Base on Reference s
		Heat transfer	flow friction		
Joshi and Webb [58] 1987	$\text{Re} \leq \text{Re}^*$	$j = 0.53 \text{Re}^{-0.5} (l / D_h)^{-0.15} \alpha^{-0.14}$	$f = 8.12 \text{Re}^{-0.74} (l / D_h)^{-0.41} \alpha^{-0.02}$	$D_h = \frac{2(s-t)h}{[(s+h)+th/l]}$	[8, 51, 65]
	$\text{Re} \geq \text{Re}^* + 1000$	$j = 0.21 \text{Re}^{-0.40} (l / D_h)^{-0.24} (t / D_h)^{0.02}$	$f = 1.12 \text{Re}^{-0.36} (l / D_h)^{-0.65} (t / D_h)^{0.17}$		
	Where $\text{Re}^* = 257 \left( \frac{l}{s} \right)^{1.23} \left( \frac{t}{l} \right)^{0.58} D_h \left[ t + 1.328 \left( \frac{\text{Re}}{l D_h} \right)^{-0.5} \right]^{-1}$				
Mochizuki [59]	$\text{Re} \leq 2000$	$j = 1.37 (l / D_h)^{-0.25} \alpha^{-0.184} \text{Re}^{-0.67}$	$f = 5.55 (l / D_h)^{-0.32} \alpha^{-0.092} \text{Re}^{-0.67}$	$D_h = \frac{2sh}{s+h}$	[59]
	$\text{Re} \geq 2000$	$j = 1.17 (l / D_h + 3.75)^{-1} (t / D_h)^{0.089} \text{Re}^{-0.36}$	$f = 0.83 (l / D_h + 0.33)^{-0.5} (t / D_h)^{0.534} \text{Re}^{-0.20}$		
Dubrovsky and Vasiliev [60]	$\text{Re} \leq \text{Re}_{\text{lim}}$	$Nu = 0.000437 (t / D_h)^{-2.6} (l / D_h)^{-0.15} \text{Re}^x$ $where x = 2.2 (t / D_h)^{0.55} (l / D_h)^{-0.02}$	$\xi = 1.05 (t / D_h)^{-1.05} (l / D_h)^{-0.217} \text{Re}^x$ $where x = -0.277 (t / D_h)^{0.285} (l / D_h)^{0.064}$	D <sub>h</sub> not mention clearly	[123]
	$\text{Re} \geq \text{Re}_{\text{lim}}$	$Nu = 0.00723 (t / D_h)^{-1.6} (l / D_h)^{-0.9} \text{Re}^x$ $where x = 1.2 (t / D_h)^{0.34} (l / D_h)^{0.15}$	$\xi = 1.05 (t / D_h)^{-0.44} (l / D_h)^{-0.234} \text{Re}^x$ $where x = -0.0042 (t / D_h)^{-1.25} (l / D_h)^{0.39}$		
		$\text{Re}_{\text{lim}} = 3960 (t / D_h)^{0.25} (l / D_h)^{0.42}$	$\text{Re}_{\text{lim}} = 488 (t / D_h)^{-0.653} (l / D_h)^{0.09}$		



Investigator(s) / Year	Reynolds No.	Correlation		Hydraulic Dia.	Base on Reference s
		Heat transfer	flow friction		
Manglik and Bergles [64] 1985	Re < Re* (laminar flow)	$j = 0.6522 \text{ Re}^{-0.5403} \alpha^{-0.1541} \delta^{0.1499} \gamma^{-0.0678}$	$f = 9.6243 \text{ Re}^{-0.7422} \alpha^{-0.1856} \delta^{0.3053} \gamma^{-0.2659}$	$D_h = \frac{4shl}{2(sl + hl + ht) + ts}$	[8, 51, 65]
	Re > (Re* + 100) (turbulent flow)	$j = 0.2435 \text{ Re}^{-0.4063} \alpha^{-0.1037} \delta^{0.1955} \gamma^{-0.1733}$	$f = 1.8699 \text{ Re}^{-0.2993} \alpha^{-0.0936} \delta^{0.6820} \gamma^{-0.2423}$		
	Evaluate Re* same as in Joshi and Webb				
Maiti and Sarangi [124] 2002	Re ≤ Re* (laminar flow)	$j = 0.36(\text{Re})^{-0.51} (h/s)^{0.275} (l/s)^{-0.27} (t/s)^{-0.063}$	$f = 4.67(\text{Re})^{-0.70} (h/s)^{0.196} (l/s)^{-0.181} (t/s)^{-0.104}$	$D_h = \frac{2(s-t)h}{[(s+h)+th/l]}$	[8]
	Re ≥ Re* (turbulent flow)	$j = 0.18(\text{Re})^{-0.42} (h/s)^{0.288} (l/s)^{-0.184} (t/s)^{-0.05}$	$f = 0.32(\text{Re})^{-0.286} (h/s)^{0.221} (l/s)^{-0.185} (t/s)^{-0.023}$		
		$\text{Re}^* = 1568.58(h/s)^{-0.217} (l/s)^{-1.433} (t/s)^{-0.217}$	$\text{Re}^* = 648.23(h/s)^{-0.06} (l/s)^{0.1} (t/s)^{-0.196}$		

In 2011 Kim [109] has estimated the correlation on the basis of blockage ratio ( $\beta$ ) on the reference of Manglik and Bergles

$\beta < 20\%$	$j_{air} = 0.655 (\alpha)^{-0.136} (\delta)^{0.236} (\gamma)^{-0.158} (\text{Re}_{D_h})^{(0.15 \ln \text{Re}_{D_h} - 0.623)}$	$f = \exp(7.91) (\alpha)^{-0.159} (\delta)^{0.358} (\gamma)^{-0.033} (\text{Re}_{D_h})^{(0.126 \ln \text{Re}_{D_h} - 2.3)}$
$20 \leq \beta < 25\%$	$j_{air} = 1.18 (\alpha)^{-0.134} (\delta)^{0.0373} (\gamma)^{0.118} (\text{Re}_{D_h})^{(0.0445 \ln \text{Re}_{D_h} - 0.982)}$	$f = \exp(9.36) (\alpha)^{-0.0025} (\delta)^{0.0373} (\gamma)^{1.85} (\text{Re}_{D_h})^{(0.142 \ln \text{Re}_{D_h} - 2.39)}$
$25 \leq \beta < 30\%$	$j_{air} = 0.49 (\alpha)^{-0.23} (\delta)^{0.245} (\gamma)^{-0.733} (\text{Re}_{D_h})^{(0.049 \ln \text{Re}_{D_h} - 0.971)}$	$f = \exp(5.58) (\alpha)^{-0.36} (\delta)^{0.552} (\gamma)^{-0.521} (\text{Re}_{D_h})^{(0.111 \ln \text{Re}_{D_h} - 1.87)}$

$30 \leq \beta < 35\%$	$j_{air} = 0.22 (\alpha)^{-0.315} (\delta)^{0.235} (\gamma)^{-0.727} (\text{Re}_{D_h})^{(0.0313 \ln \text{Re}_{D_h} - 0.729)}$	$f = \exp(4.84) (\alpha)^{-0.48} (\delta)^{0.347} (\gamma)^{0.347} (\text{Re}_{D_h})^{(0.089 \ln \text{Re}_{D_h} - 1.49)}$
------------------------	--	--

## 2.7. Deviations from Idealized Condition

Declination of the heat exchanger performance affects its effectiveness for cryogenic applications. The most severe performance deterioration is discussed in this section. So the adverse cases that impact on the performance are

- Axial and longitudinal heat conduction
- Heat leak from or to the ambient,
- Flow maldistribution at the headers and due to manufacturing errors.
- Fluid property variation at low temperatures.

### 2.7.1 Consequence of Axial and Longitudinal Heat Conduction.

Heat conduction effects due to axial and longitudinal considered during the design of highly effective plate fin heat exchanger for the application of cryogenics.

The axial heat conduction is applied for the design of heat exchanger. The reason for the application are examined by various investigators on which Landau *et al.* [125] gave the axial heat conduction equations. Kays *et al.* 1960 [48] represent the graph showing the deterioration due to axial heat conduction and the effect is due to small temperature difference between the both fluids for balanced flow. Kroeger [126] extended the work to unbalanced and balanced flows.

Besides the axial heat conduction Kays *et al.* [48] stated the ineffectiveness due to longitudinal heat conduction by a longitudinal heat conduction parameter.

Chowdhury *et al.* [127] developed the equation to calculate the overall inefficiency. It also shows that by combining lateral resistance Kroeger [126] results can be utilized to calculate the efficiency.

Hausen [128] obtained an approximation scheme to investigate longitudinal heat conduction effect on the performance and shows the temperature declination on the graph without taking longitudinal heat conduction. Hahnemann studied the longitudinal heat conduction in a single pass counterflow heat exchanger [129] and complex expressions are presented for evaluating

the effectiveness of a heat exchanger subject to longitudinal heat conduction. Bahnke *et al.* [130] used numerical finite-difference analysis to compare their results with that of Hahnemann [129] and observed that deterioration of the heat exchanger performance is maximum when the ratio of the flow stream capacity rates is same. The numerical investigation has been done on accounting lengthwise heat conduction on different directional flow crossflow, counterflow and parallel- flow type for the different range of  $ntu$  by Chiou [131, 132]. Venkatarathnam *et al.* [133] concentrate on the longitudinal heat conduction in the outer wall to the surrounding on which less attention than the inner separating wall between two fluids. So degradation in the performance of heat exchanger is due to longitudinal heat conduction through the outer walls is not insignificant and the effectiveness varies up to  $10\pm 15\%$ . Ranganayakulu [134] investigated on the longitudinal heat conduction of plate-fin compact heat exchangers.

### **2.7.2 Effect of Heat Transfer to The Ambient**

Furthermore, heat leak from the surrounding through the wall degrade the performance of the cryogenics heat exchanger as the temperature difference between the ambient and heat exchanger is too high. So the heat leak is dramatically more as compared to the ordinary system, therefore, reviewing the longitudinal heat conduction through wall and heat leak from surrounding was investigated by the various researcher. Associated document presented for insulating the system to prevent heat interaction between the fluid and the surrounding. Wood and Kern [135] resolve a solution for longitudinal heat conduction and heat leak from surrounding to the wall unconventionally and develop governing differential equations. They clarified the needs of the design engineer and achieved a closed iterative technique to govern heat exchanger effectiveness since heat loss to the atmosphere is an inadequate assessment. Chowdhury and Sarangi [136] provide the equation for effectiveness without an iterative procedure by considering heat leak terms. Barron [137] derived the equation for two cases i.e. heat loss from the hot side to the surrounding and second is gain of heat from the surrounding to the cold side. Gupta [138] considered the degradation factor for the decline in the performance of the heat exchanger due to heat leak from surrounding and longitudinal conduction through wall by experiment. Shown in Temperature graph of hot and cold fluid flow lengthwise also considered the effect of heat capacity and heat in leak parameter on degradation. They showed the comparison between numerical results with experiment.

### 2.7.3 Effect of Flow Maldistribution

The execution disintegration of plate-fin heat exchangers because of stream mal distribution is also a genuine problem. Mueller [139] and Mueller *et al.* [139] considered different sorts of flow mal distribution in heat exchangers and discussed their reasons. The impacts of a few sorts and examples of mal distribution in heat exchangers on the exchanger heat execution explored. The examination demonstrated that a littler diminishment in execution happens in heat exchangers, with the turbulent flow than with laminar flow. A foremost experimental study on the impact of the flow arrangement on plate-fin heat exchangers has done by Jiao and R. Zhang [140]. Kitto *et al.* [141] pointed out that the two-phase flow heat exchangers still poses a formidable challenge if poor performance resulting from maldistribution of flow. Lalot and bergles [142] suggested the simple and regulated way of misdistribution and its calculation with high-quality by studying the flow distribution. Zhang [143, 144] reported the effect of flow maldistribution by using CFD simulation. A large portion of the past works predominantly concentrated on the impact of flow on consistency on heat exchanger taking into account their particular flow maldistribution model. Whereas Wen [145] utilized C.F.D method to explain the heat transfer and pressure drop in the header. He suggested, an opening to introduce baffle in the header to enhance the execution of flow appropriation. On the reference of numerical analysis [146], flow examples of the flow field in the header of plate-balance heat exchanger have been explored by a method for particle image velocimetry (PIV). Jiao *et al.* [147] perform an experiment for uniform flow distribution by applying the second header with patterns of coaxial holes in increasing order on the both side of the middle hole. The effect of the second header improves the performance of heat exchanger. Consequently, Wen *et al.* [145] placed a baffle plate in the header of three varying size of the various hole to improve the maldistribution and study the flow pattern. By this analytical approach Wen *et al.* [148] performed an experimental and numerical examination.

### 2.7.4 The effect of variable fluid properties

The properties are changing along the length as due to the absolute temperature deviation between the stream and the surrounding or between the fluid causes the occurrence of variation in fluid properties. The variation in the fluid decline the effectiveness of heat exchanger in that respect Choudhury *et al.* [136] generated the explicit expression for

variable fluid properties considered along with axial conduction. So the variation in specific heat which depends on the temperature considered on the performance of cryogenic heat exchangers.

The variation in fluid property such as local heat transfer coefficient due to the change in temperature over the length are also affected by the formation of the boundary layer. Shah [149] introduced a method to include these effects on the performance of heat exchanger having two streams. Variation of fluid properties affect temperature along with the longitudinal heat conduction has incorporated by Paffenbarger [150] using computationally intensive numeric model. Multistream heat exchanger performance also effected and illustrated the effect by them through an example.

Although there are tremendous uses of PFHX and but a very fewer work on Experimental studies performed on plate fin heat exchanger using liquid nitrogen. Previously no one focused on the performance or the effectiveness of plate fin heat exchanger using the present method of experimental studies at cryogenic temperature. This method seems to be simplest of available methods.

## **Chapter III**

# **DESIGN SPECIFICATION OF PLATE FIN HEAT EXCHANGER**

In this session, heat exchanger design or sizing problem is discussed. The predominant effect of heat exchanger size on process plant is the major problem. It was concluded that large heat exchanger size has negative influence on assessment of the equipment. So, the sizing of heat exchanger is an imperative part of design process which decides exchanger size and geometry to fulfil the required capacity for the equipment.

The most widely recognized issues in plate fin heat exchanger configuration are estimating the size and the rating. The rating issue is to evaluate the thermo-hydraulic performance of a fully specified exchanger. The rating program decides the heat transfer rate and the fluid outlet temperatures for recommended fluid flow rates, inlet temperatures, and the pressure drop for an existing heat exchanger; consequently, the heat transfer area and the dimensions of flow geometries are available. The sizing issue, on the other hand, is deal with the determination of the measurement of length of the heat exchanger. In the sizing problem, an applicable heat exchanger type is chosen and the size to meet the predefined hot and cold fluid inlet and outlet temperatures, flow rates, and pressure drop are resolved. The flow chart of design is shown schematically in Figure 3.1.

### **3.1 Brief Outline of Design Method**

In design process, Colburn and friction factor are an essential term. To find these terms, several correlations were developed on the basis of experimental data for plate fin heat exchanger. In this work, some important correlations are used to correlate data for specified heat exchanger by an equation provided by various researcher. In this chapter, few correlations are presented which had been established [45, 68,70]. Although the desired effectiveness is computed through appropriate correlations but the performance of the heat exchanger is effected by various factors such as fouling factor, longitudinal heat conduction,

heat loss to the surroundings, flow maldistribution at the headers, manufacturing irregularities etc. Among these factors, some have not much effected on the gas to gas type of Plate fin heat exchanger. It is required to consider the longitudinal heat conduction which have predominant effect on the effectiveness of cryogenics heat exchanger. In general, longitudinal heat conduction is neglected in some conventional heat exchanger. Kroeger [126] proposed the equation for correct prediction of performance for Plate fin heat exchanger.

The step-by-step procedure to design the heat exchanger are provided. The parameters of PFHX is designed for low pressure [1]. At low temperature, selection of heat exchanger depends upon the inlets temperatures of hot and cold sides. Even though there is a significant change in temperature but the fluid is in single phase during the flow due to which density does not differ significantly throughout the length. So, for approximate analysis mean temperature was used to evaluate the properties. The procedures of design are as follows [1].

1. To compute the outlet temperatures of cold and hot fluids designed for the estimated effectiveness, the following equations have been used.

$$T_{co} = T_{ci} + \varepsilon (T_{hi} - T_{ci}) \quad 3.1$$

$$T_{ho} \approx T_{hi} - \varepsilon \frac{cp, c \times \dot{m}_c}{cp, h \times \dot{m}_h} (T_{hi} - T_{ci}) \quad 3.2$$

2. Evaluate the properties from the mean temperature using equation (3.3) and (3.4) and iterate the value of  $T_{ho}$ .

$$T_{cm} = \frac{(T_{ci} + T_{co})}{2} \quad 3.3$$

$$T_{hm} = \frac{(T_{hi} + T_{ho})}{2} \quad 3.4$$



3. To improve the value of  $T_{ho}$ , optimize the specific heat of hot gas up to the insignificant variation in specific heat to the previous evaluated values obtained from mean temperature of hot gas. Again calculate  $T_{hm}$  from the improved value of  $T_{ho}$ .
4. The fluid properties at mean temperatures are evaluated for cold and hot gas.

	Hot Gas	Cold Gas
$\mu$	$Pa.s$	$Pa.s$
$c_p$	$kJ / kg.k$	$kJ / kg.k$
Pr	-----	-----
$\rho$	$kg / m^3$	$kg / m^3$

5. Calculate the NTU from given equation.

$$NTU = \frac{1}{1-c^*} \ln \frac{1-c^* \varepsilon}{1-\varepsilon} \quad 3.5$$

Where

$$c^* = \frac{c_{\min}}{c_{\max}}$$

Such that  $c_{\min} = c_c$  &  $c_{\max} = c_h$  if  $c_h > c_c$  else  $c_{\max} = c_c$  &  $c_{\min} = c_h$

In which  $c_c = (\dot{m}c_p)_c$  and  $c_h = (\dot{m}c_p)_h$

6. Calculation of heat transfer area from the specified geometry.

Fin spacing,  $s$  (excluding the fin thickness)  $= \left( \frac{1-f \times t}{f} \right) \quad 3.6$

Free flow area to frontal area ratio,

$$\sigma = a_{ff} / a_{fr} = \frac{s \times (h - t)}{(h + t)(s + t)} \quad 3.7$$

Heat transfer area / fin,

$$a_s = 2hl + 2ht + 2sl \quad 3.8$$

Ratio of fin area to heat transfer area,

$$\frac{2h(l + t)}{2(hl + sl + ht)} \quad 3.9$$

7. Equivalent diameters obtained from different correlations [3.10 (a), (b), (c)]

Equivalent Diameter,

$$D_e = \frac{(4 \times \text{Free flow area} \times \text{length})}{\text{heat transfer area}} \quad 3.10$$

Joshi and Webb,

$$D_h = \frac{2(s - t)h}{[(s + h) + th / l]} \quad (a)$$

Manglik and Bergles,

$$D_h = \frac{4shl}{2(sl + hl + ht) + ts} \quad (b)$$

Maiti and Sarangi,

$$D_h = \frac{2(s - t)h}{[(s + h) + th / l]} \quad (c)$$

Distance between plates,

$$b = h + t \quad 3.11$$

8. Calculation for heat transfer area,

Total area between plates,

$$A_{frh} = b \times N_h \times W \quad 3.12$$

Total free flow area,  $A_{ffh} = \sigma \times A_{frh}$  3.13

Wall conduction area on hot side,  $a_{wh} = A_{frh} - A_{ffh}$  3.14

Total heat transfer area,  $A_h = \frac{4 \times A_{ffh} \times L}{D_e}$  3.15

9. calculate core mass velocity,  $G = \frac{m}{A_{ff}}$  3.16

10. Reynolds number,  $Re = \frac{GD_e}{\mu}$  3.17

11. Evaluate Reynolds number for laminar and turbulent boundary regimes and analyze j and f factor for the fluid from Table 3.1 to 3.3.

Table 3.1 Joshi and Webb correlation

Reynolds No.	Correlation	
	Heat transfer	flow friction
$Re \leq Re^*$	$j = 0.53 Re^{-0.5} (l / D_h)^{-0.15} \alpha^{-0.14}$	$f = 8.12 Re^{-0.74} (l / D_h)^{-0.41} \alpha^{-0.02}$
$Re \geq Re^* + 1000$	$j = 0.21 Re^{-0.40} (l / D_h)^{-0.24} (t / D_h)^{0.02}$	$f = 1.12 Re^{-0.36} (l / D_h)^{-0.65} (t / D_h)^{0.17}$
Where $Re^* = 257 \left( \frac{l}{s} \right)^{1.23} \left( \frac{t}{l} \right)^{0.58} D_h \left[ t + 1.328 \left( \frac{Re}{l D_h} \right)^{-0.5} \right]^{-1}$		

Table 3.2 Manglik and Bergles correlation

Reynolds No.	Correlation	
	Heat transfer	flow friction
Re < Re* (laminar flow)	$j = 0.6522 \text{ Re}^{-0.5403} \alpha^{-0.1541} \delta^{0.1499} \gamma^{-0.0678}$	$f = 9.6243 \text{ Re}^{-0.7422} \alpha^{-0.1856} \delta^{0.3053} \gamma^{-0.2659}$
Re > (Re* + 1000) (turbulent flow)	$j = 0.2435 \text{ Re}^{-0.4063} \alpha^{-0.1037} \delta^{0.1955} \gamma^{-0.1733}$	$f = 1.8699 \text{ Re}^{-0.2993} \alpha^{-0.0936} \delta^{0.6820} \gamma^{-0.2423}$
Where $\text{Re}^* = 257 \left( \frac{l}{s} \right)^{1.23} \left( \frac{t}{l} \right)^{0.58} D_h \left[ t + 1.328 \left( \frac{\text{Re}}{l D_h} \right)^{-0.5} \right]^{-1}$		

Table 3.3 Maiti and Sarangi correlation

Reynolds No.	Correlation	
	Heat transfer	flow friction
Re < Re* (laminar flow)	$j = 0.36(\text{Re})^{-0.51} (h/s)^{0.275} (l/s)^{-0.27} (t/s)^{-0.063}$	$f = 4.67(\text{Re})^{-0.70} (h/s)^{0.196} (l/s)^{-0.181} (t/s)^{-0.104}$
Re > Re* (turbulent flow)	$j = 0.18(\text{Re})^{-0.42} (h/s)^{0.288} (l/s)^{-0.184} (t/s)^{-0.05}$	$f = 0.32(\text{Re})^{-0.286} (h/s)^{0.221} (l/s)^{-0.185} (t/s)^{-0.023}$
Where	$\text{Re}^* = 1568.58(h/s)^{-0.217} (l/s)^{-1.433} (t/s)^{-0.217}$	$\text{Re}^* = 648.23(h/s)^{-0.06} (l/s)^{0.1} (t/s)^{-0.196}$

12. Compute heat transfer coefficient,

$$h_c = \frac{(j_c \times C_p \times G_c)}{(\text{Pr})^{0.667}} \quad 3.18$$

13. Fin parameter,

$$M = \sqrt{\frac{(2 \times h_c)}{(K_f \times t)}} \quad 3.19$$

14. Calculate fin effectiveness,  $\eta_f = \frac{\tanh(Ml_e)}{(Ml_e)}$  3.20

15. Overall effectiveness, (Where  $\eta_{fo}$  is efficiency of inner fin [126]).  $\eta_{fo}$  is the same equation as equation 3.20 with  $l_e$  replaced by  $l_e/2$ .

$$\eta_o = 1 - \left[ \left( \frac{a_f}{a_s} \right) \times (1 - \eta_f) \times \frac{(N_p - 2)}{N_p} \right] - \left[ \left( \frac{a_f}{a_s} \right) \times (1 - \eta_{fo}) \times \left( \frac{2}{N_p} \right) \right] \quad 3.21$$

16. Determine overall heat transfer coefficient (U) on each side of fluid flow putting values obtained from eqn. (3.18) to (3.21).

$$\frac{1}{(U_o A_o)} = \frac{1}{\eta_{oh} h_h A_h} + \frac{a}{K_w A_w} + \frac{1}{\eta_{oc} h_c A_c} \quad 3.22$$

17. Considering the value of NTU from eqn. (3.5). Compute the  $U_o A_o$  which is calculated for core mass velocity.

$$U_o A_o = NTU * c_{\min} \quad 3.23$$

18. Equate eqn. (3.23) and (3.22) to calculate heat transfer area.

$$U_o A_o = U_1 A_1 = U_2 A_2 \quad 3.24$$

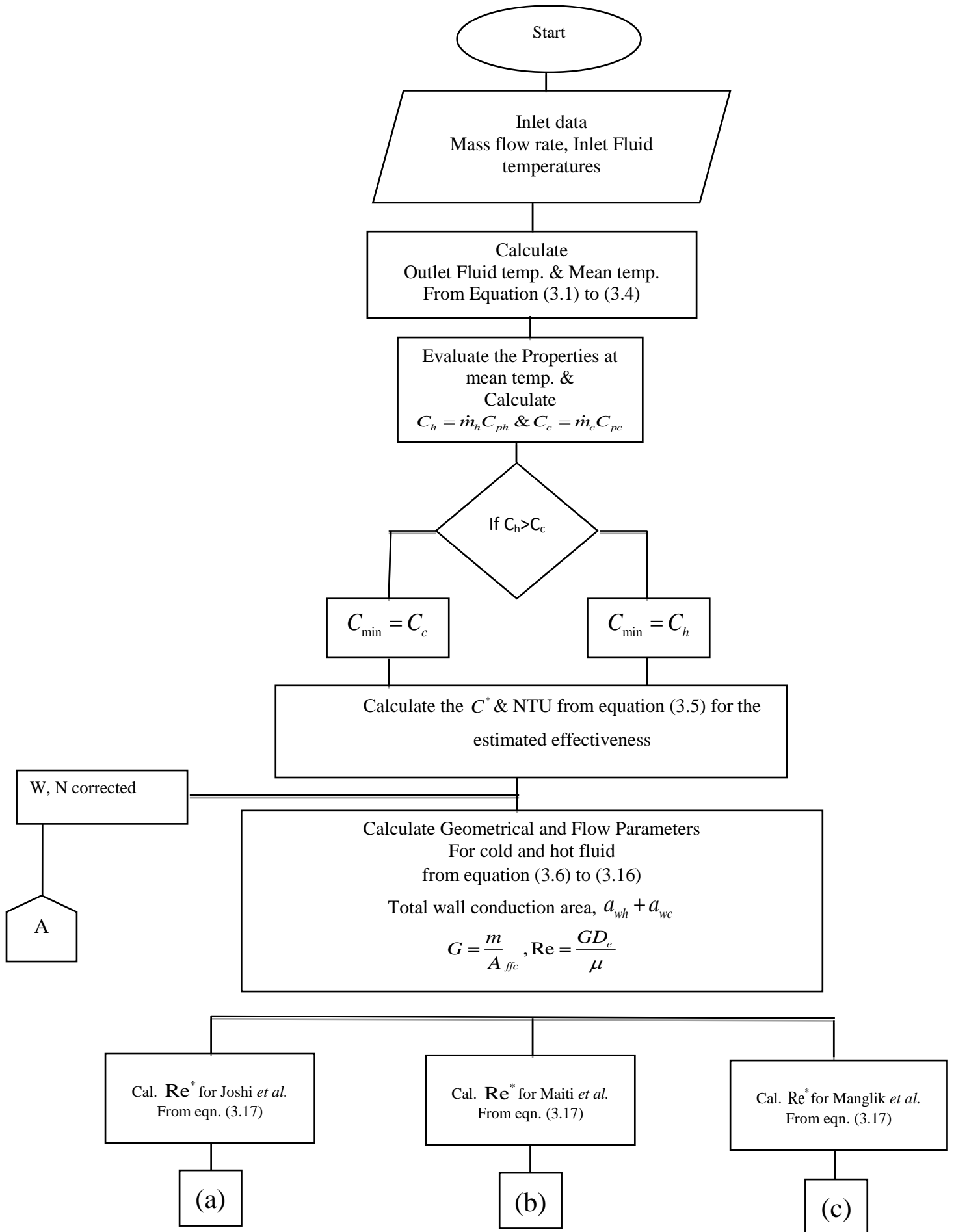
19. Obtained the required length of heat exchanger from hydraulic diameter.

$$L = \frac{D_o A_o}{4 A_{ff}} \quad 3.25$$

$$\therefore D_o = \frac{(4 \times \text{Free flow area} \times \text{length})}{\text{heat transfer area}}$$

20. Determine the pressure drop on the fluid side, using standard f factors.

21. Optimized the fin geometry on the basis of pressure drop.



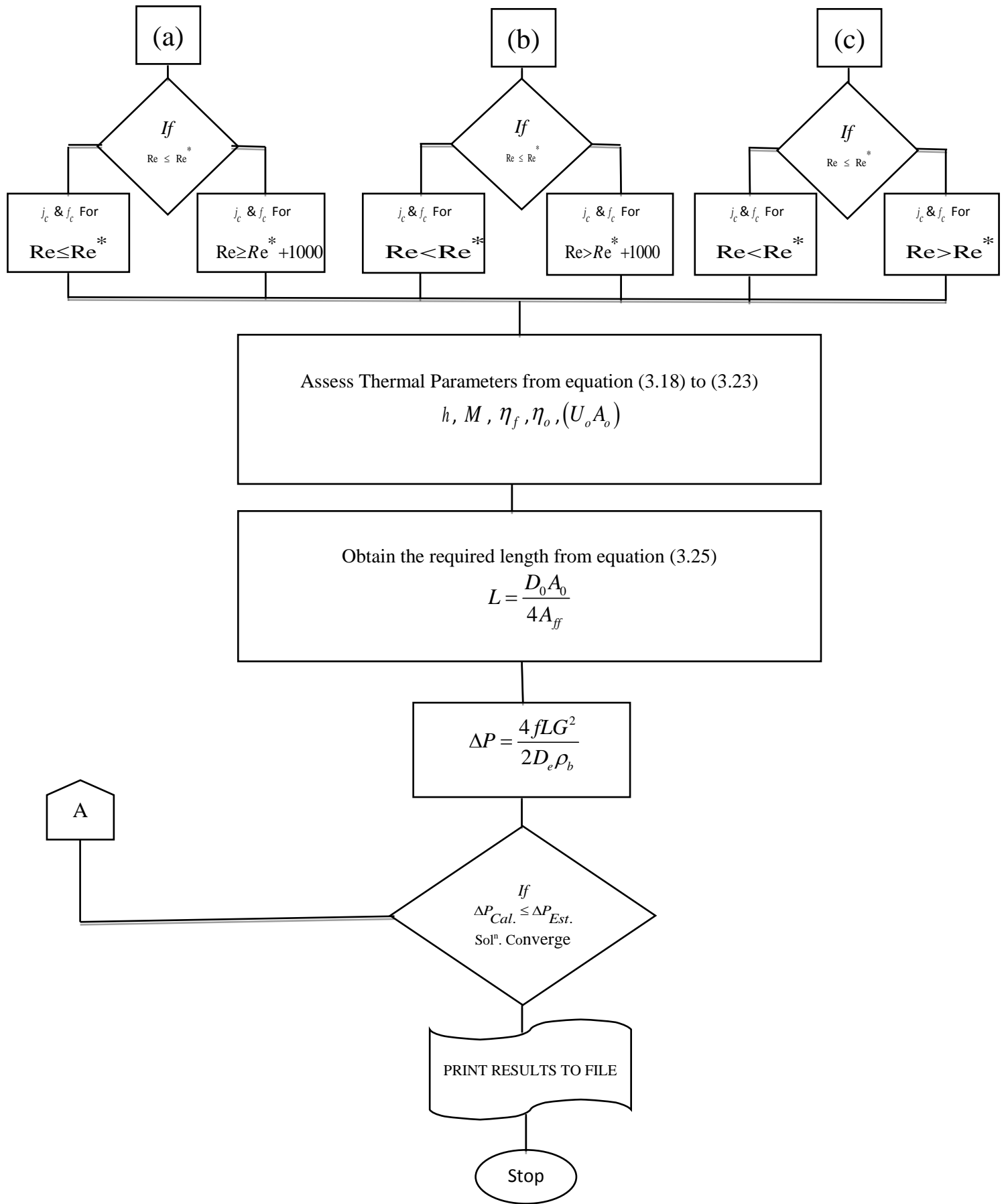


Figure 3.1 Flow diagram to optimize the Plate fin heat exchanger geometry using iterative design process for desired effectiveness

## 3.2 Specification of Fin Geometry and Input Parameters

The performance assessment of plate fin heat exchanger depends upon its selection criteria. In this section, the systematic procedure for design of heat exchanger is specified as follows.

### 1. Conclude the surface geometrical parameters

Figure 3.2 demonstrates a diagram of a general counter flow offset plate fin heat exchanger strip. Figure 3.3 represents the geometry in which the structure parameters are fin spacing ( $s$ ), fin height ( $h$ ), fin thickness ( $t$ ), and fin length ( $l$ ) for offset strip of plate fin heat exchanger. The dimensionless terms incorporate as:

$$a = s/h, d = t/l \text{ and } c = t/s$$

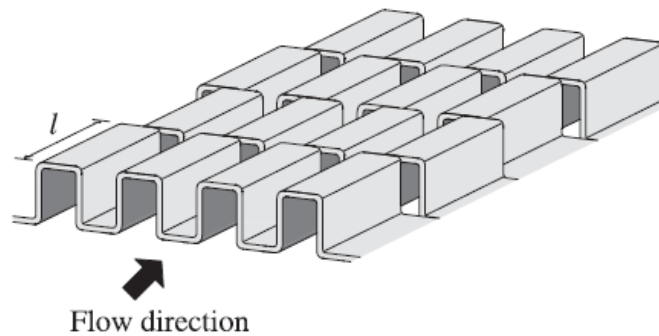


Figure 3.2 Counter flow offset plate fin heat exchanger strip

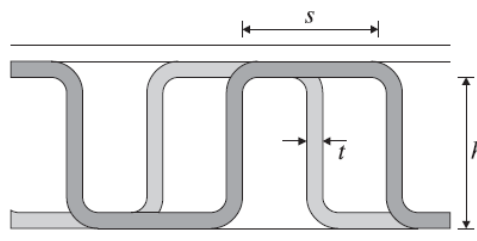


Figure 3.3 Geometrical of strip fin



Table 3.4 Fin geometry used in heat exchanger

FIN GEOMETRY	H.P SIDE (Hot Fluid)	L.P SIDE (Cold Fluid)
Fin Type	Serrated	Serrated
Fin frequency, f	714 fins /meter	588 fins/ meter
Fin length, l	3 mm	5 mm
Fin thickness, t	0.2 mm	0.2 mm
Fin height, h	9.3 mm	9.3 mm
No. of layers	5	4

2. Dimensions associated with the preferred fin geometry. Some associated dimensions are calculated from equation 3.6 to 3.11.

3. Calculation of heat exchanger dimensions,

i) Width of the core,  $W = 73$  mm

ii) Total Number of layers,  $N = 9$ .

4. Fluid flow parameters.

Table 3.5 Specified Input Data for Plate Fin Heat Exchanger used for LN2 plant

Fluid Flow Parameter	H.P SIDE (Hot gas)	L.P SIDE (Cold gas)
Mass flow rate (kg/s)	0.0822	0.07791
Inlet pressure (bar)	8	1.15
Fluid inlet temp. (K)	310	99.716
Fluid outlet temp. (K)	124.26	301.54
Allowable pressure drop (bar)	0.05	0.05

Note:- Estimated Design Effectiveness  $\geq 0.95$

Table 3.6 Effective properties at mean temperature

Fluid Properties	Hot fluid at mean temprature	cold fluid at mean temprature
Sp. Heat ( $C_p$ ) (J/kg-K)	1043	1043
Viscosity( $\mu$ ) (N/m <sup>2</sup> -s)	0.0000134	0.00001295
Peclet number	0.74767	0.75
Density (kg/m <sup>3</sup> )	1.583	1.711

Table 3.7 Flow configurations for both sides of counter flow

Heat transfer area	Hot side (m <sup>2</sup> )	Cold side (m <sup>2</sup> )
Total area between plates	$A_{frh} = 0.0035$	$A_{frc} = 0.0028$
Total free flow area	$A_{ffh} = 0.0024$	$A_{ffc} = 0.0021$
Wall conduction area on hot side	$a_{wh} = 0.0010$	$a_{wc} = 0.00069$

### 3.3 Design Correlations of Heat Exchanger

The concluded design parameters obtained by logical reasoning using correlation developed by Joshi *et al.*, Maity *et al.*, Manglik *et al.* and simulation using Aspen-Muse<sup>®</sup> are represented. Design parameters of offset fin based on previous correlations presented in a tabular form as shown in Table 3.4. The proposed design methods for the selection of heat exchanger dimensions were developed analytically using Matlab<sup>®</sup>. The relationship between the variables to find the heat transfer and flow friction with respect to Reynolds number is established by the investigator.

Joshi *et al.* [58] developed an analytical model to correlate the  $j$  and  $f$  factors related to wake region in boundary layer separation of the fins. The offset fin arrays were used to anticipate the wake during the transition regions from laminar to turbulent flows. The equation of

Reynolds number for the wake width, i.e. the transition Reynolds number, was formulated and then  $j$  and  $f$  factors correlations for the laminar and turbulent flow was given to visualize the flow patterns in the fin wake to analyses the stress on transition.

The correlations given by Joshi and Webb shown in Table 3.1 provides the friction factor,  $f$  and Colburn factor,  $j$ . Table 3.1 also represents the critical Reynolds number on which the correlations of  $j$  and  $f$  factor depends upon. The hydraulic diameter considers for calculating  $j$  and  $f$  factor are given in equation 3.10 (a)

Manglik *et al.* [64] choose an experimental data of 18 offset plate fin surfaces from Kays *et al.* [8], London *et al.* [51] and Waiters [65]. Table 3.2 provides the correlation developed by Manglik *et al.* taking critical Reynolds number into account. The equation for hydraulic diameter is given in Eqn. 3.10 (b). Maiti *et al.* [124] used CFD simulation for developing conceptual correlation for  $j$  and  $f$  factors detailed in Table 3.3.

Experimental study is performed and a couple of readings are taken which is applied to form a wide range of data by comparing its result with the CFD model and form a trend to develop correlations. In this author used finite volume method by applying PHOTON computational software to generate the data for plate fin heat exchanger [124]. The correlation developed by the Maiti *et al.* shown in table 3.3 gives the critical Reynolds number separately for heat transfer and pressure drop and the hydraulic diameter for this case is given in Eqn. 3.10 (c). Table 3.8 represents the calculated design parameters based on these correlations.

Table 3.8 Design parameters based on correlations

Unknown Variable		Joshi and Webb	Manglik and Bergles	Maiti and Sarangi
G (kg/s-m <sup>2</sup> )	Hot Gas	2.0618	2.0618	2.0618
	Cold Gas	2.4170	2.4170	2.4170
Re <sup>*</sup>	Hot Gas	226.0105	270.2149	226.0105
	Cold Gas	344.7136	398.4808	344.7136
j	Hot Gas	0.0463	0.0346	0.0348
	Cold Gas	0.0349	0.0258	0.0247
f	Hot Gas	0.1206	0.1557	0.1602
	Cold Gas	0.0783	0.1014	0.1106
h (W/m <sup>2</sup> -K)	Hot Gas	649.95	486.5900	489.1776
	Cold Gas	574.7013	424.5993	406.8329
M (m <sup>-1</sup> )	Hot Gas	208.1588	180.1092	180.5875
	Cold Gas	195.7381	168.2457	169.6882
η	Hot Gas	0.6913	0.7375	0.7366
	Cold Gas	0.6950	0.7423	0.7487
U <sub>o</sub> A <sub>o</sub> (W/K)	Hot Gas	168.7144	136.5704	131.0826
	Cold Gas	238.2437	185.4332	181.6910
L (m)	Hot Gas	0.9078	1.3540	1.1325
	Cold Gas	0.9504	1.4115	1.2462
ΔP (Pa)	Hot Gas	1.9808e+003	2.0775e+003	3.2825e+003
	Cold Gas	1.0716e+003	3.3250e+003	1.5137e+003

### 3.4 Simulation Software for Design of Heat Exchanger

Thermal design of Plate fin heat exchanger using Simulation software:

Aspen – muse<sup>®</sup> has been used to design the plate fin heat exchanger to calculate the geometrical parameters. It supports the operation technique based on properite correlations. During design process, various losses was considered which was imposed due to longitudinal heat conduction and others.

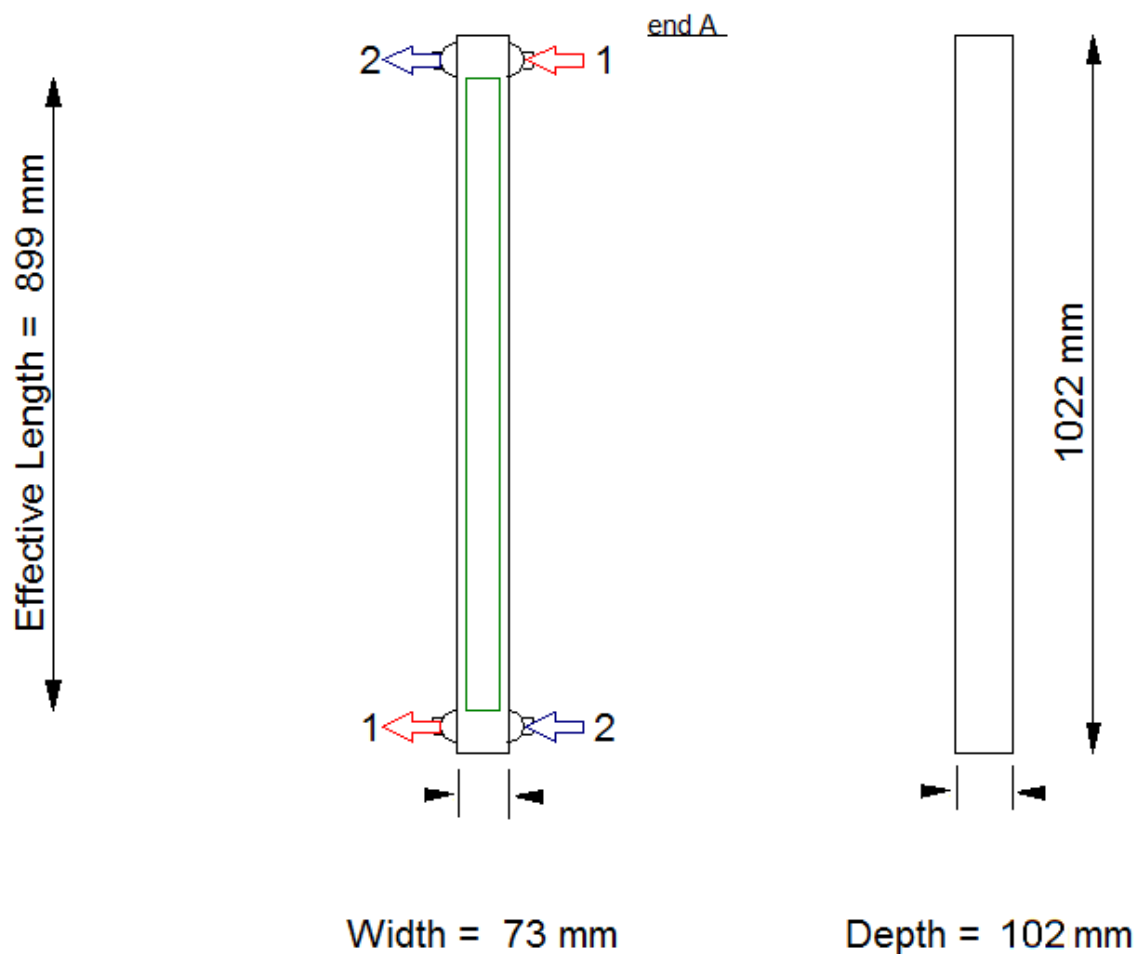


Figure 3.4 Dimensions of Plate fin heat exchanger using simulation software

### 3.5 Specification of Heat Exchanger Dimensions

The purpose of this design was to assess the dimension based on the calculated dimensions which are justified by considering various correlations and simulation. The presented dimension in Table 3.9 shows the core dimensions and total dimensions of the plate fin heat exchanger.

Table 3.9 Interior and total size of the plate fin heat exchanger

S.No.	Core Design size	Dimensions (mm)	Total Design size	Dimensions (mm)
1.	Core Width	73	Total Length	1000
2.	Core Height	93	Total Width	85
3.	Core length	900	Total Height	105

The experimental and the analytical review (Rating problem) includes the concluded dimensions for the evaluation of effectiveness of offset fins.

## Chapter IV

# RATING OF PLATE FIN HEAT EXCHANGER

In this section, rating problem of the heat exchanger was discussed. Moreover, the rating of heat exchanger determines the effectiveness of heat exchanger. The performance of a heat exchanger depends on effectiveness. It calculates the outlet temperatures of heat exchanger and computing outlet temperature is an iterative process until the outlet temperature converges. So, the sizing and rating of a heat exchanger are important because its effectiveness is directly proportional to the effective performance of the equipment.

The rating issue is assessing the thermo-hydraulic performance of a completely designated exchanger. "Rating" is the computational procedure in which the channel stream flow rates and temperatures at the inlet, thermodynamic properties of the fluid, heat exchanger measurement are taken as a factor and temperatures at outlets are to be found. The effectiveness associated with the heat transfer coefficient through correlations developed by the researchers by performing different sets of the experiment. Initially, use the pre-estimated effectiveness to find the actual effectiveness, outlet temperatures and the average fluid temperatures. Since, the outlet temperatures are not given in the rating problem therefore hypothetical value of effectiveness was taken from the previous research practices [1].

The rating issue specified the present Plate fin heat exchanger to fulfill the heat transfer load under the limited pressure drop.

Brief outline of rating process of Plate Fin Heat Exchanger:

- Evaluate the mean temperature for both side of fluid flow and estimate the mean bulk temperature.
- Determine the properties from Refprop at mean temperature for each side of fluid.
- Specify heat exchanger input parameter.
- Calculate the heat transfer area.
- Calculate Reynolds number, heat transfer coefficient and Colburn factor (j).
- Determine NTU and effectiveness.

- Compute the outlet temperatures of hot and cold fluid.
- Determine the pressure drop and friction factor (f) for both the sides.

## 4.1 Specified Heat Exchanger and Input Parameter

The detail evaluation processes for calculating unknown parameters are given. Generally, rating problems have the following criteria as referred in Table 4.1.

Table 4.1 Rating Process

Data	Rating Method
Specified data	Length, Width, and Height
Inlet data	Mass flow rate, Fluid temperatures
Output data	Thermal duty

Whereas in design problem the main objective is to find out the block size as mentioned in Table 4.2.

Table 4.2 Design Process

Data	Rating Method
Specified data	Thermal duty
Inlet data	Mass flow rate, Fluid temperatures
Output data	Length, Width, and Height

The detail specifications of plate fin heat exchanger are given in Table [4.3, 4.4, 4.3] represents the core dimensions including the thickness of separating plate, end plate and end bar. Table [4.4] represents the dimensions of the fin geometry of the core.

Table 4.3 Size of the offset Plate Fin Heat Exchanger interior

ITEM NO.	ITEM DISCRIPTION	SIZE IN MM	QUANTITY IN NOS
1.	Edge bar	9.5x6x79	18
2.	Side bar	9.5x6x950	18
3.	Offset serrated fin	9.5Hx73Wx900L	4/5
4.	Separating sheet	105Wx900Lx0.8THK	10
5.	End plate	105Wx900Lx6THK	2



Table 4.4 Core size of a Plate Fin Heat Exchanger

S.No.	Design size	Dimensions in mm
1.	Core width	73
2.	Core height	93
3.	Core length	900

The detail dimension of geometry of a fin and the fin frequency of serrated fin is given in Table 4.5

Table 4.5 Dimensions of Fin Geometry

FIN GEOMETRY	H.P SIDE (Hot Fluid)	L.P SIDE (Cold Fluid)
Fin Type	Serrated	Serrated
Fin frequency (f)	714 fins /meter	588 fins/ meter
Fin length (l)	3 mm	5 mm
Fin thickness (t)	0.2 mm	0.2 mm
Fin height (h)	9.3 mm	9.3 mm
No. of layers	5	4

## 4.2 Rating of Specified Heat Exchanger Through Different Correlations.

Different correlations are used for rating to determine the effectiveness and pressure drop for specified mass flow rate and inlet temperatures at the cold and hot ends. In order to find out the effectiveness and pressure drop, other responses are also drawn out from the rating analysis from the available variables and constants. The analytical examination of plate fin heat exchanger uses three different correlations developed by Joshi *et al.*, Maity *et al.* and Manglik *et al.* in the present assessment. The rating problem uses a similar formulation as in sizing problem to find the output data from specified data and input data. The only difference is that it draws out the specified data (Length, Width and Height) from the design (chapter-3) and determines the effectiveness and pressure drop. The step of finding the responses is summarized below.

### 4.2.1 Performance Evaluation Using the Correlation of Maiti and Sarangi

Table 4.6 Input values of Plate Fin Heat Exchanger

Inlet	Temperature (K)	Pressure (Bar)	Mass flow rate (g/s)
Hot	307.5	1.05	6.029
Cold	107.8	1.037	6.029

1. First compute the outlet temperatures of cold and hot fluid which is designed for the estimated effectiveness i.e. 95% using the following equation.

$$T_{c,o} = T_{c,i} + \varepsilon (T_{h,i} - T_{c,i}) \quad 4.1$$

$$T_{h,o} \approx T_{h,i} - \varepsilon \frac{\dot{m}_c}{\dot{m}_h} (T_{h,i} - T_{c,i}) \quad 4.2$$

Since the mass flow rate is same therefore by evaluating the above equation

$$T_{c,o} = 291.508 \text{ and } T_{h,o} = 123.592$$

2. Evaluate the properties from the mean temperature using equation (3) and (4)

$$T_{c,m} = \frac{(T_{c,i} + T_{c,o})}{2} \quad 4.3$$

$$T_{h,m} = \frac{(T_{h,i} + T_{h,o})}{2} \quad 4.4$$

Therefore, the mean temperature on each side of fluid.

$$T_{c,m} = 199.55 \text{ and } T_{h,m} = 215.54$$

3. The fluid properties of Nitrogen at these mean temperatures are evaluated for cold and hot gas.

Table 4.7 Fluid properties of hot and cold gas

	Hot Gas	Cold Gas
$\mu$	0.00001374 Pa-s	0.00001289 Pa-s
$c_p$	1042.9 J / kg.k	1043.6 J / kg.k
Pr	0.7331	0.7371
$\rho$	1.644 kg / m <sup>3</sup>	1.7548 kg / m <sup>3</sup>

4. Calculation for heat transfer area from the selected geometry

Fin spacing,  $s$  (excluding the fin thickness)  $= \left( \frac{1-f \times t}{f} \right)$  4.5

Free flow area to frontal area ratio,  $\sigma = a_{ff} / a_{fr} = \frac{s \times (h-t)}{(h+t)(s+t)}$  4.6

Heat transfer area / fin,  $a_s = 2hl + 2ht + 2sl$  4.7

Ratio of fin area to heat transfer area of fin,  $\frac{2h(l+t)}{2(hl + sl + ht)}$  4.8

Equivalent Diameter,	$D_e = \frac{(4 \times \text{Free flow area} \times \text{length})}{\text{heat transfer area}}$	4.9
----------------------	---	-----

Maiti and Sarangi,	$D_h = \frac{2(s-t)h}{[(s+h)+th/l]}$	4.10
--------------------	--------------------------------------	------

Distance between plates,	$b = h + t$	4.11
--------------------------	-------------	------

Heat transfer area,

Total area between plates,	$A_{frh} = b \times N_h \times W$	4.12
----------------------------	-----------------------------------	------

Total free flow area,	$A_{ffh} = \sigma \times A_{frh}$	4.13
-----------------------	-----------------------------------	------

Wall conduction area on hot side,	$a_{wh} = A_{frh} - A_{ffh}$	4.14
-----------------------------------	------------------------------	------

Total heat transfer area,	$A_h = \frac{4 \times A_{ffh} \times L}{D_e}$	4.15
---------------------------	---	------

The evaluated values Heat transfer area from equation 4.5 to 4.14

Table 4.8 Fluid flow Parameter of hot and cold gas

Parameters	High pressure side	Low pressure side
Fin spacing, s (m)	0.001201	0.001501
Free flow area to frontal area ratio	0.69936	0.748699
Heat transfer area / fin (m <sup>2</sup> /fin)	0.00006672	0.000112
Ratio of fin area to heat transfer area of fin	0.892041	0.865683
Equivalent Diameter (m)	0.001674	0.002165
Distance between plates (m)	0.0095	0.0095

Table 4.9 Heat transfer area (m<sup>2</sup>)

	High pressure side	Low pressure side
Total area between plates	0.003468	0.002774
Total free flow area,	0.002425	0.002077
Wall conduction area on hot side	0.001042	0.000697
Total heat transfer area	5.216633	3.452948

Total wall conduction area of the fin is obtained from the calculation is 0.00174 m<sup>2</sup>.

5. Calculate core mass velocity,  $G = \frac{m}{A_{ff}}$  4.16

6. Reynolds number,  $Re = \frac{GD_e}{\mu}$  4.17

Evaluate Reynolds number for laminar and turbulent boundary regimes

7. Analyze j and f factor for the fluid obtained from the Reynolds number

Various correlations presented in the literature which emphasize on the performance of heat exchanger on the basis of Colburn factor and Friction factor. Here we use only three out of them to find out j and f factor. The first one is Maiti *et al.* correlation.

Table 4.10 Maiti and Sarangi correlation

Reynolds No.	Correlation	
	Heat transfer	flow friction
Re < Re* (laminar flow)	$j = 0.36(\text{Re})^{-0.51}(h/s)^{0.275}(l/s)^{-0.27}(t/s)^{-0.063}$	$f = 4.67(\text{Re})^{-0.70}(h/s)^{0.196}(l/s)^{-0.181}(t/s)^{-0.104}$
Re > Re* (turbulent flow)	$j = 0.18(\text{Re})^{-0.42}(h/s)^{0.288}(l/s)^{-0.184}(t/s)^{-0.05}$	$f = 0.32(\text{Re})^{-0.286}(h/s)^{0.221}(l/s)^{-0.185}(t/s)^{-0.023}$
Where	$\text{Re}^* = 1568.58(h/s)^{-0.217}(l/s)^{-1.433}(t/s)^{-0.217}$	$\text{Re}^* = 648.23(h/s)^{-0.06}(l/s)^{0.1}(t/s)^{-0.196}$

8. Compute overall heat transfer coefficient

$$h_c = \frac{(j_c \times C_p \times G_c)}{(\text{Pr})^{0.667}} \quad 4.18$$

9. Fin parameter,

$$M = \sqrt{\frac{(2 \times h_c)}{(K_f \times t)}} \quad 4.19$$

10. Calculate fin effectiveness,

$$\eta_f = \frac{\tanh(Ml_e)}{(Ml_e)} \quad 4.20$$

11. Overall effectiveness,

$$\eta_o = 1 - \left[ \left( \frac{a_f}{a_s} \right) \times (1 - \eta_f) \times \frac{(N_p - 2)}{N_p} \right] - \left[ \left( \frac{a_f}{a_s} \right) \times (1 - \eta_{fo}) \times \left( \frac{2}{N_p} \right) \right] \quad 4.21$$

Table 4.11 Heat transfer coefficient and effectiveness

Parameters	High pressure side	Low pressure side
core mass velocity, G	2.49	2.90
Reynolds number, Re	302.98	487.53
heat transfer coefficient	95.63	74.43
core mass velocity,	75.00	66.16
Overall effectiveness, $\eta_{oh}$	0.964081	0.935129

12. Determine U on each side of fluid flow putting values obtained from equation (4.18) to (4.21)

$$\frac{1}{U_o A_o} = \frac{1}{\eta_{oh} h_h A_h} + \frac{a}{K_w A_w} + \frac{1}{\eta_{oc} h_c A_c} \quad 4.22$$

13. Considering the value of NTU from equation (4.5). Compute the  $U_o A_o$  using equation.

calculate core mass velocity,  $NTU = \frac{U_o A_o}{c_{\min}} \quad 4.23$

14. Equate equation (4.23) and (4.22) to calculate heat transfer area.

15. Effectiveness with heat conduction along the axial direction.

It is necessary to consider the longitudinal heat conduction which has predominant effect on the effectiveness for high-effectiveness cryogenics heat exchanger. In general, longitudinal heat conduction is neglected in convention heat exchanger. Hence for the same Kroeger [126] prescribe the equation on the effectiveness for the

correct prediction of performance. The expressions by Kroeger for ineffectiveness are given as.

Ineffectiveness,

$$i = \frac{1 - \frac{C_{\min}}{C_{\max}}}{\psi e^{r_1} - \frac{C_{\min}}{C_{\max}}} \quad 4.24$$

Where

$$r_1 = 1 - \left( \frac{C_{\min}}{C_{\max}} \right) \frac{NTU}{1 + \lambda \times NTU \left( \frac{C_{\min}}{C_{\max}} \right)} \quad \text{and} \quad \psi = \frac{1 + \gamma\phi}{1 - \gamma\phi}$$

Where

$$\phi = \left( \frac{\alpha}{1 + \alpha} \right)^{1/2} \frac{1 + \gamma}{\frac{1}{\alpha} - \gamma - \gamma^2}$$

$$\gamma = \frac{1 - C^*}{1 + C^*} \frac{1}{1 + \alpha} \quad (\text{Where } C^* = \frac{C_{\min}}{C_{\max}})$$

$$\alpha = \lambda \times NTU \times \frac{C_{\min}}{C_{\max}}$$

$$\lambda = \frac{K_w a_w}{LC_{\min}}$$

Therefore, effectiveness due to longitudinal heat conduction

Effectiveness,

$$\varepsilon = 1 - i \quad 4.25$$

With the following effectiveness calculation is done for the cold and hot exit temperatures from equation (4.26) and (4.27). If the outlet temperatures are same or near to that as computed from estimated effectiveness iteration is terminated otherwise iteration is again initiated using previously obtained outlet temperatures from step 2 to 15 until the assumed and computed outlet temperatures converge up to the preferred values.

$$T_{h,o} = T_{h,i} - \varepsilon \frac{C_{\min}}{C_h} (T_{h,i} - T_{c,i})$$



Hot outlet temperature,

4.26

Cold outlet temperature,

$$T_{c,o} = T_{c,i} + \varepsilon \frac{C_{\min}}{C_c} (T_{h,i} - T_{c,i})$$

4.27

Table 4.12 Heat transfer coefficient and effectiveness

Effectiveness	$T_{ho}$	$T_{co}$
0.920162	123.4361	291.5404

16. Determine the pressure drop on each side of fluid using standard ‘f’ factors are shown in Table 4.9.

Pressure drop,

$$\Delta P = \frac{4fLG^2}{2D_e\rho_b}$$

4.28

So, the pressure comes out from the calculation on accounting the friction factor ‘f’ for hot and cold side fluids.

Table 4.13 Evaluated values of friction factor and pressure drop

	Friction factor, f	Pressure drop, $\Delta P$
Hot side	0.13047	527.22
Cold side	0.08697	347.38

Since, the pressure drop is under the allowable limit of 0.0056 bar there is no need of further iteration.

#### 4.2.2. Performance evaluation using the correlation of Manglik and Bergles

Manglik *et al.* correlation is carried out for prediction of outlet temperatures, effectiveness and pressure drop including thermal and hydraulic performance of heat exchanger. The above equation is used to predict the dimensions of heat exchanger. The only

difference is observed in hydraulic diameter, Colburn factor and the friction factor equation as given below in equation 4.29 and Table 4.14.

Manglik and Bergles,

$$D_h = \frac{4shl}{2(sl + hl + ht) + ts} \quad 4.29$$

Table 4.14 Manglik and Bergles correlation

Reynolds No.	Correlation	
	Heat transfer	flow friction
Re < Re* (laminar flow)	$j = 0.6522 \text{ Re}^{-0.5403} \alpha^{-0.1541} \delta^{0.1499} \gamma^{-0.0678}$	$f = 9.6243 \text{ Re}^{-0.7422} \alpha^{-0.1856} \delta^{0.3053} \gamma^{-0.2659}$
Re > (Re* + 1000) (Turbulent flow)	$j = 0.2435 \text{ Re}^{-0.4063} \alpha^{-0.1037} \delta^{0.1955} \gamma^{-0.1733}$	$f = 1.8699 \text{ Re}^{-0.2993} \alpha^{-0.0936} \delta^{0.6820} \gamma^{-0.2423}$
Where $\text{Re}^* = 257 \left( \frac{l}{s} \right)^{1.23} \left( \frac{t}{l} \right)^{0.58} D_h \left[ t + 1.328 \left( \frac{\text{Re}}{l D_h} \right)^{-0.5} \right]^{-1}$		

The calculated effectiveness from the above correlation is 0.9504 without considering of longitudinal effect and with longitudinal effect it is 0.9085. The pressure drop across the heat exchanger on the both side of hot and cold side is 0.003 bar and 0.002 bar which is under the allowable pressure.

### 4.2.3. Performance evaluation using the correlation of Joshi and Webb

Rating of heat exchanger by using the correlation of Joshi *et al.* is similar to that of Maiti *et al.* and Manglik *et al.* Same equations are used for the hydraulic diameter as in Maiti *et al.* The only change occurs in Colburn and friction factor and as given below in Table 4.15.

Table 4.15 Joshi and Webb correlation

Reynolds No.	Correlation	
	Heat transfer	flow friction
Re ≤ Re*	$j = 0.53 \text{ Re}^{-0.5} (l / D_h)^{-0.15} \alpha^{-0.14}$	$f = 8.12 \text{ Re}^{-0.74} (l / D_h)^{-0.41} \alpha^{-0.02}$
Re ≥ Re* + 1000	$j = 0.21 \text{ Re}^{-0.40} (l / D_h)^{-0.24} (t / D_h)^{0.02}$	$f = 1.12 \text{ Re}^{-0.36} (l / D_h)^{-0.65} (t / D_h)^{0.17}$

$$\text{Where } Re^* = 257 \left( \frac{l}{s} \right)^{1.23} \left( \frac{t}{l} \right)^{0.58} D_h \left[ t + 1.328 \left( \frac{Re}{lD_h} \right)^{-0.5} \right]^{-1}$$

The draw out effectiveness from the above correlation is 0.9712 without consider longitudinal effect and with longitudinal effect is 0.9280. The pressure drop across the heat exchanger on the both side of hot and cold side is 0.003 bar and 0.002 bar which is under the allowable pressure.

### 4.3 Rating based on simulation software

Aspen Muse<sup>©</sup> is used for rating of plate fin heat exchanger. It provides better precision results to simulate the performance of presented exchangers. It provides the thermal and hydraulic analysis of fluid flow on a multi-layer fins.

Figure 4.1 and 4.2 represent the variation of temperature and pressure with respect to the longitudinal distance. The inclination and declination of lines shows the fall and rise of temperature on each stream of both the sides vice versa. It shows the variation of pressure with respect to longitudinal distance. The curve shows drop in pressure on the both side of stream. The graph is obtained from the analysis of plate fin heat exchanger by Aspen Muse<sup>©</sup>.

The simulated result of effectiveness using Aspen Muse<sup>©</sup> along with the effectiveness developed by using various correlations is tabulated below in Table 4.16.

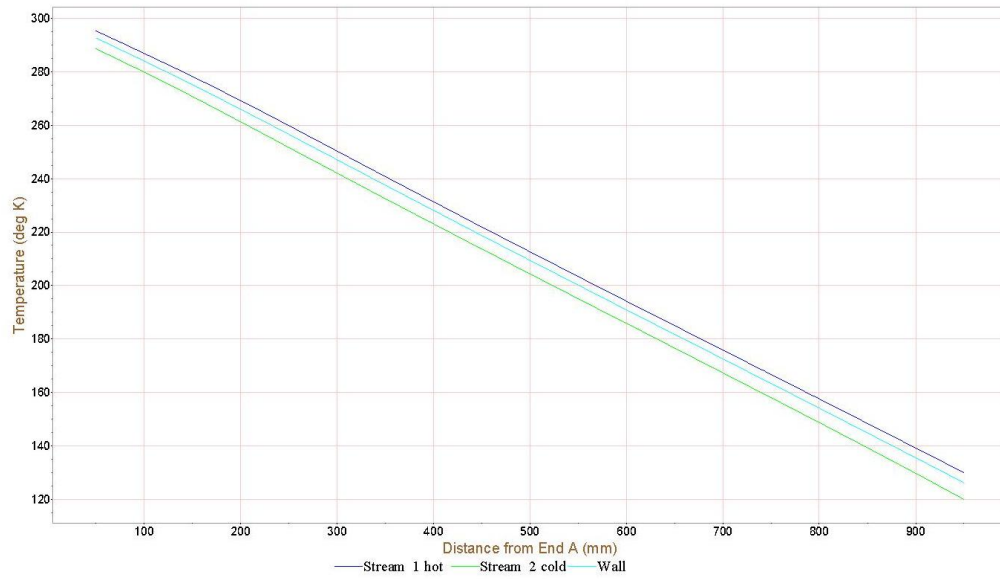


Figure 4.1 Temperature with respect to the longitudinal distance Aspen Muse<sup>©</sup>

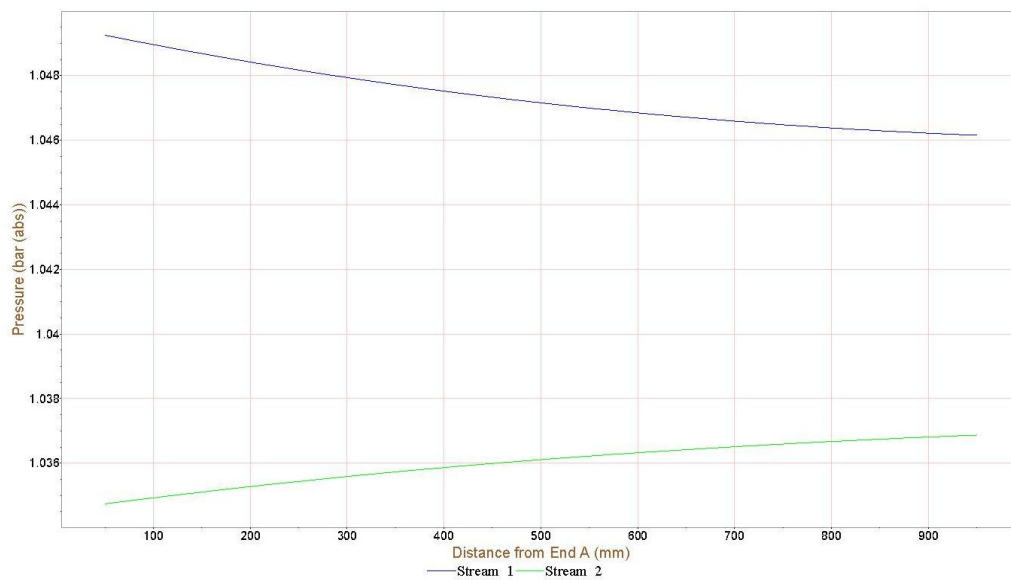


Figure 4.2 Pressure with respect to the longitudinal distance Aspen Muse<sup>©</sup>

Table 4.16 Effectiveness at mass flow rate

Mass flow rate (g/s)	Effectiveness			
	Maiti & Sarangi	Manglik and Bergles	Joshi & Webb	Aspen - Muse <sup>©</sup>
6.029	0.92	0.90	0.92	0.88

Table 4.17 and 4.18 represents the pressure drop using Aspen Muse<sup>®</sup> and analytically using different correlations at hot and cold side of heat exchanger respectively.

Table 4.17 Pressure drop (Hot End) at mass flow rate

Mass flow rate (g/s)	Pressure drop at Hot Side			
	Maiti & Sarangi	Manglik and Bergles	Joshi & Webb	Aspen - Muse <sup>®</sup>
6.029	0.005272	0.003679	0.003928	0.00441

Table 4.18 Pressure Drop (Cold End) at mass flow rate

Mass flow rate (g/s)	Pressure drop at cold side			
	Maiti & Sarangi	Manglik and Bergles	Joshi & Webb	Aspen - Muse <sup>®</sup>
6.029	0.003474	0.002386	0.002445	0.00278

## 4.4 Effect of heat leak to surroundings

Highly effective heat exchanger is required for cryogenics applications. The temperature difference between the cryogenic equipment to that of surrounding is very large. Due to this temperature differences, the effectiveness of the cryogenic equipment is strongly affected by the losses such as longitudinal heat conduction and the heat leak from the surrounding. The heat leak to the surrounding can be controlled up to some extent by applying proper insulation. So, excellent methods is required for thermal insulation in cryogenic systems. Some cryogenic systems are placed in the vacuum chamber to insulate the system.

In the present experimental examination, the performance of the plate fin heat exchanger is investigated at cryogenic temperature. The temperature difference from the surrounding to that of the test system as quite high therefore it is highly necessary to design support structure to reduce the heat leak and also bear the instrumentation and control systems. Bulk filling of

expanded perlite is used here in the present experimental setup to provide cost effective and better insulation.

Expanded perlite offer better insulation. It has low thermal conductivity, incombustible and easy to handle. Expanded perlite sustains reliable measures at low temperature about in the range of 4.26 K to 1366 K and prevent the system from moisture. The thermal conductivity of perlite varies according to temperature and density. The demerit of expanded perlite dust is it causes chronic poisoning.

The plate fin heat exchanger put inside the cold box filled with perlite and then covered with thermocol and the pipelines are insulated with foam and expanded perlite supported with thermocol. The RTD's sensors were placed inside the insulation and insulated perfectly from ambient temperature. The conducted wire of RTD's taken out from the insulation through the tiny holes.

## **Chapter V**

# **THE EXPERIMENTAL STUDIES**

## **5.1 Experimental setup and procedure**

The experimental setup comprises with counter flow offset plate fin heat exchanger as a test piece along with other components. The pressurized nitrogen gas from the liquid nitrogen storage tank through the vaporizer is made to pass through the plate fin heat exchanger on the high-pressure side and gets cooled with the help of chiller and pass again to the low-pressure side. This session describes the major component, arrangement of the experimental set-up and the calibration process of the apparatuses used.

In this experiment, the mass flow rate for both the side is constant for a single set of experiment. Inlet and outlet temperatures and pressure are measured when flow achieves steady state. The same process is repeated for different mass flow rate. Process and instrumentation modules are represented in process chart as shown in Figure 5.1. The pressurized nitrogen as a working fluid from the vaporizer is collected in the reservoir tank and made to pass. The impurities of gas affect the experimental results and also increase the

fouling factor which affects the performance of the heat exchanger. Therefore, Nitrogen gas supplied to the test system is pure to avoid the fouling factor. Control valve manages to bring the flow of nitrogen gas at different flow rates. The gas enters to the high-pressure entry side of the heat exchanger and comes out from the high-pressure exit side thereafter it is allowed to pass through the chiller unit. The chiller unit is comprised of the cryogenic vessel (wide neck Dewar) in which a coil type heat exchanger is dipped in the liquid nitrogen bath in which the temperature of nitrogen gas decreases. The chilled gas is again sent back to the heat exchanger through the low-pressure entry side of the heat exchanger where it exchanges the heat from high temperature to the low temperature which can be realized by visualizing Figure 5.2 (during the commissioning process of experimental test plant). After that, nitrogen gas comes out from the heat exchanger through the low-pressure exit side of the heat exchanger.

In the course of the flow process, valves and taps have to be evaluated in support of the performance perspective of the heat exchanger. For this purpose, instrumentation is added to the test rig for measuring the pressure, temperature and the mass flow rate. Pressure gauges are placed at the inlet on the hot side and also provide at the outlet of the cold side to measure the pressures of the fluids. U-tube manometers are coupled with a high-pressure side and low-pressure side to measure the drop in pressure on the both sides of the heat exchanger. A provision is added to attach the RTD module along with the data adequate system for the measurement of temperature at the inlets and outlets of the hot and cold streams. Unconventional automation designs consist of six RTD response channels ADAM-4015 enclosed with ADAM-4520 which is connected to the computer. It is used for sensing different temperatures at different points of the test setup.

The required section is carefully insulated separately. The pipe connections are properly wrap with insulation tapes along with perlite powder casing and heat exchanger is shielded with perlite powder supported with the thermocol sheets to reduce the thermal conduction as well as convection interacting with the environments as shown in Figure 5.2.

In Figure 5.1 green dotted lines indicate the Resistance Temperature Detector (RTD's) connection with the test rig to the data adequate system (ADAM VIEW) while yellow dotted lines are linked with the manometer. Instrumentation and fittings are listed below the figure 5.1. The photograph of the actual model during the commissioning process is in Figure 5.2.

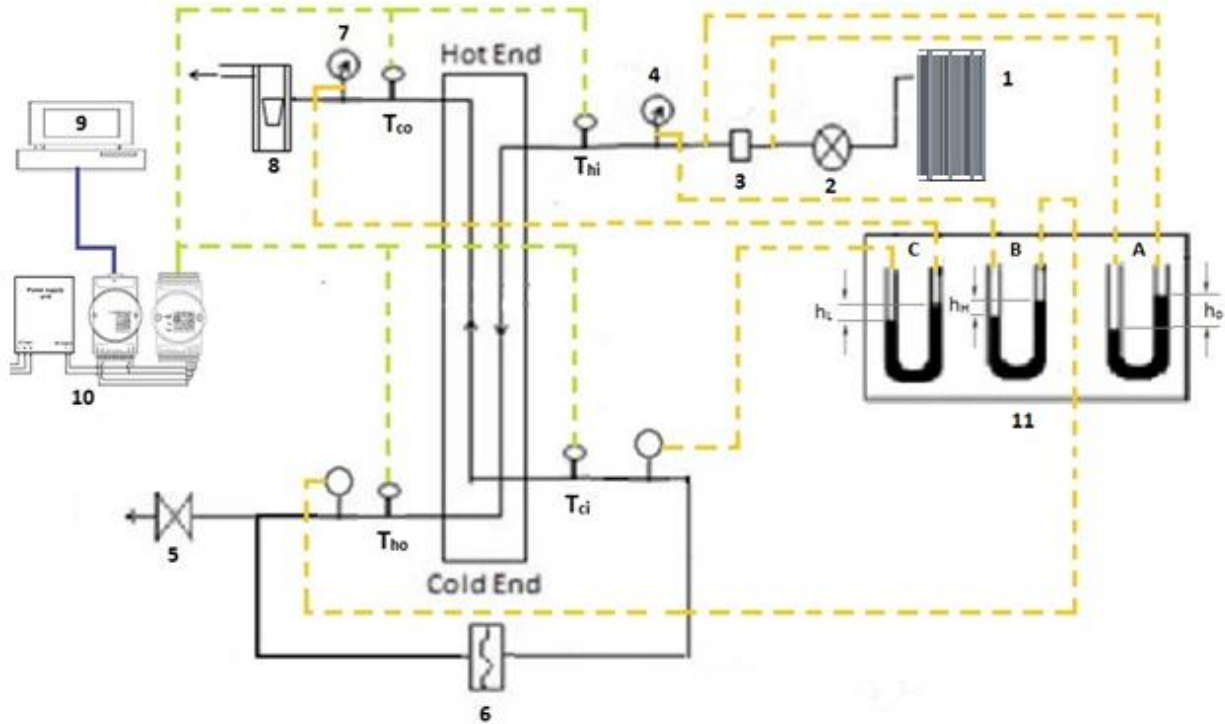


Figure 5.1 Process Flow & Instrumentation diagram of the experimental test rig

- |                              |                              |
|------------------------------|------------------------------|
| 1: Vaporizer                 | 2: Control Valve             |
| 3: Orifice                   | 4: Inlet Pressure Indicator  |
| 5: Bypass valve              | 6: Chiller Unit (Sub cooler) |
| 7: Outlet Pressure Indicator | 8: Rotameter                 |
| 9: Monitor                   | 10: ADAM View                |
| 11: Manometer                |                              |

$T_{hi}, T_{ho}, T_{ci}, T_{co}$ : PT100 Resistance Temperature Detectors (RTD's).





Figure 5.2 Photograph during commissioning



Figure 5.3 Image of Final Experimental setup

### 5.1.1 Simple representation of Fluid Flow Facility of Experimental setup

Above explained fluid flow facility of the experimental setup is clarifying by the schematic fluid flow diagram as shown in Figure 5.4. The fluid from the vaporizer flows into the chiller through heat exchanger. The chilled gas again comes back into the heat exchanger where it exchanges heat and comes out to the atmosphere.

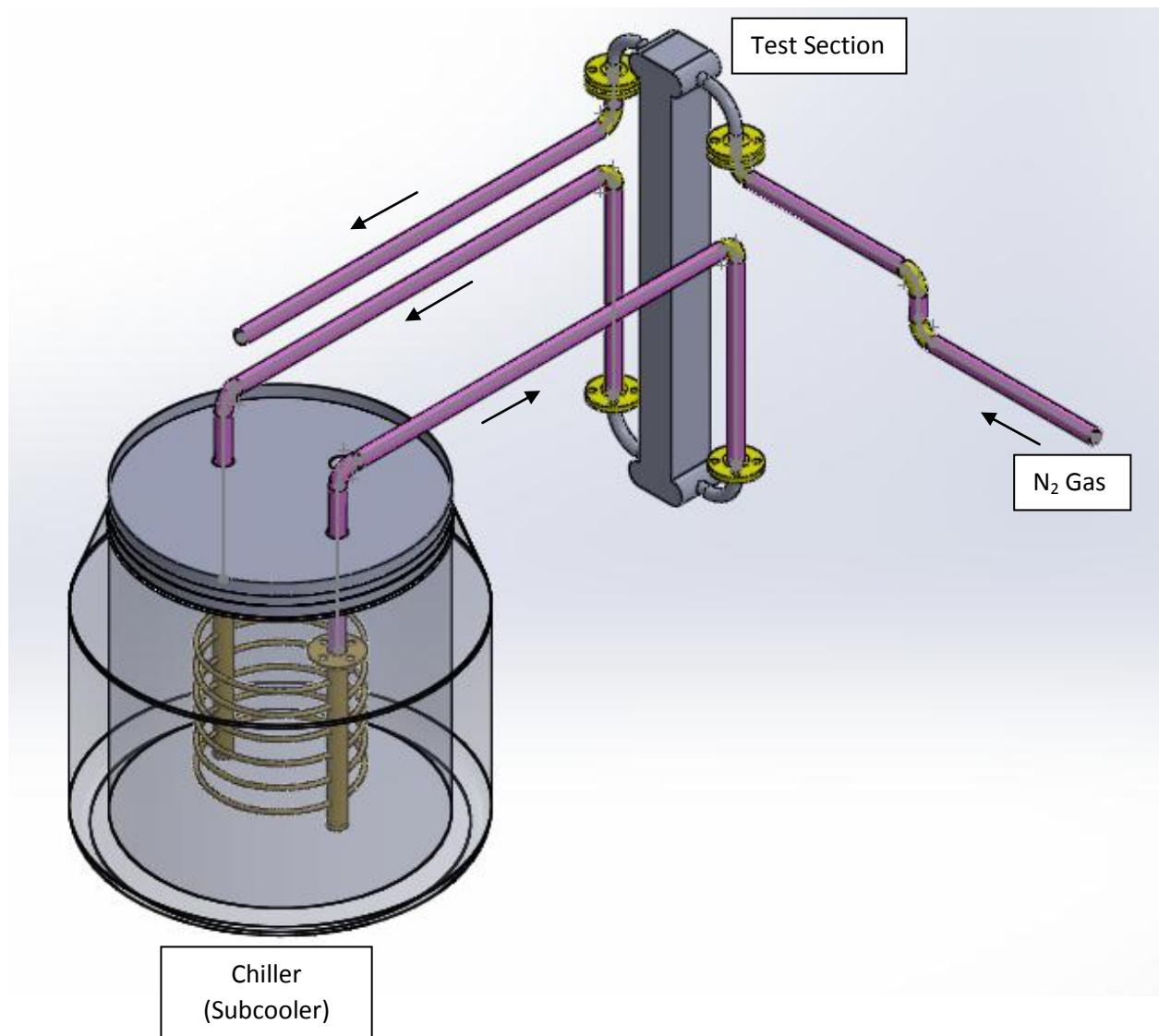


Figure 5.4 Schematic Fluid Flow diagram of Experimental setup

## 5.2. Description of associated equipment and instruments

The experimental setup consists of the following component.

- Liquid storage tank unit
- Vaporizer
- Test Section (Plate Fin Heat Exchanger)
- Chiller unit
- Temperature measurement devices (RTD)
- Fluid metering device (Orifice and Rotameter)
- Pressure measurement devices (Manometers and Pressure Gages)

### 5.2.1. Storage tank

The storage tank of liquid nitrogen and other cryogenics are often called as Dewar. The vessel name is in the name of its inventor called James Dewar. It is made up of two layers of wall. Vessels have high levels of vacuum in between them to reduce the axial conduction and convection. The inner layer is of glass supported by an outer layer of metal for an extremely cold substance like liquid helium, another layer of the liquid nitrogen shield is provided to reduce the evaporation rate.

Table 5.1 Basic Technical Specifications of Storage Tank

Volume	75 Ltr.
Diameter	550 (mm)
Height	760 (mm)
Neck width	450 (mm)
Isolation	Multi-Layer in High Vacuum
Inside layer	SS 304
External layer	CS
Automatic jacket over pressure relief	YES
Weight	45 Kgs. (Approx.)

### 5.2.2. Vaporizers

The vaporizer is a kind of heat exchanger which is used to change the phase by transferring thermal energy from an external source of the fluid. Cryogenic liquid ( $N_2$ ) changes from a liquid state to the vapour state by exchanging heat with the ambient temperature.

There are mainly two types of vaporizers

- Natural draft vaporizers

Natural draft vaporizers utilize free convection as the heat transfer mechanism. In the experiment this type of vaporizer is used.

- Forced draft vaporizers

Forced draft vaporizers utilize forced convection as the heat transfer mechanism. Multiple fans mounted at the top of the vaporizer supplies high-velocity of air downward through the heat exchange array providing maximum heat transfer and high evaporation rates.

Table 5.2 Technical Specification of Star Fin Vaporizer

Volume	200 Nm <sup>3</sup> / Hr
Design Pressure	20 bar
Design Temperature	-198 ° C
Design Code	ASME Sec VIII Div 1 ED 2004 AD 2005

### 5.2.3. Plate Fin Heat Exchanger

The plate fin heat exchanger used in this experiment was manufactured by Apollo Heat Exchangers, Mumbai. The diagram for the manufacturing point of view has been shown in Fig.5.6 with all of its dimensions. The high-pressure side has five layers, and the low-pressure side has four layers. Flow arrangement data is provided in Table 5.1. The core dimensions and fin geometry data has been tabulated in Table 5.2 and 5.3 respectively. The design data for this heat exchanger is given in Table 5.4.

Table 5.3 Flow arrangement of the heat exchanger

	HIGH-PRESSURE SIDE (Hot Fluid Side)	LOW-PRESSURE SIDE (Cold Fluid Side )
Fin	Offset-Strip Fin(OSF)	Offset-Strip Fin(OSF)
No. of Passage	5	4
No. of Pass	Single	Single
Flow Rate	Counter Flow	Counter Flow

Table 5.4 Core size of the heat exchanger

Core Length	900 Mm
Core Width	73 Mm
Core Height	93 Mm
Total Length	1000 Mm

Total Width	85 Mm
Total Height	105 Mm

Table 5.5 Fin Geometry of the heat exchanger

FIN GEOMETRY		HIGH PRESSURE SIDE (Hot Fluid Side)	LOW PRESSURE SIDE (Cold Fluid Side)
1	Fin frequency, f	714 fins /meter	588 fins/ meter
2	Fin length, l	3 mm	5 mm
3	Fin thickness, t	0.2 mm	0.2 mm
4	Fin height, h	9.3 mm	9.3 mm
5	No. of layers	5	4

Table 5.6 Flow parameters of the heat exchanger

	HOT SIDE	COLD SIDE
Fluid	Nitrogen (HP)	Nitrogen (LP)
Flow Rate	5 g/s	4.8 g/s
Inlet Temperature	310K	83.65 K
Outlet Temperature	92.85 K	301.67 K
Allowable Pressure Drop	0.05 bar	0.05 bar
Pressure At Inlet	7.35 bar	1.15 bar
Heat Load	5.5 KW	5.5 KW

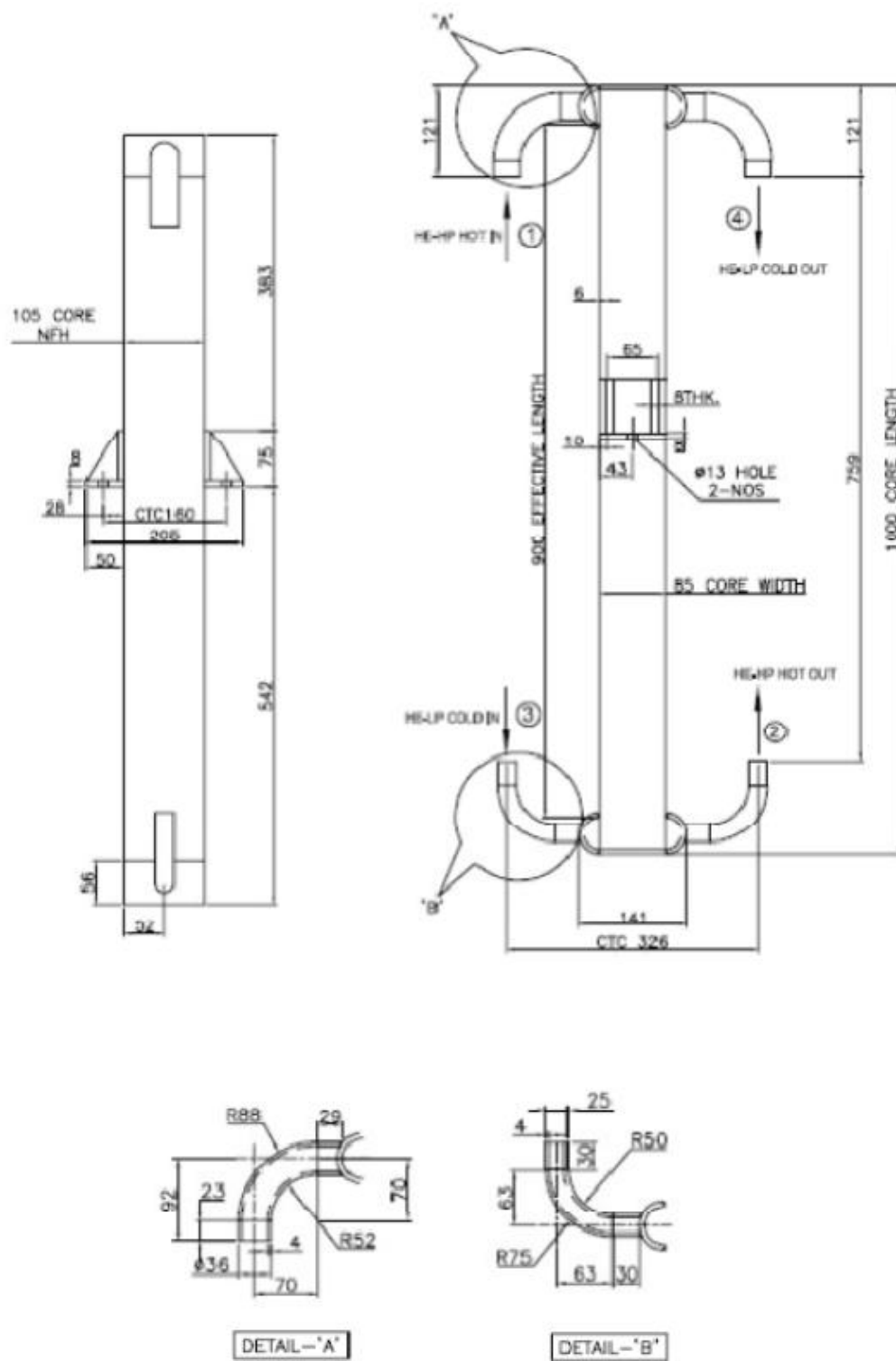


Figure 5.5 Sketch of Plate Fin Heat Exchanger

#### 5.2.4. Chiller unit

The chiller unit consists of coil type heat exchanger dipped in a broad neck Dewar filled with liquid nitrogen. Liquid nitrogen extracts heat from the gaseous nitrogen. The temperature of nitrogen gas can be controlled by controlling the level of liquid nitrogen in the Dewar. The sub-cooler (chiller) is used for supplying cold gas to the plate fin heat exchanger. It is designed and developed in our cryogenics lab.

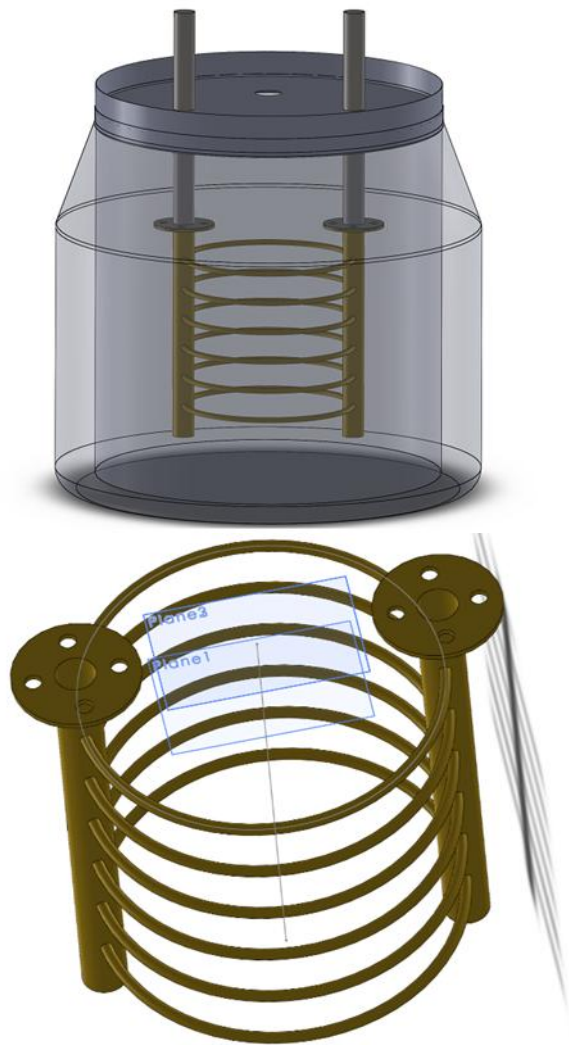


Figure 5.6 Design Model of Chiller Heat Exchanger

The present work in this dissertation clarified the design criteria of the chiller to implement in the cold testing of Plate Fine Heat Exchanger. The LMTD method has been provided in the literature to estimate the length and number of tubes required for the Heat

Exchanger. This new type heat exchanger has been used as a chiller for obtaining cryogenic temperature. The concept is developed here for the implementation in experimental work.

It was concluded that the heat exchanger was explained by two main factors one is a low-pressure drop across inlet and outlet, and the other one is the high coefficient of performance. The equipment shown in Figure 5.6 is used for obtaining the outlet temperature up to 100K and it will connect to the plate fin heat exchanger for cold testing. Nitrogen gas flow inside the tube and the tube dipped inside the liquid nitrogen. The outlet temperature of the nitrogen gas is controlled by refilling liquid nitrogen up to the certain interval of time using supply line. Graph in the figure 5.7 shows the inlet temperature and the liquid nitrogen temperature on which process is deigned.

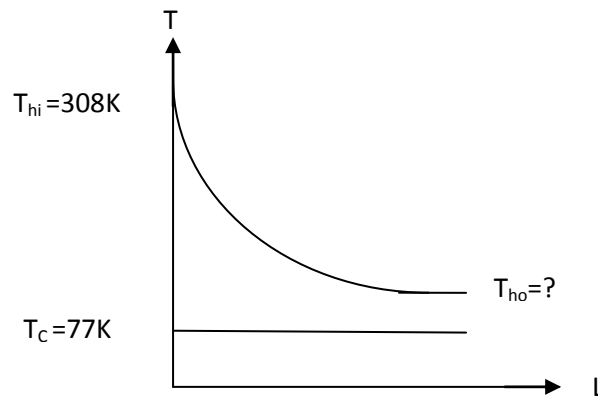


Figure 5.7 temperature profile w.r.t length

#### 5.2.4.1 Design of chiller unit

##### 1. MATHEMATICAL MODEL

###### a. Inside tube heat transfer coefficients of nitrogen gas

For calculating Reynolds number, mass flow rate of compressed fluid is 5.77 g/s

$$\therefore R_e = \frac{DG}{\mu}$$

5.1



Where

$$G = \frac{\dot{m}}{A} = \rho V$$

If  $Re > 3500$  flow is Turbulent [2] since in our case it is more than 3500

$$\therefore J_H = 0.023 R_e^{-0.2} B_1 \quad 5.2$$

Where

$$B_1 = 1 \text{ for Gasses}$$

$$J_H = \frac{h_c P_r^{\frac{2}{3}}}{C_p G} \quad 5.3$$

From equation-5.3, we can calculate the heat transfer coefficients ( $h_c$ ) of gaseous nitrogen inside the tube.

**b. Convective Heat transfer coefficient from the tube wall to liquid nitrogen at 77k**

Since the heat transfer is taken place between the tube wall and static fluid. So we will consider free convection

Therefore, for free convection Nusselt number is given as [135]

$$Nu = 0.53(Gr Pr)^{1/4} \quad 5.4$$

Where

$$Gr = \frac{D^3 g \beta \Delta T}{\nu^2}$$

$$Pr = \frac{\mu C_p}{K}$$

And also

$$N_u = \frac{hD}{K} \quad 5.5$$

By equating 5.4 and 5.5 equations, we will get the Heat transfer coefficient (h) from the tube wall to liquid nitrogen

### c. Boiling heat transfer coefficient

For calculating boiling heat transfer coefficient, the convective contribution of heat transfer may be determined as follows [135]

$$N_u = 0.62 \left( \frac{R_{ab}}{J_{aG}} \right)^{\frac{1}{4}} \quad 5.6$$

The Nusselt number involves the properties of the vapor as

$$N_u = \frac{h_B D}{k} \quad 5.7$$

The  $R_{ab}$  is the film boiling Rayleigh number defined as

$$R_{ab} = \frac{g \rho_G (\rho_L - \rho_G) D^3 \rho_{rg}}{(\mu_G)^2} \quad 5.8$$

and Jakob number is defined as,

$$J_{aG} = \frac{C_G (T_w - T_{sat})}{(i_{fg})_e} \quad 5.9$$

Where  $(i_{fg})_e$  is an effective heat of vaporization [135]

$$(i_{fg})_e = i_{fg} + 0.34 C_G (T_w - T_{sat}) \quad 5.10$$

By equating 5.6 and 5.7 above equations, we will get the boiling heat transfer coefficient ( $h_B$ ) for liquid nitrogen.

For calculating overall heat transfer co-efficient,

$$\frac{1}{U} = \frac{1}{\left(\frac{r_0}{r_i}\right) \frac{1}{h_c} + \frac{r_0}{k} \ln\left(\frac{r_0}{r_i}\right) + \frac{1}{h_B}} \quad 5.11$$

Where,  $r_0$  &  $r_i$  is outer & inner radius of the tube

- - Heat transfer rate

$$Q = UA(LMTD) \quad 5.12$$

And also

$$Q = m_g c_{pg} \Delta T \quad 5.13$$

Equating (5.12) & (5.13) we get the length of the tube

$$\ln \left( \frac{T_{ho} - T_c}{T_{hi} - T_c} \right) = - \frac{UA}{C_{\min}} = -NTU \quad 5.14$$

Where  $A = 2\pi rL$  and  $C_{\min} = m_g C_{pg}$

$$\text{or, } \left( \frac{T_{ho} - T_c}{T_{hi} - T_c} \right) = \exp(-NTU) \quad 5.15$$

$$\therefore \varepsilon = \left( \frac{T_{hi} - T_{ho}}{T_{hi} - T_c} \right) \quad 5.16$$

$$\therefore \varepsilon = 1 - \exp(-NTU) \quad 5.17$$

The mathematical analysis represented in this section gives the calculated heat transfer coefficient of inner tube between the shell wall and liquid nitrogen. It calculates the heat transfer rate and predict the length of the tube required.

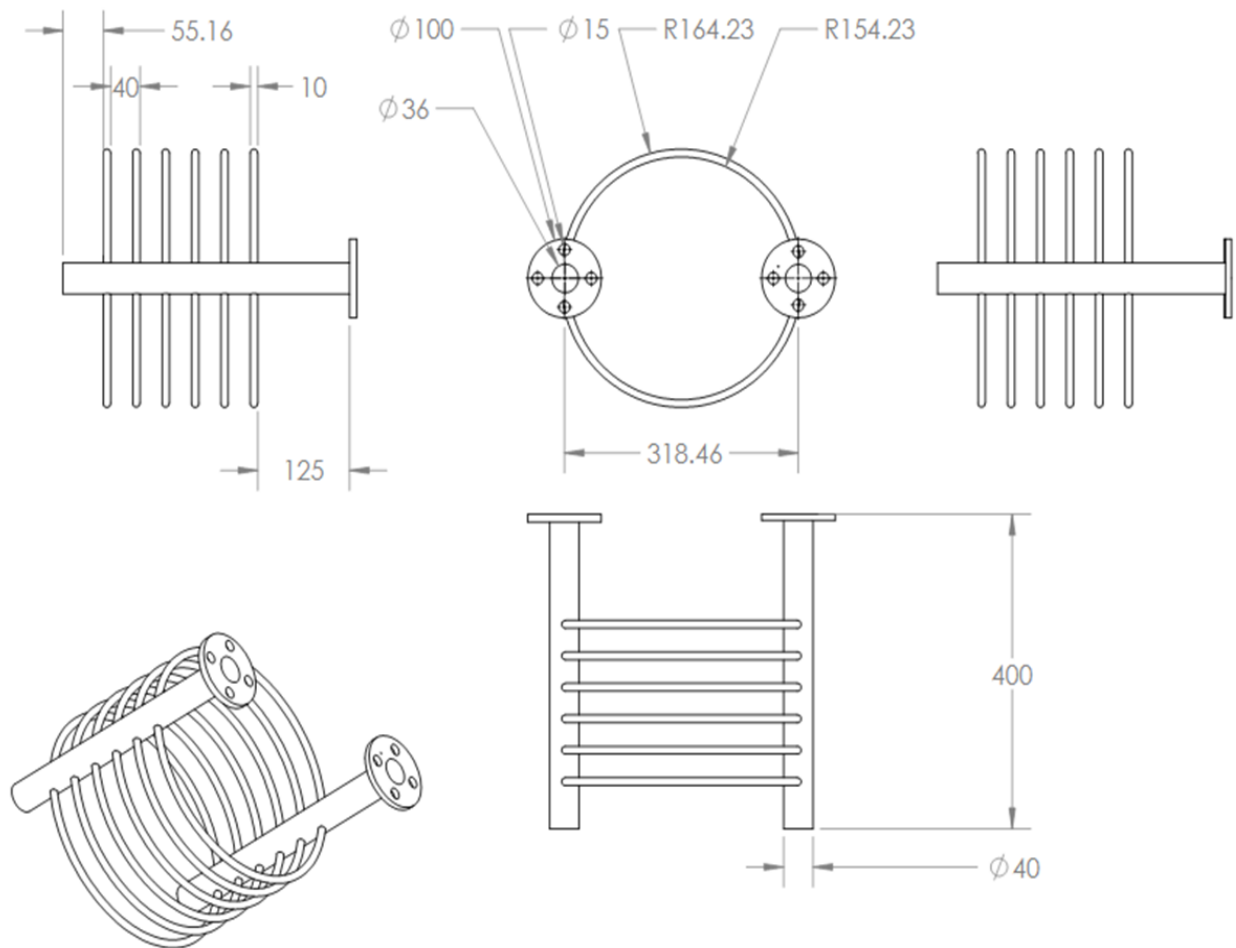


Figure 5.8 Design Sketch of Chiller Heat Exchanger

The geometrical model presented in Figure 5.8 designed by considering the thermal requirement and the inner shell geometry of the Penguin wide neck cryogenic Dewar. The construction of chiller unit also considers the other dimensions for the cold testing of heat exchanger. The traverse and crosswise movement of the fluid particle cause the turbulence inside the coil which increases the heat transfer rate as compared to that of the straight tube

whereas the pressure drop is comparatively low as compared to the helical coil type heat exchanger.

## 2. NUMERICAL MODEL

The heat transfers from liquid nitrogen in the wide neck cryogenic Dewar sustained at  $196\text{K} \pm 0.5\text{K}$  to hot gas flowing inside the coil was evaluated through CFD analysis and compared its result with the analytical solution. The CFD contour as shown in Figure 5.9 the result explains the outlet temperature which verifies the analytical statement. An experiment has performed to analyse the predicted data developed by CFD. The recorded database shown in Table 5.7 represents the comparison and variation between the outlet temperatures of nitrogen gas flowing in a coil to that of mass flow rate of nitrogen gas under the isothermal state.

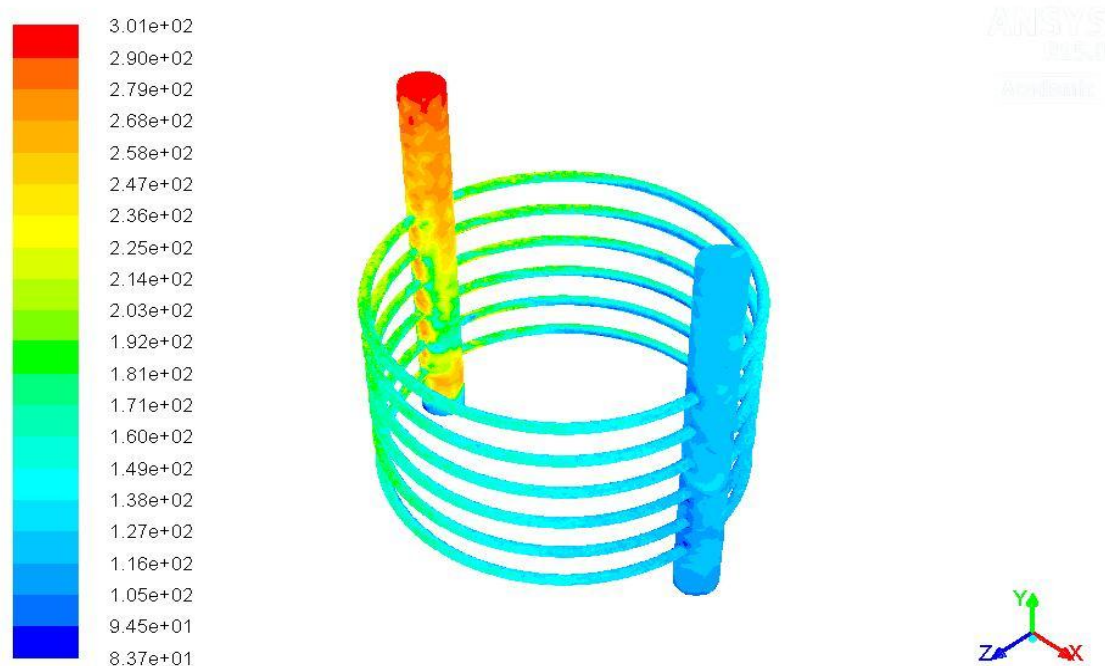


Figure 5.9 Temperature contour of Heat Exchanger of Chiller

Table 5.7 Outlet Temperature as a function of mass flow rate

S.No.	Mass flow rate (Litre/min)	Outlet Temperature (K)		
		Analytical	Numerical	Experimental
1.	300	100.48	111.26	106.4
2.	350	106.14	114.46	111.4
3.	400	110.72	118.15	114.1
4.	450	116.01	122.35	118.3
5.	500	120.34	127.64	122.8

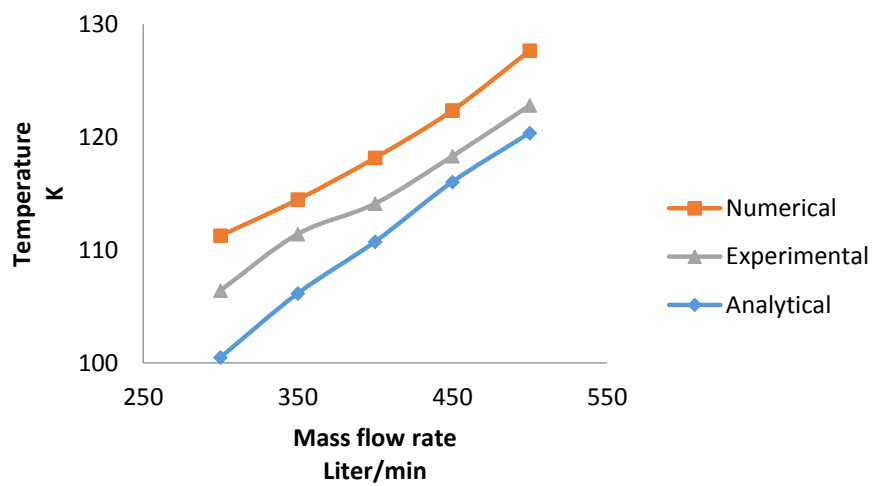


Figure 5.10 Temperature Vs Mass flow rate variation

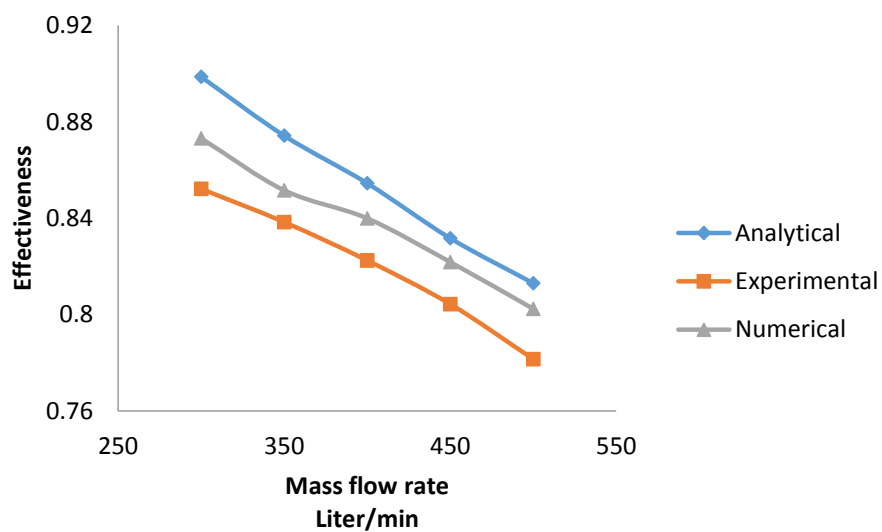


Figure 5.11 Effectiveness Vs Mass flow rate variation

Estimations were performed for various flow rates of nitrogen gas supplied by a gas vaporizer. The measurements are taken at steady state conditions. The cooling process is due to the absorption of heat by the liquid nitrogen which boils off during the cooling process. Figure 5.10 demonstrates that the outlet temperature from the chiller due to change in the mass flow rate of the nitrogen gas. These show an increase in the outlet temperature as the mass flow rate increases. It also illustrates the minimum temperature 100.48K attended at 300 liters/min. In Figure 5.11, the effectiveness of heat exchanger is plotted against the mass flow rate.

## 5.4 Instrumentation

The instrumentation is one of the most important parts of the experimental setup in which the Pressure gauges are placed at the inlet on the hot side and at the outlet of the cold side to measure the pressures of the fluids. The U-tube manometers are coupled with high-pressure side and low-pressure sides to measure the drop in pressure on the both sides of the heat exchanger. A provision is added to attach the RTD module along with the data accusation system for the measurement of temperature at the inlets and outlets of the hot and cold streams. The details of the instruments are given below.

### 5.4.1 Temperature measurement

To quantify the performance of the Plate-fin type of heat exchanger, it is necessary to measure the temperature at various stages.

#### Resistance temperature detector (RTD)

Platinum resistance thermometers PT-100 a resistance temperature detector (RTD) is used as a temperature sensor. Platinum resistance thermometers (PRTs) has good precision over a varied temperature array (from  $-200$  to  $+850$  °C). The fluctuating property, the electrical resistance of a material change with the change of temperature and this concept is utilized to measure or to sense the temperature through RTD. In operation, a small current excitation across the component, leads to also the voltage that is related to resistance is then measured and changed to a unit of temperature calibration.

PT-100 is the most common type of RTD. In PT-100, platinum resistance is changed to 100 ohms at  $0^{\circ}\text{C}$  to 138.4 ohms at  $100^{\circ}\text{C}$  respectively. Accordingly, resistance changes at a



different temperature range, but their nominal resistance unremarkably classifies RTD's at 0°C. So the relation between the resistance and temperature is linear given as follow

$$R_t = R_0 \times \left[ 1 + A \times t + B \times t^2 + C(t - 100) \times t^3 \right] \quad 5.18$$

Where

$R_t$  is the resistance at temperature ( $t$ )

$R_0$  is the resistance at 0

$A = 3.9083 \text{ E} - 3$

$B = -5.775 \text{ E} - 7$

$C = -4.183 \text{ E} - 12$  (below 0 °C)

$C = 0$  (above 0 °C)

The change in resistance as the temperature changes is used to determine the temperature. Temperature is measured at the four points of outlet and the inlet of the cold and hot region through resistance temperature detector (RTD). Two more RTDs are added into the chiller unit to record the chiller temperature to maintain the steady temperature of the flow. Before measurement, RTD's is calibrated to ensure the correct result. Comparison method is commonly used. Since it is cost effective process hence several sensors can be calibrated simultaneously which are connected with multi-channel RTD sensor.

Process of calibration of RTDs

- Put three-fourth portions of the RTDs into the uniformly stable bath of liquid Paraffin in a beaker.
- Attach the RTDs wires to the multi-channel RTD sensor. As shown in Figure 5.12.
- This arrangement is electrically heated slowly and well-stirred bath to maintain uniformity.
- The reading of all the RTDs are recorded respectively. Repeat the procedure for different temperature range and plot the graph.

A reference measuring thermometer is additionally inserted to record the temperature.



Figure 5.12 RTD calibrations Setup with PT100

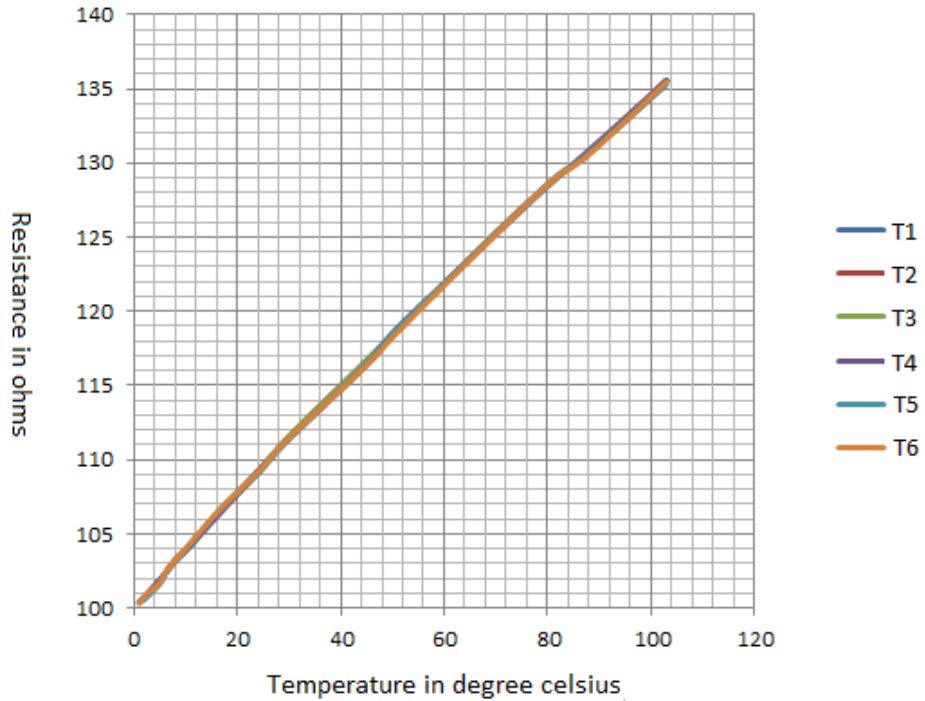


Figure 5.13 RTD calibrations graph

Table 5.8 Temperature at different T100

Thermometer	RTD1	RTD2	RTD3	RTD4	RTD5
1	0.94	0.91	1.1	1	0.84
1.9	1.87	1.96	1.92	1.52	2.02
5	4.38	4.39	4.89	4.27	4.47
6	6	6.05	6.06	5.99	6.15
8.4	8.52	8.34	8.16	8.16	8.36
11.1	11.22	10.9	11	11.38	11.42
17	17.25	17.66	17.32	17.68	17.8
24.1	24.05	24.22	24.44	23.92	24.17
30.7	30.63	30.8	30.29	30.28	30.48
45.8	45.18	45.07	44.27	44.52	44.21
52.5	51.89	51.89	52.16	52.26	51.81
70.4	70.71	70.84	70.45	70.43	70.35
81.4	81.76	81.48	81.86	81.95	81.85
88.2	87.93	87.63	87.6	87.55	87.34
103.8	103.84	103.67	104	102.97	103.51

The error calculate after calibration of RTD sensors is 13.7%. (Appendix-I)

To study the performance of the heat exchanger and to monitor the cooldown behavior, it is necessary to measure the temperature. So temperature is measured by using the Platinum Resistance Temperature Detector (RTD). It is the most linear and stable temperature sensor. The Pt-100 type RTDs is fitted at different locations to measure the temperatures. ADAM-

4015 data acquisition modules are used, and it provides a data output view in PC by using an ADAM-4520 converter. Figure 5.14 shows the connection of ADAM View with the RTD's to the monitor through the power supply unit. The actual picture of ADAM is presented in Figure 5.15. ADAM.NET utility software is used to connect it with a computer through VGA cable. The screen of software display is illustrated in Figure 5.16.

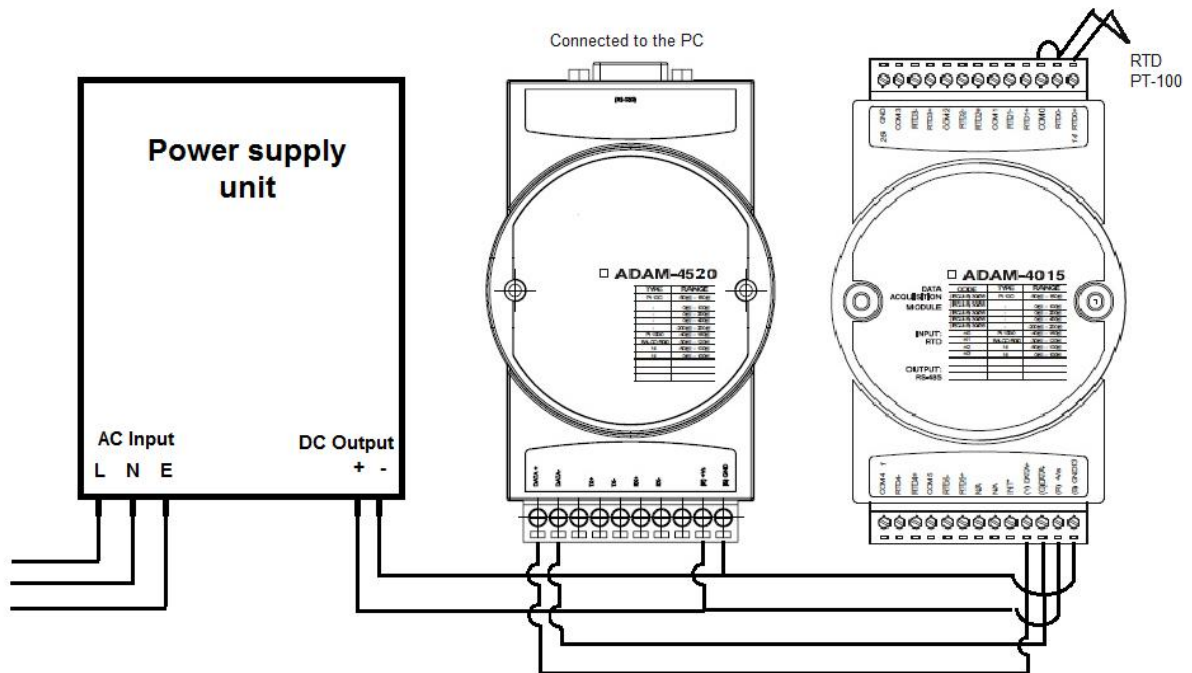


Figure 5.14 ADAM View Connections



Figure 5.15 Photograph of ADAM View

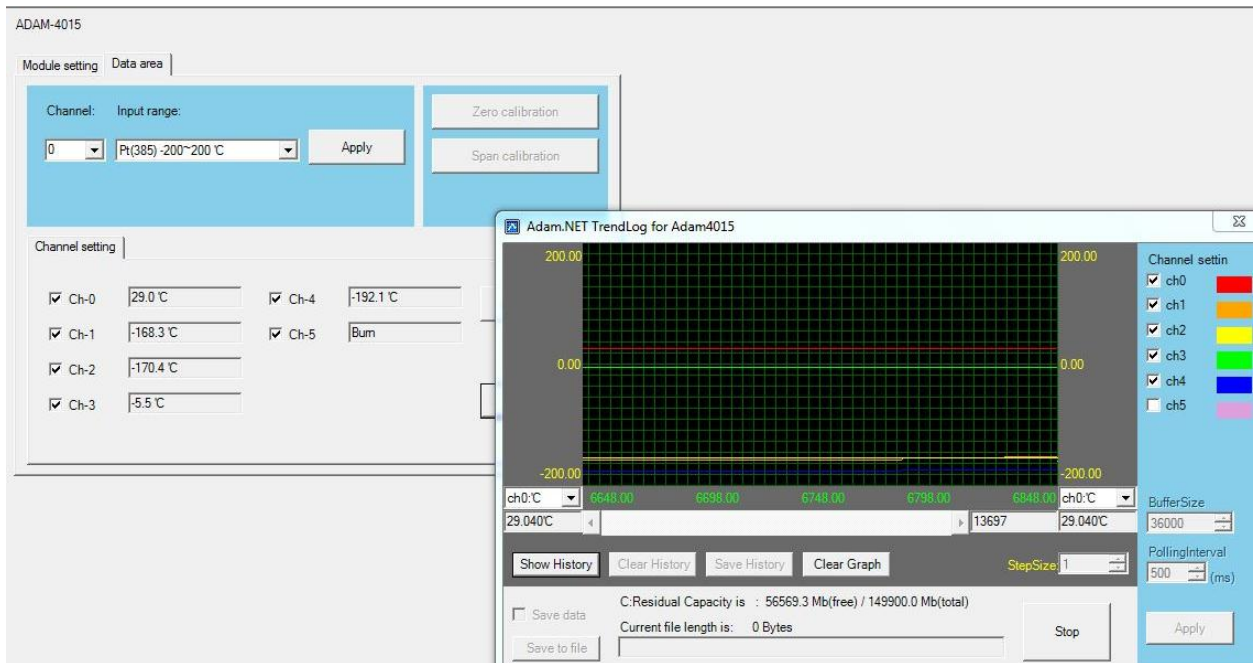


Figure 5.16 Display of ADAM View S/W

## 5.4.2 Orifice mass flow meter

Orifice mass flow meter devices are used to determine the rate of flow through pipe. It consists of a flat circular plate which has sharp edged hole called an orifice concentric in the pipe.

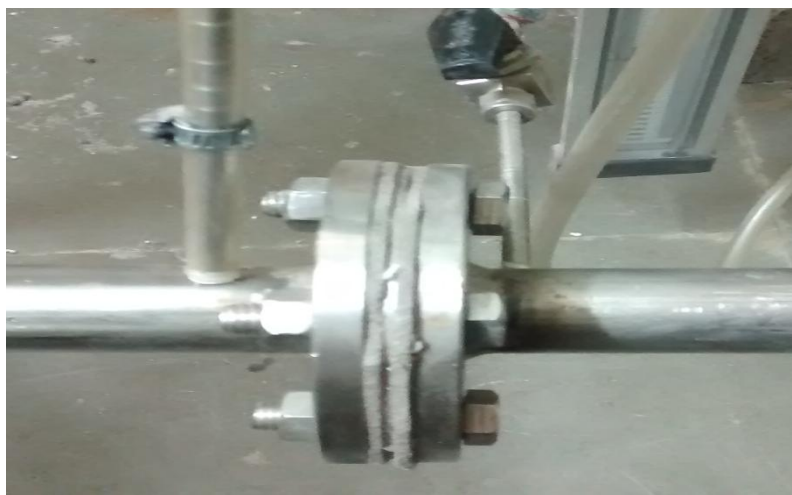


Figure 5.17 Photograph of Orifice

Orifice plate placed in between the flow in a pipe restrain the flow causes a drop in pressure or a pressure difference across the orifice plates. The change in pressure is measured by a manometer to calculate the mass flow rate.

As shown in the Figure 5.17 nitrogen gas passing through the pipe of 1-inch diameter which is restricted by an orifice of diameter 1 cm. The pressure difference across the orifice obtained from manometer through pressure tap.

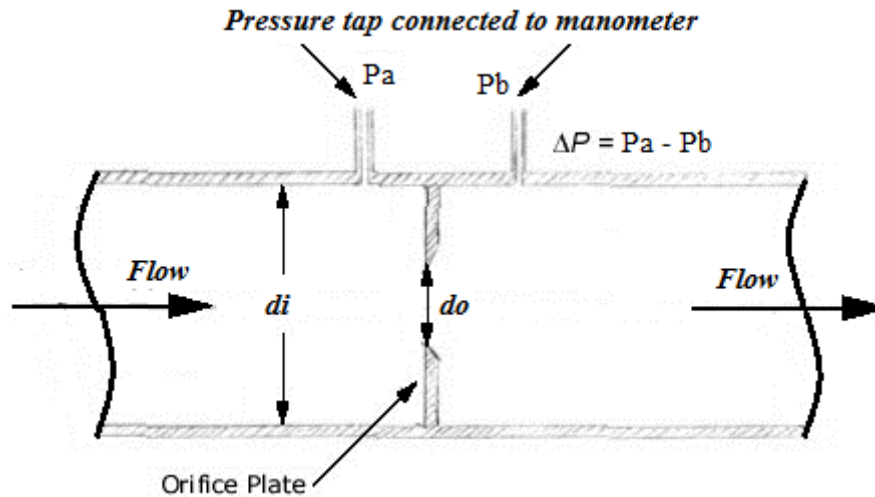


Figure 5.18 Sketch of Orifice

Therefore, The actual flow rate

$$q = C_f A_o \sqrt{\frac{2\Delta p}{\rho}}$$

5.19

The coefficient of flow  $C_f$  is in the range of 0.6 to 0.9 for most of the orifice. Since  $C_f$  is depending on the mass flow rate (Reynolds number) and the diameter of pipe and orifice as required for a standard graph.

Multiplying  $Q$  with density result the mass flow rate as,

$$Q_{mass} = \rho q$$

5.20

Therefore, the input parameters required to calculate flow rate are as follows

- Diameter of pipe,  $d_i$
- Orifice plate diameter,  $d_o$
- Pressure difference through manometer,  $\Delta P$
- Density of Fluid at flow, temperature and pressure,  $\rho$
- Flow Coefficient,  $C_f$

Table 5.9 Gas mass flow rate ( $Q_{\text{mass}}$ ) at various pressure differences  $\Delta P$

Pressure differences $\Delta P$ (Manometer reading in mmHg)	Pressure differences $\Delta P$ (KN/m <sup>2</sup> )	Volume flow rate $Q$ (m <sup>3</sup> /s)	Mass flow rate $Q_{\text{mass}}$ (Kg/s)
41	5.466217	0.0052	0.00591
74	9.865855	0.0068	0.00809
120	15.99868	0.0085	0.01053
138	18.39849	0.0091	0.01134
166	22.13151	0.0099	0.0125
200	26.66447	0.0107	0.01395
228	30.3975	0.0112	0.0152

The validation of measured mass flow rate through an orifice is calibrated through Rotameter

Table 5.10 Gas mass flow rate ( $Q_{\text{mass}}$ ) at various

Rota meter reading Lit/min	Volume flow rate m <sup>3</sup> /s	Density Kg/m <sup>3</sup>	Mass flow rate kg/s
300	0.00500	1.1980	0.00599
400	0.00667	1.2154	0.008107
500	0.00833	1.2444	0.010366
550	0.00917	1.2530	0.011490
600	0.01000	1.2733	0.012733
650	0.01083	1.3022	0.014103
700	0.01167	1.3312	0.015535

Table 5.11 Error Differences in between Orifice and Rotameter

Run Number	Mass flow rate (kg/s)		Error (kg/s)
	Orifice	Rotameter	
1	0.00591	0.00599	0.00008
2	0.00809	0.00810	0.00001
3	0.01053	0.01036	-0.00017
4	0.01134	0.01149	0.00015
5	0.01250	0.01273	0.00023
6	0.01395	0.01410	0.00015
7	0.01520	0.01553	0.00033

Average error:- 0.00011 kg/s

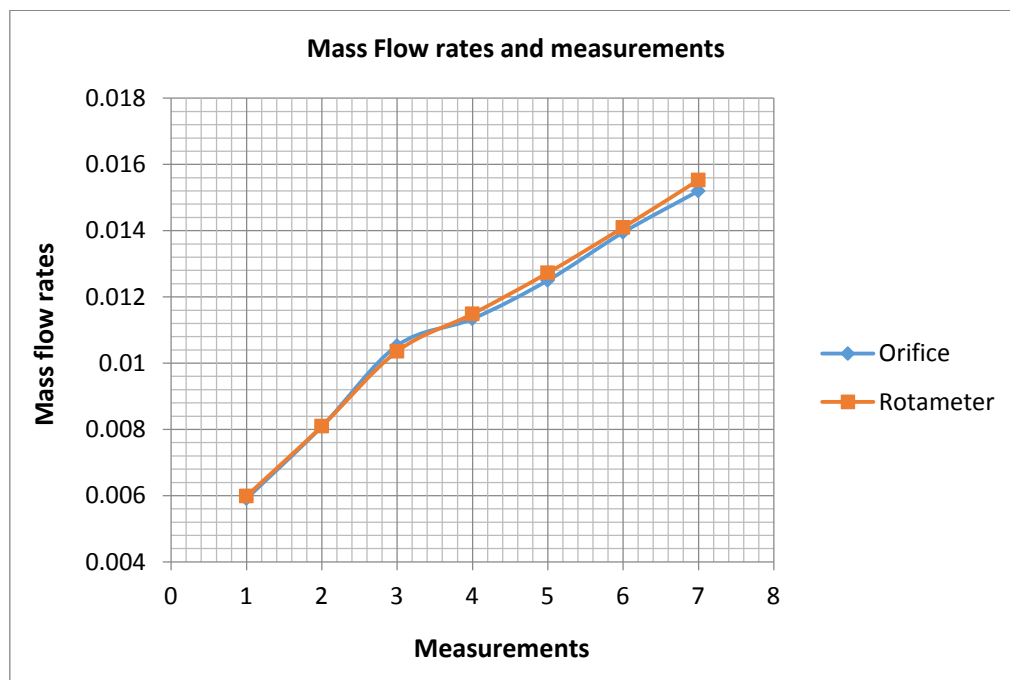


Figure 5.19 Mass flow rates of Devices



## 5.5. Estimation of heat exchanger Performance

The performance evaluation based on the calculation are presented below

The calculations present of this experiment are:

- a) Apply the energy balance equation on a Plate-Fin Heat exchanger
- b) Examine the effect of change of flow rates on the effectiveness of the Plate-Fin Heat exchanger
- c) Determine the heat transfer and pressure drops for fins of the heat exchanger.
- d) Compare the performance between hot and cold flow test.

## 5.6. Effect of heat leaks surrounding

Heat leak to the surroundings through the wall degrade the performance of the cryogenics heat exchanger as the temperature difference between the ambient and heat exchanger is too high. So the heat leak is dramatically more as compared to the ordinary system. Therefore, many researchers investigated heat leak from surrounding. Associated document presented for insulating the system to prevent heat interaction between the fluid and the surrounding.

Wood *et al.* [135] resolve a solution for longitudinal heat conduction and heat leak from surrounding to the wall unconventionally and develop governing differential equations. They justified the needs of the design engineer and achieved a closed iterative technique to govern heat exchanger effectiveness since heat loss to the atmospheres is an inadequate assessment. Chowdhury *et al.* [136] provide the equation for effectiveness without an iterative procedure by considering heat leak terms. Barron [137] derived the equation for two cases i.e. first is for the heat loss from the hot side to the surrounding and second is to gain heat from the surrounding to the cold side. Gupta [138] consider the degradation factor for the decline in the performance of the heat exchanger due to heat leak from surrounding and longitudinal conduction through the wall by experiment.

The heat leak from surrounding is prohibited or minimized by using thermal insulation. The thermal insulations for cryogenics systems required a high level of a prevention method. The temperature difference between the insulation layers might be in between the range of 4K to 400K. The purpose of insulation is to interrupt the interaction between cold and hot

boundaries by interposing some thermal resistance. Thermal resistance reduces the heat conductivity. As the relationship between thermal conductivity (k) and thermal resistance (R) given as

$$k = \frac{d}{R}$$

5.21

Where

‘d’ is the distance of heat flow

In the present test apparatus ‘bulk filling’ technique is used for insulation. The experimental setup is supported with steel structure covered with thermacol filled with perlite powder. So the main component of insulation is perlite powder. Expanded perlite offers better insulation. It has low thermal conductivity; it is incombustible and easy to handle. Expanded perlite sustained reliable measures at low temperature about in the range of 4.26 K to 1366 K and it prevents the system from moisture. The demerit of expanded perlite dust is that it causes chronic poisoning.

The plate fin heat exchanger put inside the cold box filled with perlite covered with thermocol and the pipelines are insulated with foam and perlite dust supported with thermocol. The RTD’s sensors were placed inside the insulation and insulated perfectly from ambient temperature. The conducted wire of RTD’s taken out from the insulation through the tiny holes.

## 5.7. Experimental error analysis

Error estimation in an experimental setup is accomplished by uncertainty analysis. Uncertainty analysis is comprised with two errors one is fixed and another is random error. In every experimental test performance, uncertainty analysis depends on the accuracy of the instruments and gauges to define the result properly. The session describes the work process to achieve the consistency by calculating the uncertainty. So this section contains the experimental error analysis which occurs due to the instrumentation error from the measurement.

Although there are different methods are there to find uncertainty in the experimental setup, a suitable method is adopted in this session. The more accurate method was presented by Kline *et al.* [152]. The Kline-McClintock Method determines the uncertainty of a calculation given certain measurements and the tolerances on those measurements. Root –Sum squared method is used to determine the uncertainty in which the uncertainty in the result depends upon on the variable.

Since the present work is mainly effected by temperature and mass flow rate through which effectiveness is evaluated. Therefore, effectiveness has been admitted for error analysis as followed.

Suppose the uncertainty or error is denoted by  $\pm\delta R$  (i.e. Change in the result ‘R’)

Since R is a function of the variable  $x_1, x_2, \dots, x_n$

$$\text{Or } R = R(x_1, x_2, \dots, x_n)$$

5.22

Then,  $x_1, x_2, \dots, x_n$  is the variance of Result ‘R’ and  $\pm\delta x_1, \pm\delta x_2, \dots, \pm\delta x_n$  are the uncertainties of the variables.

For the uncertainty for one independent variable, the resulting uncertainty is given by

$$\delta R = \left( \frac{\partial R}{\partial x_1} \delta x_1 \right)$$

5.23

∴ For ‘nth’ numbers of independent variable using Taylor theorem

$$\delta R = \left( \frac{\partial R}{\partial x_1} \delta x_1 + \frac{\partial R}{\partial x_2} \delta x_2 + \frac{\partial R}{\partial x_3} \delta x_3 + \dots + \frac{\partial R}{\partial x_n} \delta x_n \right)$$

5.24

$$\text{or } \delta R = \sum_{i=1}^n \left( \frac{\partial R}{\partial x_i} \delta x_i \right)$$

5.25

But according to Kline *et al.* [152] the uncertainty is described by the expanding the equation (5.26) regarding root-sum-square i.e.

$$\delta R = \left\{ \sum_{i=1}^n \left( \frac{\partial R}{\partial x_i} \delta x_i \right)^2 \right\}^{1/2} \quad 5.26$$

$$\text{or } \delta R = \left\{ \left( \frac{\partial R}{\partial x_1} \delta x_1 \right)^2 + \left( \frac{\partial R}{\partial x_2} \delta x_2 \right)^2 + \dots + \left( \frac{\partial R}{\partial x_n} \delta x_n \right)^2 \right\}^{1/2} \quad 5.27$$

In the present experiment, the result is in the form of effectiveness represented by the equation

$$\eta = \frac{m_1(T_2 - T_1)}{m_2(T_3 - T_1)} \quad 5.28$$

So, the uncertainty in the result of the present experimental setup occurs due to an error in the measurement of temperature and flow rate. The mass flow rate individually depends upon the other variables, mainly on the pressure drop. The resultant  $\eta$  is partial differentiate with the individual variables  $m_1$ ,  $m_2$ ,  $T_1$ ,  $T_2$ ,  $T_3$  accordingly.

$$\frac{\partial \eta}{\partial m_1} = \frac{(T_2 - T_1)}{m_2(T_3 - T_1)} \quad 5.29$$

$$\frac{\partial \eta}{\partial m_2} = \frac{-m_1(T_2 - T_1)}{m_2(T_3 - T_1)} = \frac{-1(T_2 - T_1)}{m_2(T_3 - T_1)} = \frac{(T_1 - T_2)}{m_2(T_3 - T_1)} \quad 5.30$$

$$\frac{\partial \eta}{\partial T_1} = \frac{m_2(T_3 - T_1) \frac{\partial(m_1(T_2 - T_1))}{\partial T_1} - m_1(T_2 - T_1) \frac{\partial}{\partial T_1} m_2(T_3 - T_1)}{m_2^2(T_3 - T_1)^2} \quad 5.31$$

$$\frac{\partial \eta}{\partial T_1} = \frac{m_2(T_3 - T_1)(-m_1) - m_1(T_2 - T_1)(-m_2)}{m_2^2(T_3 - T_1)^2} \quad 5.32$$

$$\frac{\partial \eta}{\partial T_1} = \frac{(m_2T_3 - m_2T_1)(-m_1) - (m_1T_2 - m_1T_1)(-m_2)}{m_2^2(T_3 - T_1)^2} \quad 5.33$$

$$\frac{\partial \eta}{\partial T_1} = \frac{-m_1m_2T_3 + m_1m_2T_1 + m_1m_2T_2 - m_1m_2T_1}{m_2^2(T_3 - T_1)^2} \quad 5.34$$

$$\frac{\partial \eta}{\partial T_1} = \frac{m_1(T_2 - T_3)}{m_2(T_3 - T_1)^2} \quad 5.35$$

$$\frac{\partial \eta}{\partial T_2} = \frac{\partial}{\partial T_2} \left( \frac{m_1(T_2 - T_1)}{m_2(T_3 - T_1)} \right) \quad 5.36$$

$$\frac{\partial \eta}{\partial T_2} = \frac{\partial}{\partial T_2} \left( \frac{m_1T_2}{m_2(T_3 - T_1)} - \frac{m_1T_1}{m_2(T_3 - T_1)} \right) \quad 5.37$$

$$\frac{\partial \eta}{\partial T_2} = \frac{1}{T_3 - T_1} \quad 5.38$$

$$\frac{\partial \eta}{\partial T_3} = \frac{\partial}{\partial x} \left( \frac{m_1(T_2 - T_1)}{x} \right) \frac{\partial x}{\partial T_3} \quad 5.39$$

$$\frac{\partial \eta}{\partial T_3} = \left( \frac{-m_1(T_2 - T_1)}{m_2(T_3 - T_1)^2} \right) \quad 5.40$$

$$\partial \eta = \sqrt{\left( \frac{\partial \eta}{\partial m_1} \partial m_1 \right)^2 + \left( \frac{\partial \eta}{\partial m_2} \partial m_2 \right)^2 + \left( \frac{\partial \eta}{\partial T_1} \partial T_1 \right)^2} \quad 5.41$$

The experiment was conducted in sets under the various range of temperature from 106 K to 308 K. The accuracy of the experimental setup depends on upon the experiences of the person and mainly the "precision" of the measurement devices. The error occurred due to the measurement of the experimental data is mainly for mass flow rate and temperature.

The mass flow rate is calculated through the volumetric flow rate to take by using Rotameter at the outlet of the heat exchanger at a particular pressure and temperature. The calibration chart provided shows the accuracy of the Rotameter, which is within the limit error of  $\pm 12$  litres/min described by the supplier of the instrument.

Resistance temperatures detectors (RTD) are attached at the inlet and the outlet of the high-pressure stream and to the low-pressure stream and calibrated through an experimental procedure explain earlier. The supplier provides the accuracy of about  $\pm 0.5\%$  or  $\pm 0.1^\circ\text{C}$ .

## Chapter VI

# PERFORMANCE ANALYSIS

A cryogenic heat exchanger setup is designed and fabricated to study the heat exchanger performance in a practical and efficient manner. It is necessary to test the performance of a heat exchanger which performs under cryogenic temperature. The performance analysis is conducted to find out the effectiveness and pressure drop of the heat exchanger.

In this section tabulated experimental data are presented in Table 6.1 to 6.4. The Tables depict the test condition to determine the performance of Plate- Fin heat exchanger at cryogenic temperature. The experiment is conducted to collect the data for both the sides (high-pressure side and low-pressure side) at a different flow rate ranging from 6.02 gm/sec to 14.41 gm/sec and at different inlet temperatures to calculate effectiveness and pressure drop across both the sides (hot and cold loops). The calculate data represented in a form of a graph, comparing experimental results with the existing correlations. Aspen MUSE<sup>®</sup>, which is a proprietary software available for design and rating of plate fin heat exchangers, uses proprietary correlations for j–f factors of fins.

### 6.1. Experimental results of cold and hot tests

Table 6.1 Test Data for a range of Mass Flow Rate at cold inlet temperature of 107K

Mass flow rate Lt/min	Hot inlet Pressure	Cold inlet pressure	Pressure drop Hot Inlet	Pressure drop Cold Inlet	Hot Inlet Temperature	Hot Outlet Temperature	Cold Inlet Temperature	Cold Outlet Temperature
300	0.05	0.037	5	5	307.5	128.2	107.8	281.5
400	0.09	0.059	7	6	307.4	127.0	106.7	282.1
500	0.14	0.089	9	8	307.4	124.6	106.1	282.5
550	0.16	0.097	11	10	308.1	124.8	106.8	283.1
600	0.18	0.119	13	12	307.9	125.2	107.8	282.6
650	0.20	0.147	15	14	308.2	125.0	108.1	282.6

Table 6.2 Test Data for a range of Mass Flow Rate at cold inlet temperature of 111K

Mass flow rate Lt/min	Hot inlet Pressure	Cold inlet pressure	Pressure drop Hot Inlet	Pressure drop Cold Inlet	Hot Inlet Temperature	Hot Outlet Temperature	Cold Inlet Temperature	Cold Outlet Temperature
300	0.05	0.037	6	5	308.8	133.0	111.2	281.6
400	0.09	0.059	8	6	308.8	131.2	111.1	283.8
500	0.14	0.089	10	8	308.5	129.3	110.9	283.8
550	0.16	0.097	11	10	308.8	129.3	111.4	284.0
600	0.18	0.119	13	12	307.9	129.4	110.8	282.6
650	0.20	0.147	15	14	308.2	129.0	112.1	282.8

Table 6.3 Test Data for a range of Mass Flow Rate at cold inlet temperature of 117K

Mass flow rate Lt/min	Hot inlet Pressure	Cold inlet pressure	Pressure drop Hot Inlet	Pressure drop Cold Inlet	Hot Inlet Temperature	Hot Outlet Temperature	Cold Inlet Temperature	Cold Outlet Temperature
300	0.05	0.037	6	6	307.4	138.6	117.7	281.3
400	0.09	0.059	8	7	307.6	137.1	117.9	283.5
500	0.14	0.089	9	9	307.5	134.0	116.1	283.5
550	0.16	0.097	11	10	307.8	134.8	117.6	283.9
600	0.18	0.119	13	12	307.9	133.9	116.8	283.4
650	0.20	0.147	15	14	308.2	134.5	118.2	283.6

Table 6.4 Test Data for a range of Mass Flow Rate at cold inlet temperature of 122K

Mass flow rate Lt/min	Hot inlet Pressure	Cold inlet pressure	Pressure drop Hot Inlet	Pressure drop Cold Inlet	Hot Inlet Temperature	Hot Outlet Temperature	Cold Inlet Temperature	Cold Outlet Temperature
300	0.05	0.037	6	5	308.4	142.5	122.1	282.9
400	0.09	0.059	8	6	308.5	139.6	120.5	284.8
500	0.14	0.089	11	8	308.4	137.4	119.8	284.8
550	0.16	0.097	12	10	308.4	136.7	119.4	284.5
600	0.18	0.119	14	12	308.6	137.2	120.4	284.5
650	0.20	0.147	15	14	308.8	138.0	121.8	284.5



The experimental data along with the analytical and simulated result are presented. The effectiveness and pressure drop as a function of mass flow rate is represented. The Colburn factor and friction factor Vs Reynolds number is also determined from the experimental data and it is represented with analytical values in Table 6.8 to 6.11. The flow rates various from 300 liters/min to 650 liters/min.

### **6.1.1. Effectiveness of Plate –Fin Heat Exchanger at different mass flow rate**

Effectiveness is one of the measures to test the thermal performance of a heat exchanger. Effectiveness defines as the actual rate of heat transfer to that of the maximum rate of heat transfer. The value of heat exchanger effectiveness lies in between zero to one. Ideally, the heat loss by the one stream (hot stream) must gain by the other fluid (cold stream), but there is always heat loss due to heat imbalance occurred during the experiment even after maintaining perfect insulation. Hence, the loss of energy in a form of heat develops the differences in the effectiveness of both the sides of heat exchanger i.e.  $\epsilon_h$  and  $\epsilon_c$  respectively. To achieve more efficient heat exchanger, the effectiveness should approach to 1.

The Effectiveness of Plate–Fin Heat Exchanger for different mass flow rate at various Inlet temperatures is represented by the graphs shown in Figures 6.1 to 6.4. Equation 5.8 is applied to find out the effectiveness and the outlet temperatures at the exit of both the sides of the heat exchanger. Volumetric Flow rate of Nitrogen gas from 300 liters/min to 650 liters/min are applied for both hot and cold side. The effect of mass flow rate in kg/s on the effectiveness obtained through calculation by correlations is also illustrated in Figures. It is observed from the Figure 6.1 to 6.4 that the effectiveness of a given heat exchanger increases with the increase of mass flow rate. Although primarily the flow boundary layers are laminar, but the wake effect due to the offset fins behave as turbulent flow. The flow rate enhances the performance of heat exchanger up to a certain extent by enhancing the heat transfer rate. The representation of Colburn factor against Reynolds number in a flow region represents the effect of heat transfer as shown in Figure 6.8 - 6.11.

The experimental result deviates from the analytical data by using correlation. The deviation in the result is due to the heat loss which is not considered for calculating analytical data. Therefore, the values of the effectiveness using correlation are more over a same flow rate as compared to the experimental values. The variation in the experimental and predicted value

shown in Table 6.5 in the form of error percentage when the cold inlet temperature is 107K. It is concluded from the Table that the error percentage is decreasing as the mass flow rate increases.

Table 6.5 Error percentage when the inlet temperature is 107K

Mass flow rate (g/s)	Error Percentage			
	Maity and Sarangi	Manglik and Bergles	Joshi and Webb	Muse <sup>®</sup>
6.029	3.94 %	2.72 %	4.76 %	1.73 %
8.201	4.05 %	2.63 %	5.03 %	1.77 %
10.52	3.60 %	1.87 %	4.62 %	1.76 %
11.68	3.53 %	1.67 %	4.57 %	1.75 %
12.98	3.51 %	1.50 %	4.56 %	1.75 %
14.41	3.43 %	1.27 %	4.50 %	1.75 %

Figure 6.1 – 6.4 shows the variation between experimental data simulation results and by various correlations. The axes of graph from Figure 6.1 – 6.4 representing the effectiveness with the vertical axis, while the mass flow rate by the horizontal axis. The lines with rectangular, triangular and diamond shape dotted points represent the experimental data and the line with cross shape dotted point represent the simulation data. The other three lines correspond the analytical data by various correlation developed by Maity & Sarangi, Joshi & Webb and Manglik & Barglus. It is depicted by a circle, plus and star shape dotted points.

The variation in the mean experimental value with simulated and analytical value as shown in Figures 6.1- 6.4 is due to experimental error or uncertainty for which equations are derived in earlier chapter. The variation in mean experimental value with the various correlation results because of Uncertainty and the leakage of heat to the surrounding, considering the effect due to longitudinal heat conduction. The average of percentage error for Maity & Sarangi, Manglik & Barglus and Joshi & Webb is 3.68%, 1.94% and 4.67 respectively. Whereas the the mean percentage error between the Muse<sup>®</sup> and experimental values is 1.75%.

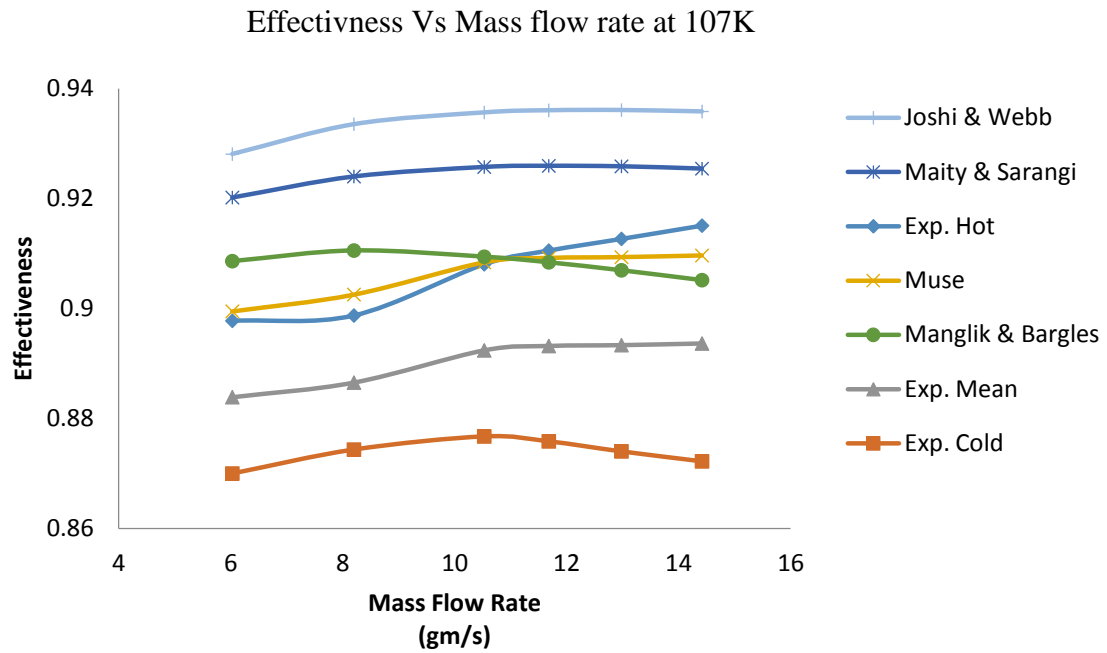


Figure 6.1 Variation of effectiveness with mass flow rate

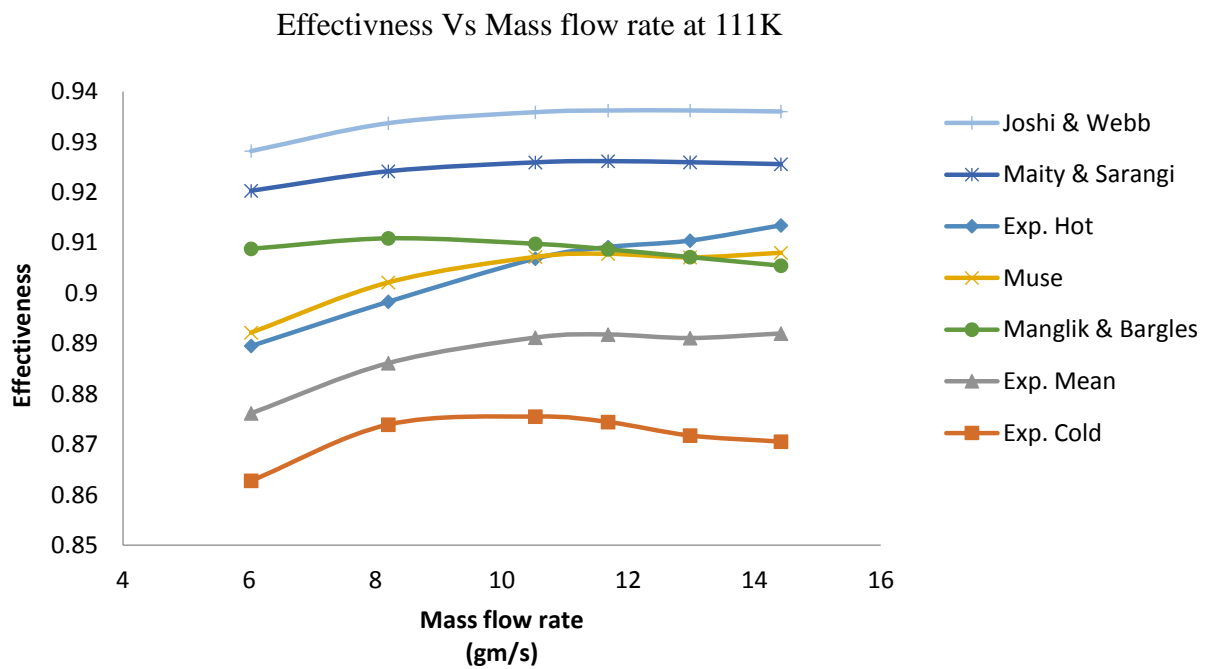


Figure 6.2 Variation of effectiveness with mass flow rate

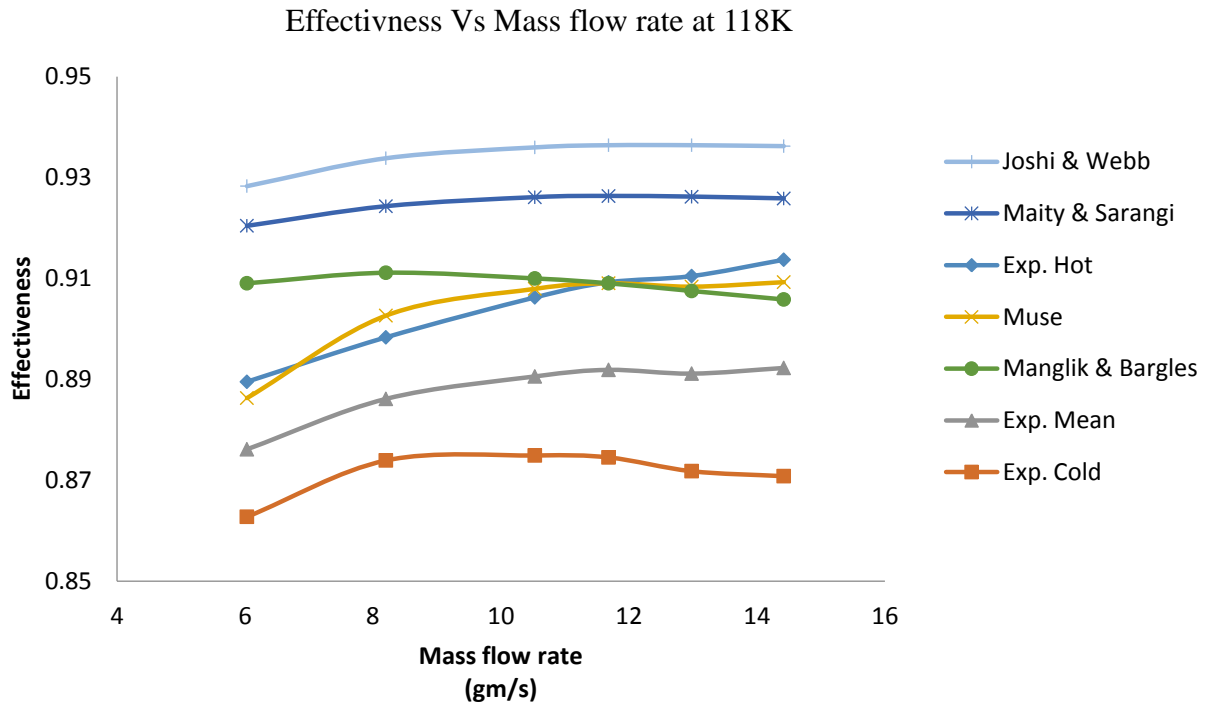


Figure 6.3 Variation of effectiveness with mass flow rate

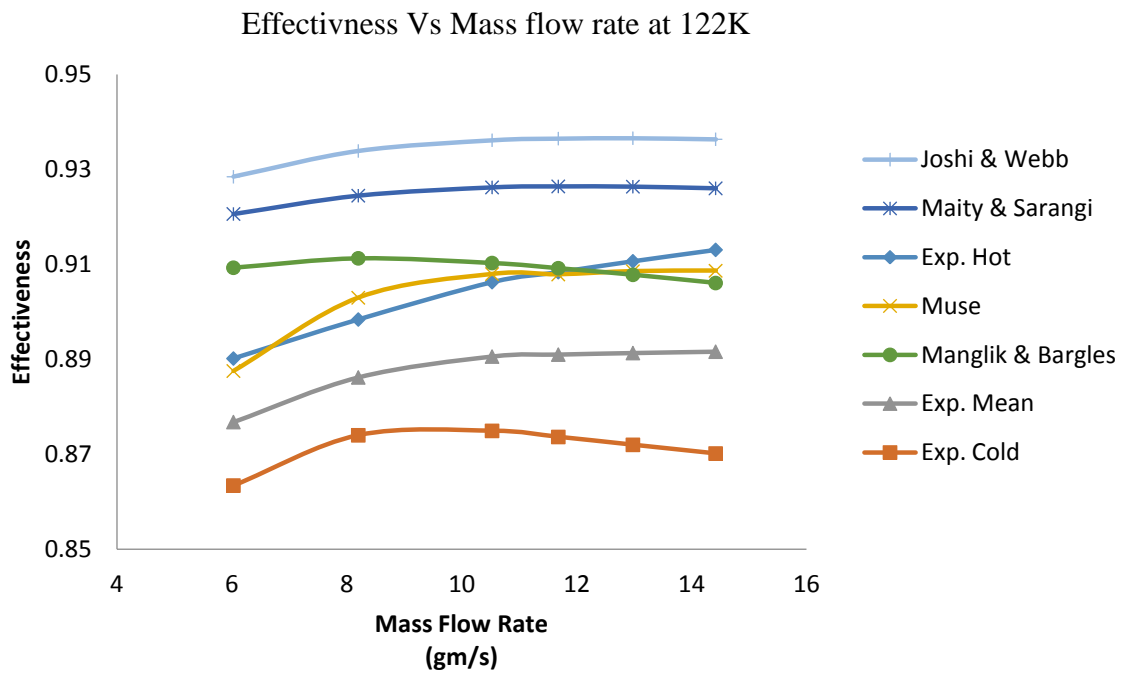


Figure 6.4 Variation of effectiveness with mass flow rate

## 6.2 Comparison of effectiveness of cold and hot tests

Present experiment performance at cold inlet temperature is compared with the earlier experiment performance at hot inlet condition by Alur [151]. The comparison is made for a set of data for each at inlet temperature of 107K for cold test and inlet temperature of 369K from hot test. In this figure different sets of data were used from hot and cold test for the range of mass flow rate of 300 liters/min to 650 liters/min. It is shown in Figure 6.5 that the initially gaining in the effectiveness in the heat exchanger at cold test goes almost same for further increment in mass flow rate at hot test. The reason behind initially gaining in the effectiveness is that at low flow rate the temperature differences are significant more between the heat transfer surface area. This means that better heat exchanger flow arrangements must have an increasing effectiveness. Even the input conditions for hot and cold test are not same and thus the effectiveness of the heat exchanger should not similar but it may be near about each other as per the experimental data.

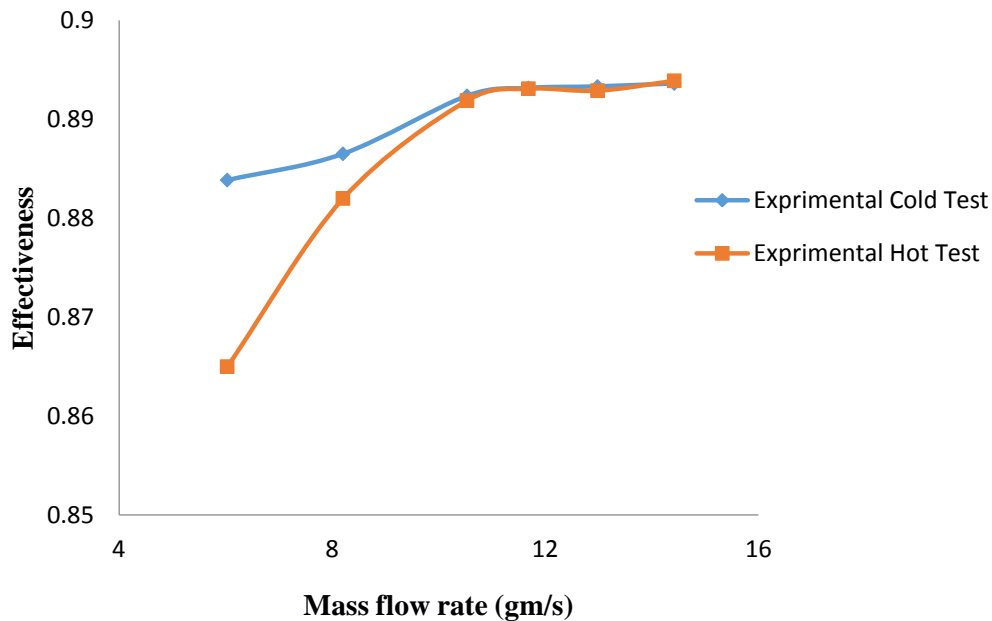


Figure 6.5 Comparison of effectiveness with cold and hot tests

## 6.3 Effect of heat transfer to surrounding

The performance of plate-fin heat exchanger is evaluated under steady state conditions; the heat transfer rate is constant i.e. heat loss by hot system is carried out by the cold system. The heat balance determines the amount of heat loss or gain by the system. To maintain heat balance in the system high quality of insulation is provided even though there

is a certain amount of heat leak from the system. Due to the heat loss, the temperature difference between the hot and cold fluid varies. The divergence in the noted value from the actual value shows the heat loss. Thus, the different value of effectiveness is evaluated for hot side and cold side.

The heat balance equation for heat exchanger is given by

$$\dot{m}c_p(T_{co} - T_{ci}) = \dot{m}c_p(T_{hi} - T_{ho}) \quad 6.1$$

•• For steady flow operation under unbalanced condition

$$\dot{m}c_p(T_{co} - T_{ci}) - \dot{m}c_p(T_{hi} - T_{ho}) = 0 \quad 6.2$$

The calculated heat leak value is substituted in leak heat option in the process of Aspen Muse<sup>®</sup>. The process of simulation also generates the two considerable values of effectiveness as indicated in Figure 6.6 by the triangular dotted line for cold effectiveness while the diamond dotted lines represents the hot effectiveness. The values obtain from the simulation under the same operating condition i.e. at a same mass flow rate at an inlet temperature of 107K. Since the simulation does not consider the uncertainty the result deviates from the experimental result and the trend of the line is as shown in Figure 6.6.

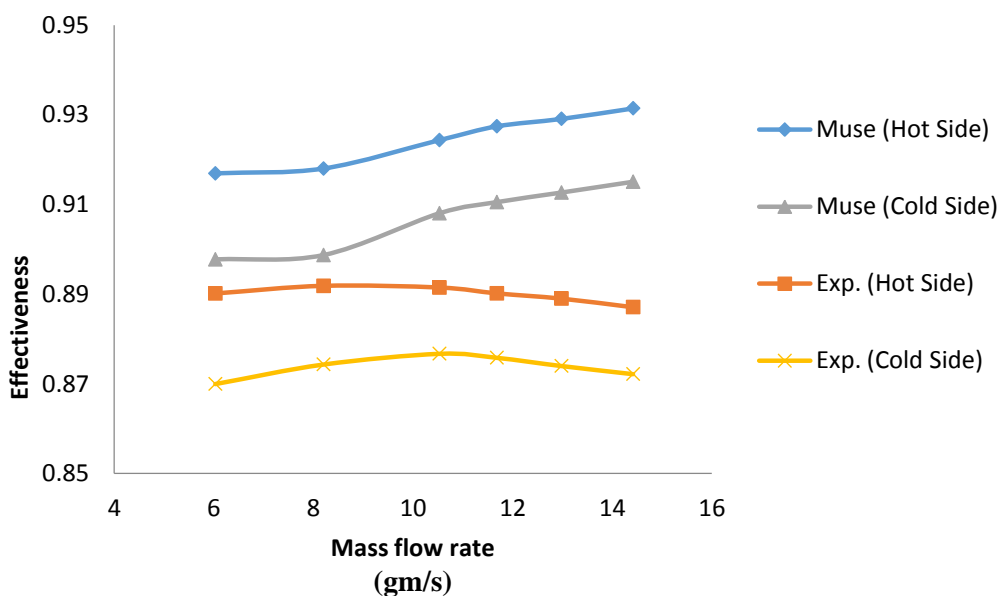


Figure 6.6 Variation of effectiveness with mass flow rate

## 6.4 Validation of effectiveness obtained with and without heat loss with cold tests

It is clear from the Figure 6.7, that the mean effectiveness of experimental result matches well with simulation result by Muse<sup>®</sup>. The points on the lines are almost coinciding with each other but a small variation occurs at low mass flow rate which is within experimental error. (Calculated heat leak in Appendix)

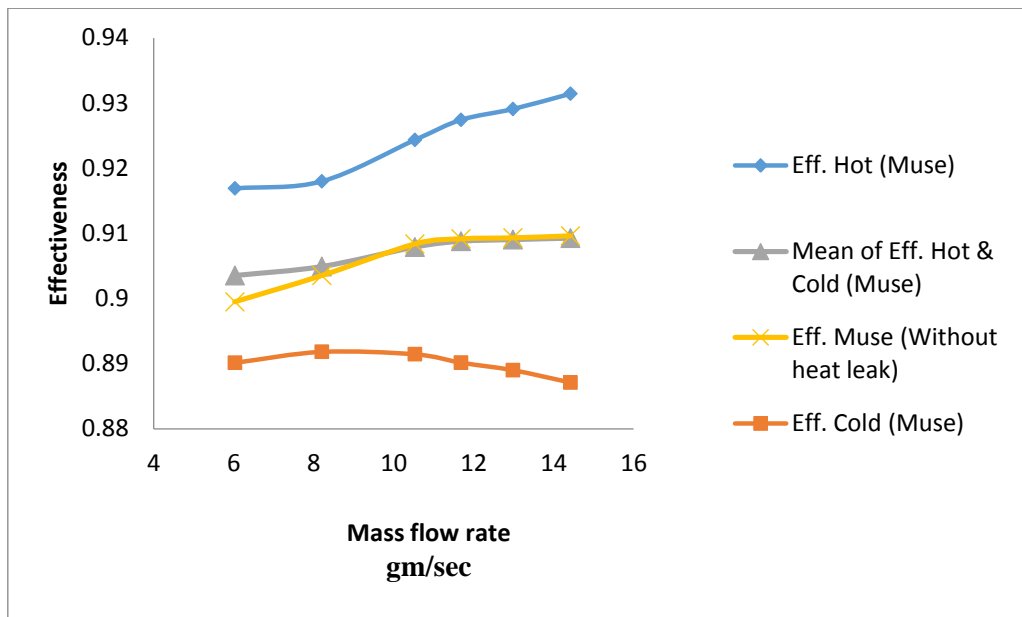


Figure 6.7 Variation of effectiveness with mass flow rate

## 6.5 Uncertainty assessment in experimental results

The uncertainty in the calculated effectiveness can be determined by using equation 5.9 to 5.14 in the earlier chapter. The error estimation is shown in Table 6.6 developed for the cold inlet temperature of 107K. It seems that the uncertainty decrease with the increase in mass flow rate.

Table 6.6 Uncertainty assessment in the effectiveness in different mass flow rate at 107K

$g / s$	$T_{h,i}$	$T_{h,o}$	$T_{c,i}$	$T_{c,o}$	$\frac{\delta\eta}{\delta m_1} = \frac{\delta\eta}{\delta m_2}$	$\delta m_1$	$\frac{\delta\eta}{\delta T_1}$	$\frac{\delta\eta}{\delta T_2}$	$\frac{\delta\eta}{\delta T_3}$	$\delta\eta$
6.02	307.	128.	107.	281.	144.29	0.00024	0.00435	0.00500	0.00449	0.04950
	5	2	8	5		3	6	8	5	1
8.20	307.	127.	106.	282.	106.60	0.00024	0.00435	0.00498	0.00447	0.03732
	4	0	7	1		8	6	3	8	3
10.52	307.	124.	106.	282.	83.26	0.00025	0.00435	0.00496	0.00451	0.02998
	4	6	1	5		5	5	8	1	2
11.68	308.	124.	106.	283.	74.97	0.00025	0.00435	0.00496	0.00452	0.02717
	1	8	8	1		6	1	8	3	2
12.98	307.	125.	107.	282.	67.33	0.00026	0.00436	0.00499	0.00456	0.02493
	9	2	8	6		2	8	8	1	5
14.41	308.	125.	108.	282.	60.48	0.00026	0.00435	0.00499	0.00457	0.02294
	2	0	1	6		8	9	8	3	7

## 6.6 Heat transfer and friction factor of Heat Exchanger

Another performance criterion is Colburn and friction factor for plate fin heat exchanger are presented below. In this, only the primary test at 107K inlet temperature at different mass flow rate is evaluated. Colburn and friction factor for each mass flow rate have been obtained from the experiment and by using various correlation and are given in Table 6.7 to 6.10. Non-dimensional graphs of Colburn and friction factors on the vertical axis and Reynolds number at horizontal axis are presented. The square dotted points show the experimental data, while the other dotted points show the predicted data by the correlations. The experimental data of Colburn factor and the analytical data calculated from the correlation shown in Table 6.7 and 6.8. These were graphically represented in Figure 6.8 & 6.9.

Table 6.7 Colburn factor at 107K on hot side of PFHX

Mass flow rate	Re	Experimental	Maity	Manglik	joshi
6.06	302.99	0.0176	0.0299	0.0269	0.0372
8.23	415.19	0.0159	0.0248	0.0228	0.0318
10.60	535.73	0.0138	0.0214	0.0200	0.0281
11.74	593.63	0.0132	0.0205	0.0190	0.0267
13.08	659.61	0.0122	0.0196	0.0180	0.0253
14.51	732.79	0.0114	0.0187	0.0171	0.0241



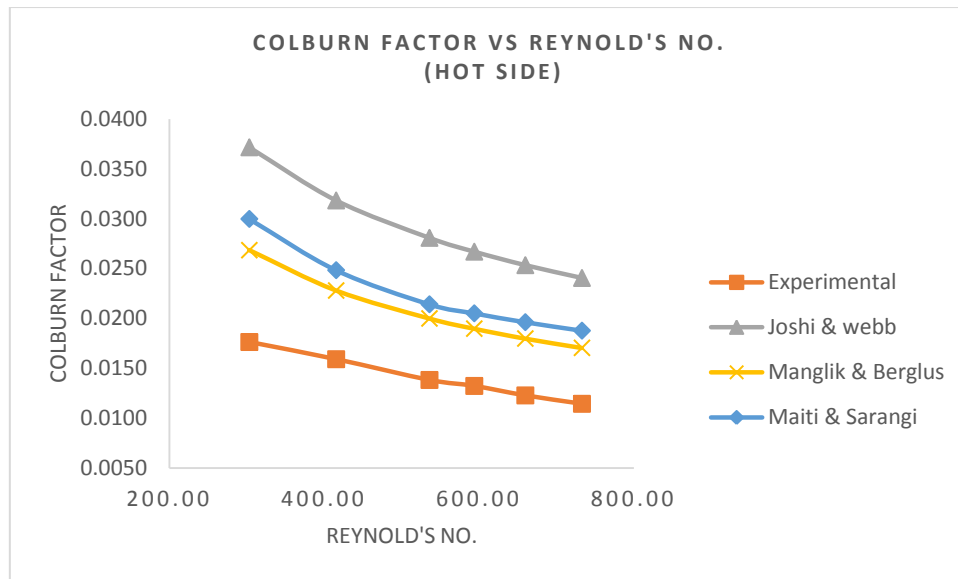


Figure 6.8 Variation of Colburn factor with Reynolds No.

Table 6.8 Colburn factor at 107K on Cold side of PFHX

Mass flow rate	Re	Experimental	Maity	Manglik	joshi
9.66	487.53	0.0180	0.0210	0.0194	0.0273
13.04	660.64	0.0150	0.0182	0.0165	0.0234
16.70	845.53	0.0125	0.0159	0.0145	0.0206
18.65	933.84	0.0113	0.0153	0.0138	0.0196
20.40	1034.22	0.0106	0.0146	0.0131	0.0186
22.61	1145.91	0.0094	0.0140	0.0124	0.0177

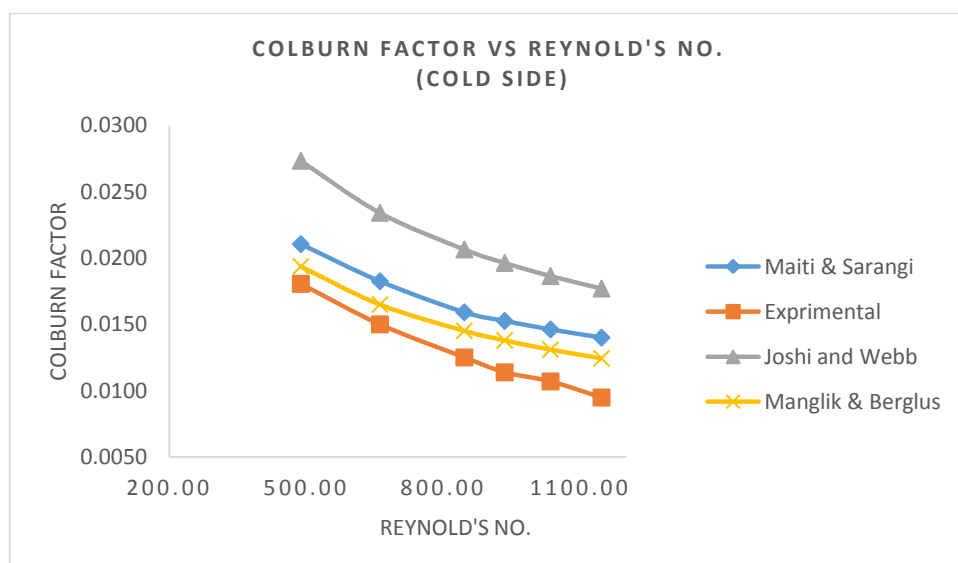


Figure 6.9 Variation of Colburn factor with Reynolds No.

Table 6.9 and 6.10 shows the calculated data of friction factors by using correlations. The experimental friction factor is also listed in the table are calculated from the measured pressure drops through the manometers. From Figure 6.10 and 6.11 it is clear that the Experimental friction factor is higher than the evaluated value, the declination is very well followed with the experimental data and the trend remain same.

Table 6.9 Friction factor at 107K on Hot side of PFHX

Mass flow rate	Re	Experimental	Maity	Manglik	joshi
6.06	302.99	0.1650	0.1305	0.1184	0.0971
8.25	415.19	0.1308	0.1047	0.0962	0.0772
10.60	535.73	0.1074	0.0876	0.0833	0.0642
11.74	593.63	0.1083	0.0815	0.0793	0.0595
13.08	659.61	0.1055	0.0757	0.0757	0.0551
14.51	732.79	0.1003	0.0703	0.0726	0.0510

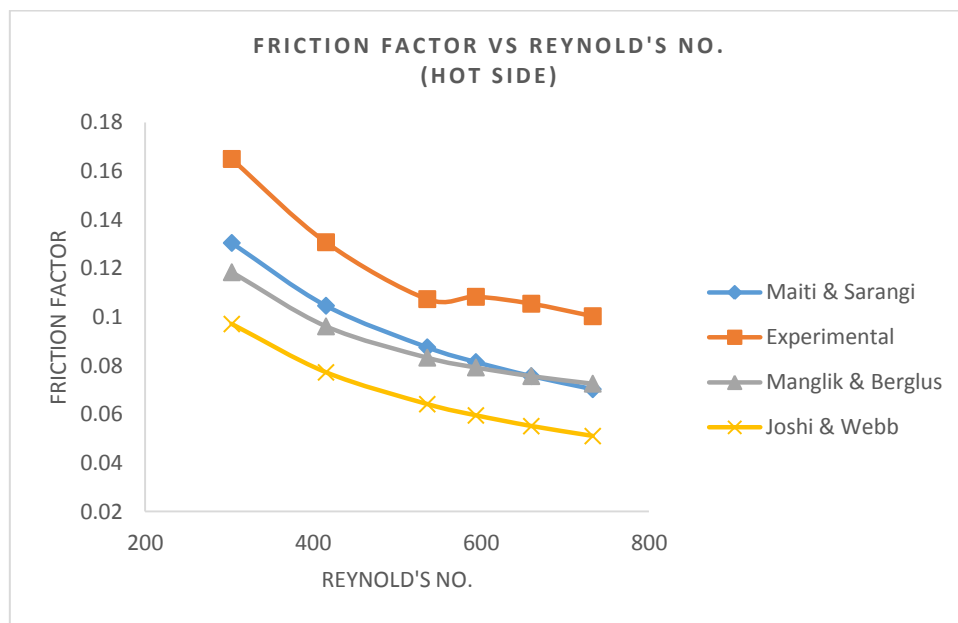


Figure 6.10 Variation of Friction factor with Reynolds No.

Table 6.10 Friction factor at 107K on Cold side of PFHX

Mass flow rate	Re	Experimental	Maity	Manglik	joshi
9.66	487.53	0.1336	0.0870	0.0750	0.0613
13.04	660.64	0.1100	0.0703	0.0619	0.0487
16.70	845.53	0.0912	0.0592	0.0547	0.0404
18.65	933.84	0.0929	0.0552	0.0525	0.0375
20.40	1034.22	0.0917	0.0551	0.0505	0.0348
22.61	1145.91	0.0885	0.0535	0.0486	0.0322

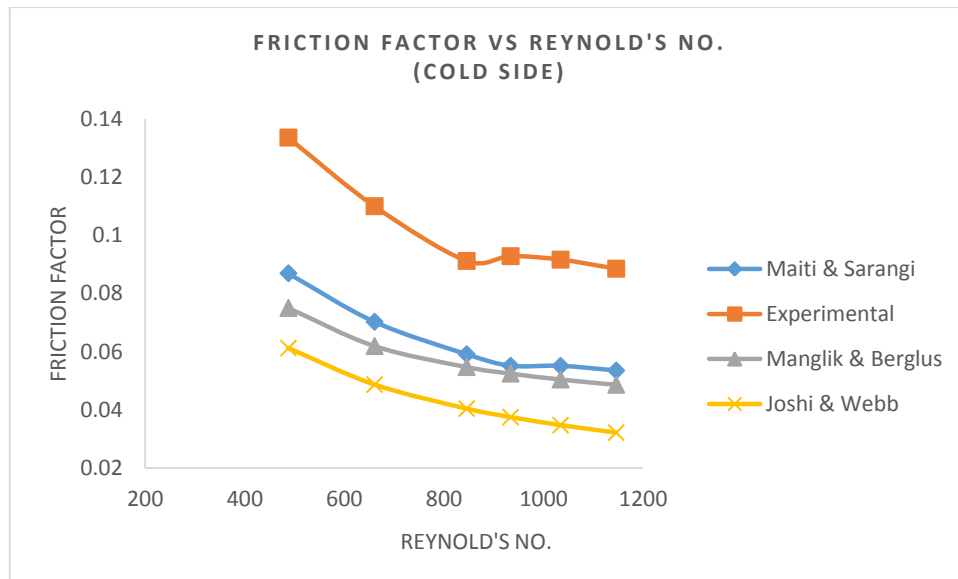


Figure 6.11 Variation of Friction factor with Reynolds No.

## 6.7 Effect of pressure drops with mass flow rate

It is observed that the flow disturbance arises due to the Fins. Fins behave as an obstacle during the flow which is responsible for the heat transfer and pressure drop. Pressure drop is the parameter which emphasizes the characterization of the heat exchanger. So on increasing the size or quantity of fin increases the pressure drop although heat transfer is also increasing. However, the pressure drop is dependent on mass flow rate as shown in figure 6.12 to 6.19. Figures indicate that the pressure drop obtained from the test set up is higher than the simulated and correlated values. The pressure enhancement is due to position of pressure gauges and experimental error in the pressure gauges. Eventually, the pressure drop occurred in the experiment is under reasonable or allowable pressure drop i.e. 0.05 bars. Therefore, it is not necessary to find out the error as it is in the acceptable limit.

For the present experiment mass flow rate varies from 0.006 to 0.021 g/s with the pressure drop variation from 0.0066 to 0.020 bars. In concern, it ensures that the pressure drop across the channel should not exceed more than the allowable pressure drop. The pressure drop across the channel of both side of heat exchanger is illustrated in Figure 6.12 below for inlet temperature of 107K. It shows that there is a slight variation in the pressure drop of the cold and hot side which is due to the differences in inlet pressure, temperature, and geometry.

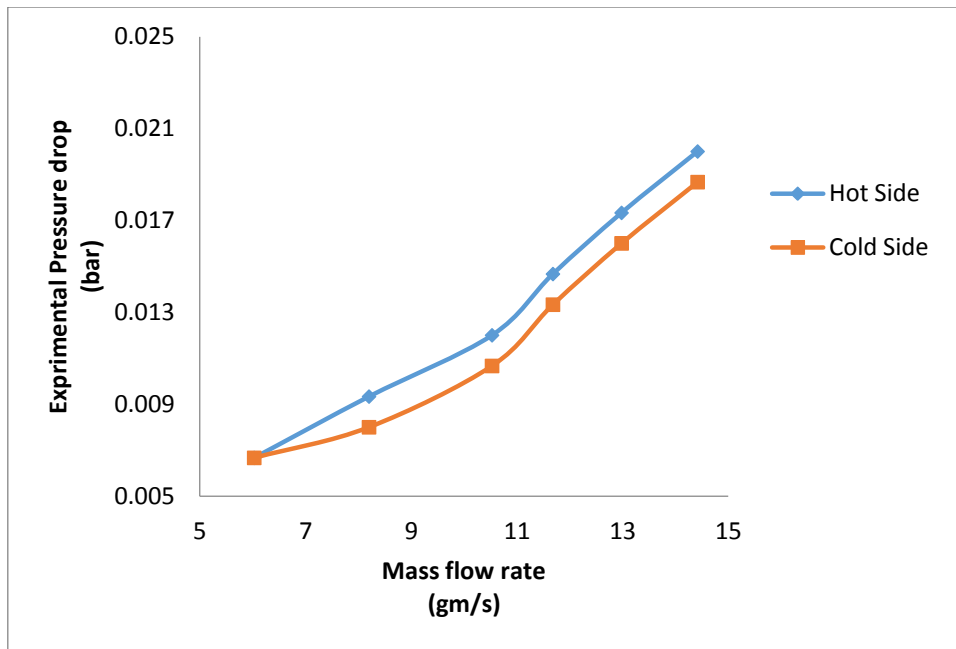


Figure 6.12 Pressure drop across the channel of both side

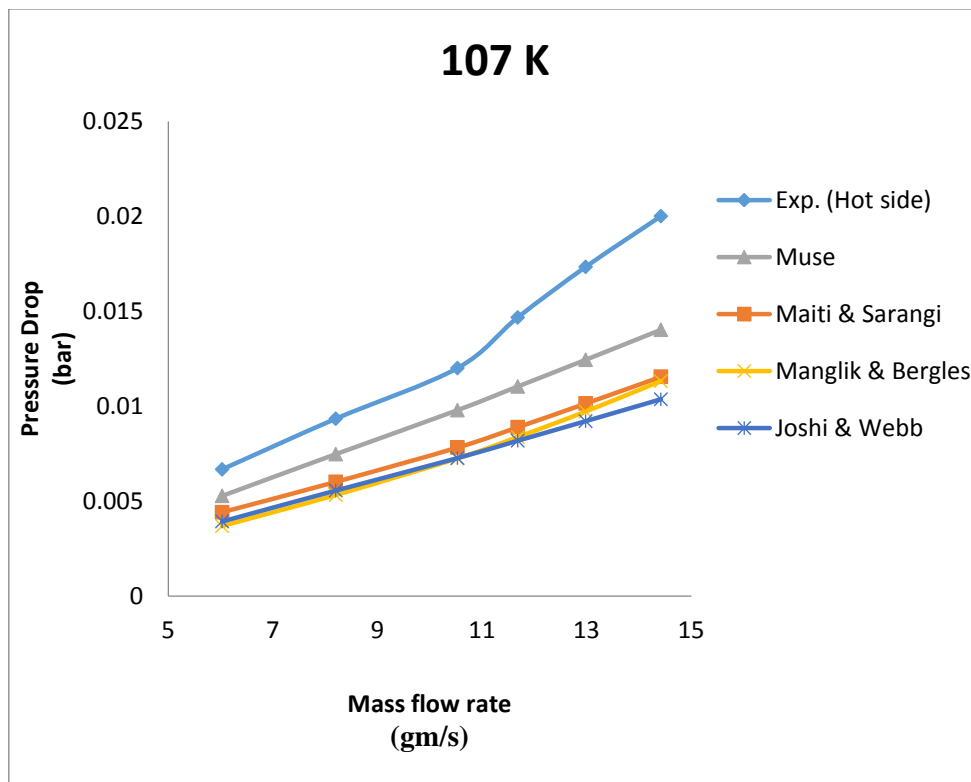


Figure 6.13 Variation of Pressure drop with mass flow rate at 107K (Hot Side)

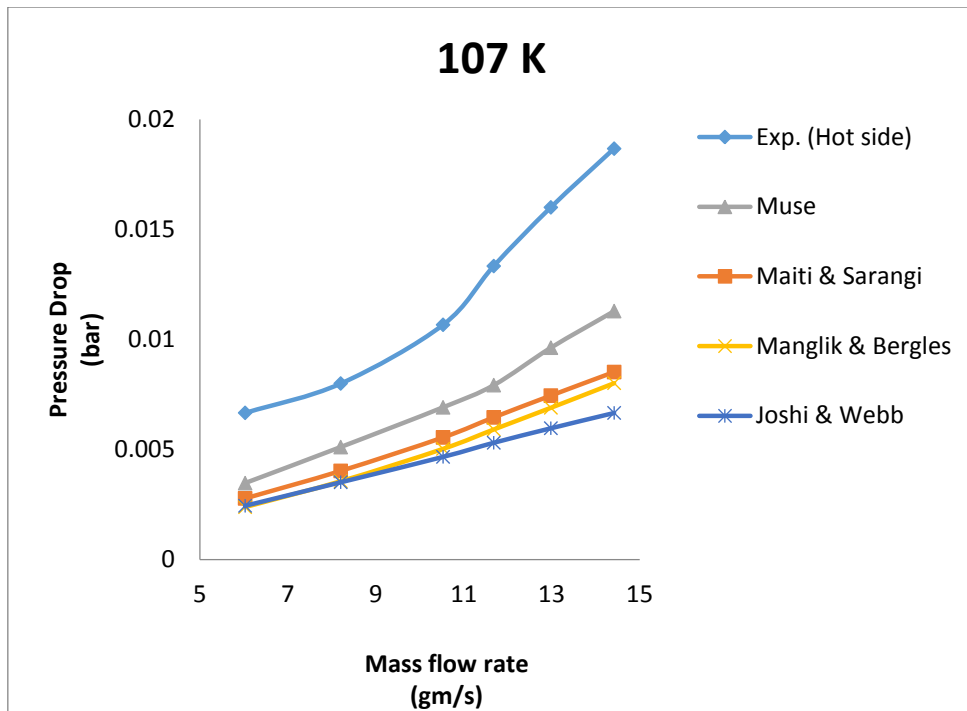


Figure 6.14 Variation of Pressure drop with mass flow rate at 107 (cold Side)

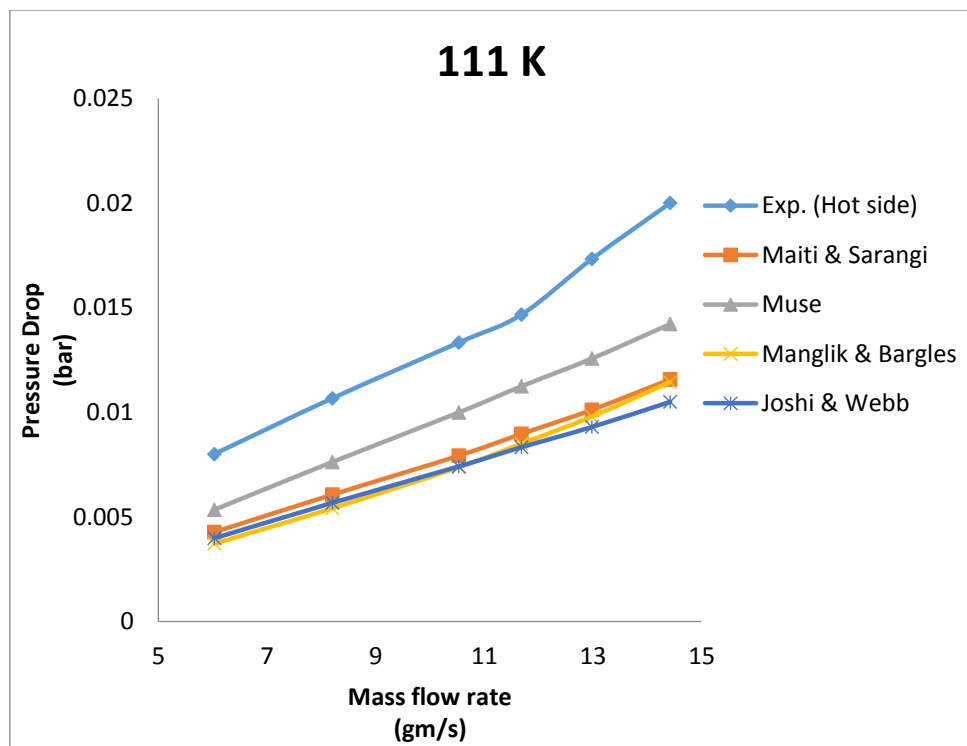


Figure 6.15 Variation of Pressure drop with mass flow rate at 111 K (Hot side)

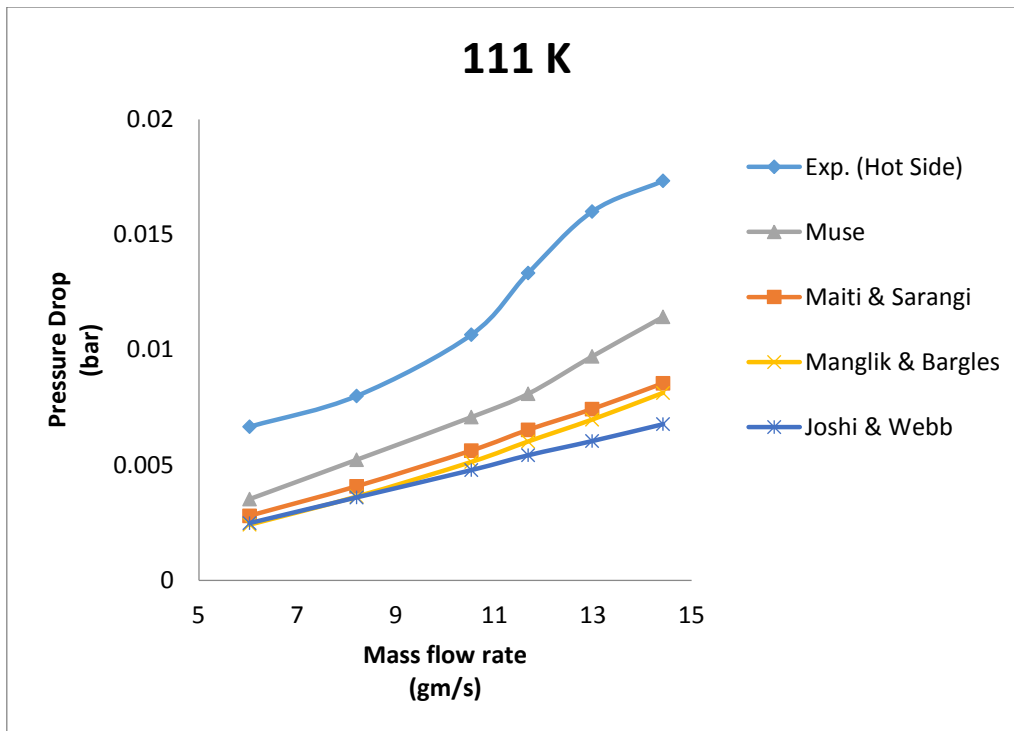


Figure 6.16 Variation of Pressure drop with mass flow rate at 111 K (Cold side)

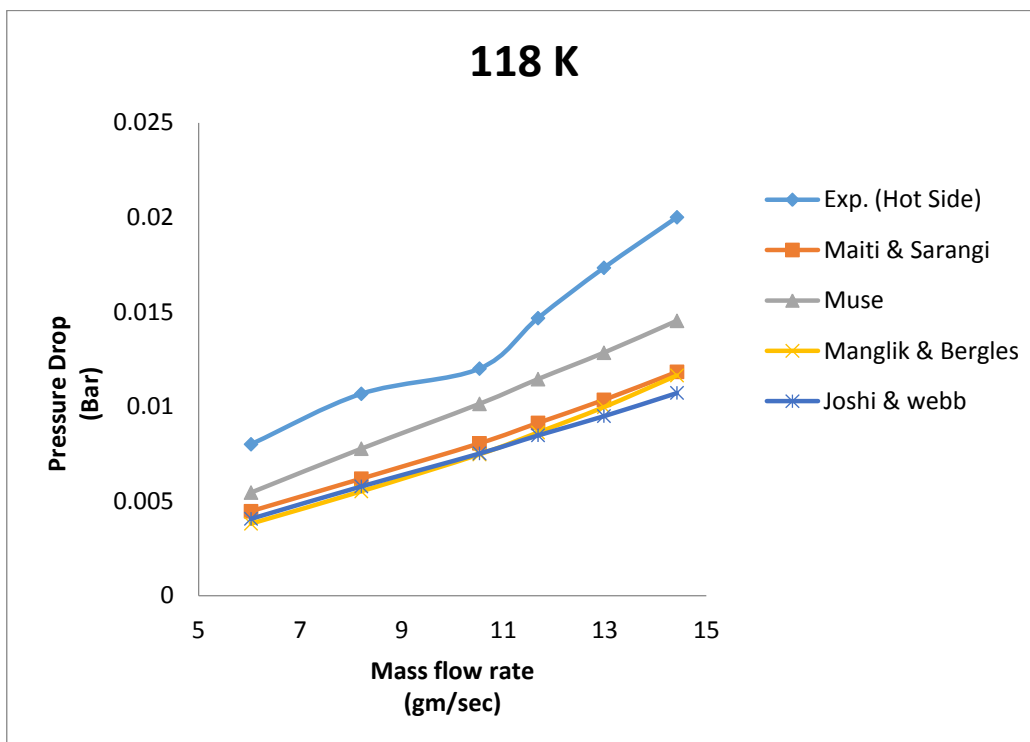


Figure 6.17 Variation of Pressure drop with mass flow rate at 118 K (Hot side)

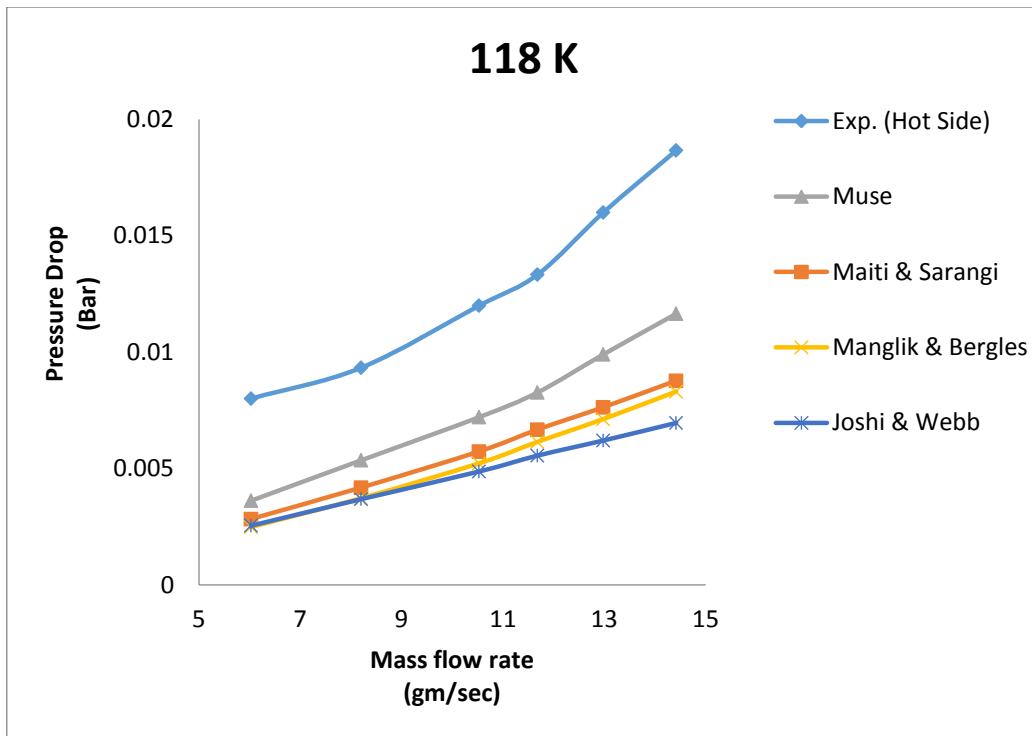


Figure 6.18 Variation of Pressure drop with mass flow rate at 118 K (Cold side)

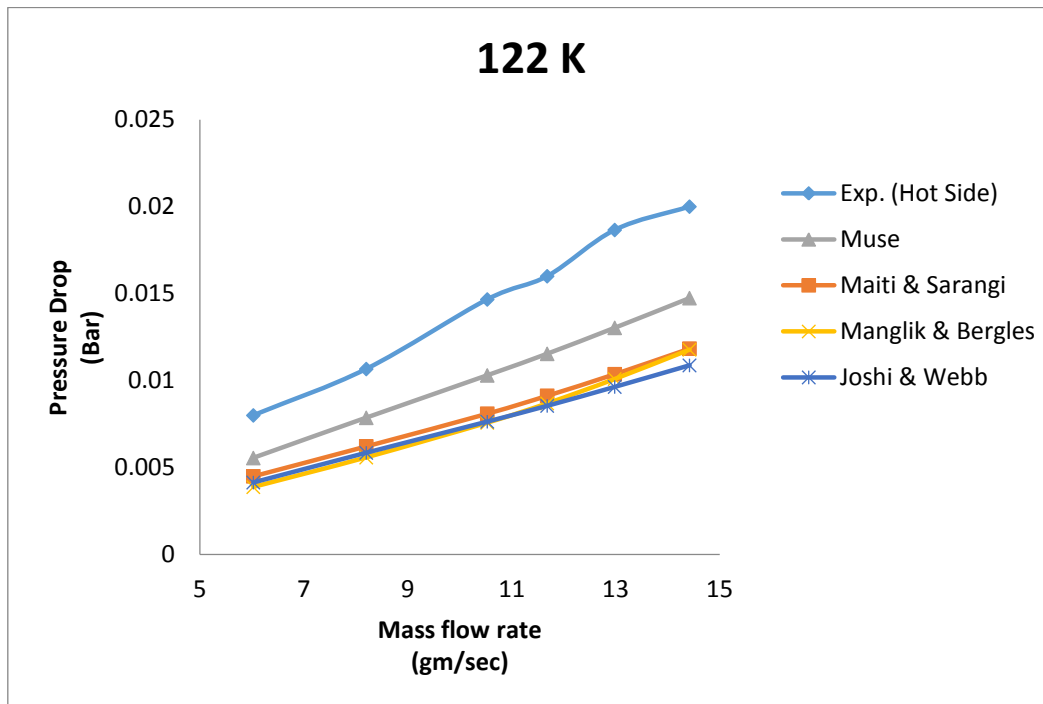


Figure 6.19 Variation of Pressure drop with mass flow rate at 122 K (Hot side)

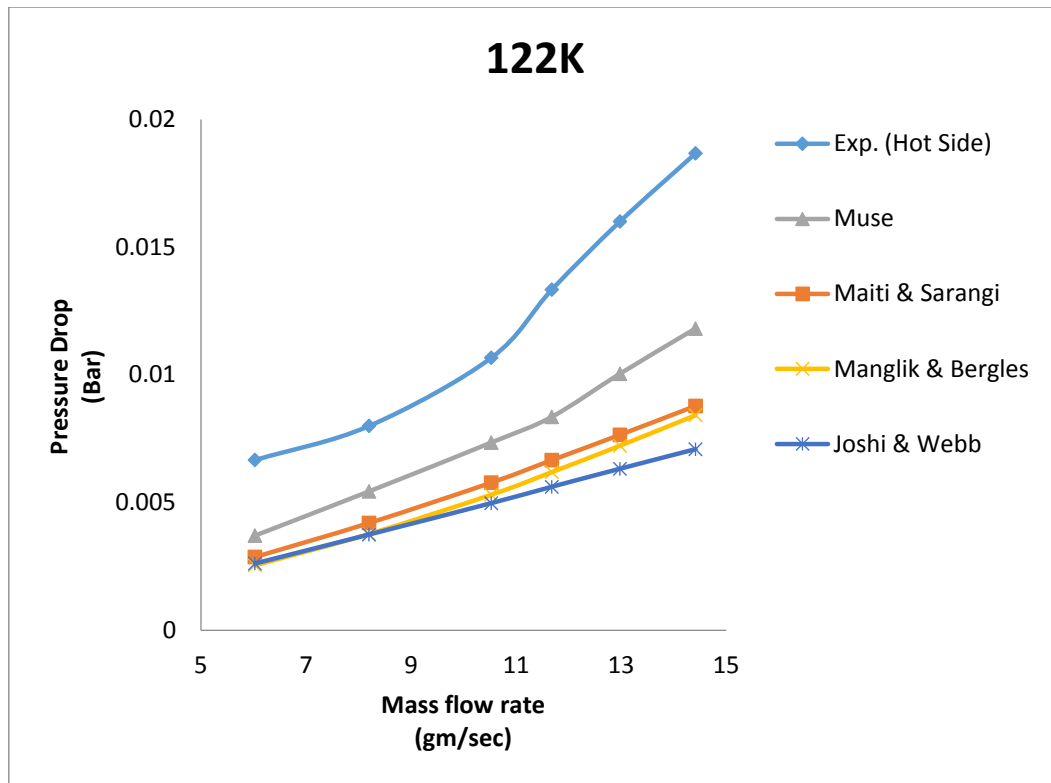


Figure 6.20 Variation of Pressure drop with mass flow rate at 122 K (Cold side)

## 6.8 Results and Discussion

The data in Figure 6.12 to 6.20 represents the calculated drop in pressure. It represents the performance of a hot and cold side of plate fin heat exchanger as a function of mass flow rate in kg/sec. The experimental results for pressure drop and friction factor are in reasonable conformity with the predicted data. It depicts that the drop in pressure rises with the increase in mass flow rate which confirm the theory.

The elevation in pressure drop is due to the obstacles of fins which causes the friction. Figure 6.10 shows that higher the Reynolds number lower is the friction factor. The slight increment in the measured friction factor than that of predicted one is due to the valves and flanges. The calculated values of the correlations and experimental result are presented in Table 6.9 and 6.10 which clearly designates the variation of pressure drop. There is a fall in friction factor due to increase in Reynolds no. as shown in Figure 6.10 and 6.11 for the cold and hot side of the heat exchanger for mass flow rate ranging from 6.02 kg/s to 14.41kg/s at 107K cold inlet temperature.

The divergence in Colburn factor between experimental and the calculated by correlation is shown in Figure 6.8 and 6.9. Deviation in both the results of outlet temperature



in experimental and predicted is effected due to the change in heat transfer. The property changes due the change in average temperature given in equation. The slight change in the average temperature effect the Colburn factor. But the trend of graph remains same shows that the value obtains through experiment is appropriate.

$$T_{h,mean} = \frac{T_{h,i} + T_{h,o}}{2} \quad \text{or} \quad T_{c,mean} = \frac{T_{c,o} + T_{c,i}}{2} \quad 6.3$$

The obtained value of effectiveness through analytical and simulation shows the conformity result with experiment result within expectable uncertainty range.

Table 6.11 shows the Percentage of error between experimental values Vs Predicted & simulated with the uncertainty at 107K cold inlet temperature.

Table 6.11 Percentage of error

	Error Percentage				
	Muse <sup>©</sup>	Maity and Sarangi	Manglik and Bergles	Joshi and Webb	Uncertainty
	1.73 %	3.94 %	2.72 %	4.76 %	4.95 %
	1.77 %	4.05 %	2.63 %	5.03 %	3.73 %
	1.76 %	3.60 %	1.87 %	4.62 %	3.00 %
	1.75 %	3.53 %	1.67 %	4.57 %	2.72 %
	1.75 %	3.51 %	1.50 %	4.56 %	2.49 %
	1.75 %	3.43 %	1.27 %	4.50 %	2.29 %
Average Percentage	1.75 %	3.68 %	1.94 %	4.67 %	3.20 %

Heat losses affect the effectiveness due to the energy imbalance in the cold and hot side of the heat exchanger. A side-by-side comparison of the present study with the earlier research on the heat exchanger is made. Compression shows that initially at low mass flow rate of 6.02 to 8.20 g/s value of effectiveness of hot test and cold test diverges from each other and subsequently it converges.

## Chapter VII

# CONCLUSIONS

### 7.1 Conclusion

The experiment performed to evaluate the performance of a plate fin heat exchanger under cryogenic temperature. The performance of plate fin heat exchangers in cryogenics environment was examined experimentally. An investigation is made to demonstrate the effect of mass flow rate on the effectiveness and on the pressure drop. The calculated effectiveness and pressure drop find out from the experiment are validated by comparing with the values obtained by means of correlations. The correlation used for comparisons with that of present experimental data are taken from the available literature by Maiti and Sarangi, Manglik and Bergles and Joshi and Webb. Eventually the following conclusions were drawn out from the present study.

❖ Variation of Effectiveness with respect to mass flow rate

Effectiveness gives a scheme to predict the performance of a specified heat exchanger. The outlet temperatures can be obtained from the predicted effectiveness. The obtained value of effectiveness shows the validity with the predicted values by Maity and Sarangi, Manglik and Bergles and Joshi and Webb along with them it is also compared with the simulation software Aspen Muse<sup>®</sup>. In figure 6.1 to 6.4 the deviation in the graphs shows the error due to multiple causes such as heat leak and instrumentation error. The mean percentage error for Maity & Sarangi, Manglik & Barglus and Joshi & Webb is 3.68%, 1.94% and 4.67% respectively. Whereas the mean percentage error between the Muse<sup>®</sup> and experimental values is 1.75% at cold inlet temperature 107K. It is observed that the variation in the effectiveness on the both sides of the channel hot side and cold side.

❖ Variation of heat transfer and flow friction with Reynolds number

The effect of Reynolds number on heat transfer and flow friction characteristics is studied for various mass flow rates. A discrepancy is noted between the experimental and the predicted data for Colburn factor and friction factor. It is observed that as Reynolds number increases both the quantity 'j' and 'f' factor decreases. The predicted Colburn factor through

correlations is higher than the experimentally measured Colburn factor whereas experimental friction factor is higher than the evaluated value. However, trend remains the same as that of the predicted value by the correlation.

❖ Variation of Pressure drop with respect to mass flow rate

In the present work a detailed explanation and sketch (P and I diagram) of a Test setup is reported. The process of finding factor affecting the performance of heat exchanger is presented. The reported experimental setup is thus an appropriate setup for computing other heat exchanger under cryogenics temperature.

❖ Validation of effectiveness obtained with and without heat loss using Aspen Muse<sup>®</sup>

The different value of effectiveness is evaluated for hot side and cold side using Aspen Muse<sup>®</sup>. Figure 6.6 shows the effectiveness w.r.t mass flow rate changes without heat leak matches well with the mean value of effectiveness when considering heat leak. The points on the lines are almost coinciding with each other but a small variation occurs at low mass flow rate which is within experimental error.

Aspen Muse<sup>®</sup> values are satisfying the value obtained by the experiment. The effectiveness deviation between the experimental value and value obtained from simulation software varies from 1.75% at cold inlet temperature 107K which is within error band.

❖ Comparison of effectiveness of cold and hot tests.

The effectiveness evaluated by earlier work (Alur [151] at a temperature higher than the ambient temperature) is compared with the present result, which is very much lower than the ambient temperature (cryogenic temperature). The comparisons show that the initially gaining of effectiveness in the heat exchanger at low mass flow rate in cold test due to the presence of cryogenic temperature. Further increment in mass flow rate shows almost same trend as in hot test.

The main benefit of the present work on experimental setup based on various correlation and simulation are seen to be the first successful and cheap cryogenic experimental set to detect the performance of PFHX. Secondly the accurate insertion of the correlation based on previous experimental values as purposed to validate the performance of offsets fin. It is identified that among the correlations and the Muse, Manglik and Muse provided the nearer result as in experiment. The deviation in the result is due to the

assumptions in correlation as in Manglik and Bergles has neglected the thickness of fins while calculating the free flow area. However, for the pressure drop in experiment shows the more deviations than the other it is because of the various obstacles which is not considered in the correlations. Although the pressure drop in all the cases are under the desirable limit.

### **Significant Contributions of Thesis**

- ❖ A general Experimental setup model of Plate fin heat exchanger is developed under cryogenics temperature.
- ❖ The application of control system for controlling the mass flow rate and the temperature has been calibrated and examined in the present study.
- ❖ Performance analysis on the basis of effectiveness and pressure drop has been proposed and implemented in the present study.
- ❖ The experimental model setup an effect for predicting the Colburn and friction factor characteristic of offset fin heat exchanger.
- ❖ The influence of geometrical/material parameters, Insulation scheme, support conditions and different shell geometrical configurations are examined in the present study using data acquisition modules.

## **7.2 Future work**

To a certain extent a lot of areas for future scope are available which would help from a similar experimental work presented here:

A similar experimental set up as shown in Figure 5.1 can be often used to support the assessment of performance of other type of heat exchanger under different cryogenics temperature. However, since most of the work is on the atmospheric temperature or above it is required to verify it at cryogenic temperature.

Investigation of present experimental model using three-dimensional numerical discrete simulation techniques on the fluid flow and heat transfer analysis. Validity of present experimental model is confirmed through the computational as well as with the three correlations as mentioned above in the literature. Various other parametric studies such as

variation on Nusselt number with respect to length and Reynolds number, variation of temperature and pressure along the length can be performed through CFD analysis.

Output parameter has to be optimized on the basis of input parameter of a specified heat exchanger using various optimization tools such as Genetic algorithm, simulate annealing etc. The data which is difficult to obtain by experiment can be predicted by using an adaptive neuro-fuzzy and neural network algorithm. Comparison and implementation of the best matching optimized value from different optimization techniques.

Analyses the flow distribution on a header with different shapes and size to accomplishing the pressure variation. The distribution of flow on the surface of the fin is required to be uniform. Therefore, header is supposed to modify. Another option is to install baffles inside the header that force the fluid to flow uniformly. Different form of baffles can be optimized including various shapes has to be optimized.

# REFERENCES

1. Shah, R.K. and D.P. Sekulic, Fundamentals of heat exchanger design. 2003: John Wiley & Sons.
2. Ackermann, R.A., Cryogenic regenerative heat exchangers. 1997: Springer Science & Business Media.
3. Barron, R.F., Cryogenic heat transfer. 1999: CRC Press.
4. Barron, R.F., Cryogenic systems. 1985: Clarendon Press.
5. Atrey, M., Thermodynamic analysis of Collins helium liquefaction cycle. Cryogenics, 1998. 38(12): p. 1199-1206.
6. Kanoglu, M., I. Dincer, and M.A. Rosen, Performance analysis of gas liquefaction cycles. International Journal of Energy Research, 2008. 32(1): p. 35-43.
7. Kern, D.Q.a.K., A.D, Extended surface heat transfer. 1972.
8. Kays, W.M. and A.L. London, Compact heat exchangers. 1984.
9. Ozisik, M.N., Heat transfer: a basic approach. 1985.
10. Frass.A.P., Heat Exchanger Design. 1989.
11. Shah, R.K., Compact Heat Exchangers and Enhancement Technology for the Process Industries: Proceedings of the International Conference on Compact Heat Exchangers and Enhancement Technology for the Process Industries Held at the Banff Centre for Conferences, Banff, Canada, July 18-23, 1999. 1999: Begell House Publishers.
12. Windmeier, C. and R.F. Barron, Cryogenic technology. Ullmann's Encyclopedia of Industrial Chemistry, 2000.
13. Kakac, S., H. Liu, and A. Pramuanjaroenkij, Heat exchangers: selection, rating, and thermal design. 2012: CRC press.
14. Incropera, F.P.a.D., D.P. , Fundamentals of Heat Transfer John Wiley, New York, 1985.
15. Hesselgreaves, J.E., Compact heat exchangers: selection, design and operation. 2001: Gulf Professional Publishing.
16. Cowell, T. and N. Achaichia, Compact heat exchangers in the automobile industry. Compact Heat Exchangers for the process industries, 1997: p. 11-28.
17. Webb, R.L., Advances in air-cooled heat exchanger technology. ASME-PUBLICATIONS-HTD, 1998. 365: p. 49-58.
18. Li, Q., et al., Compact heat exchangers: A review and future applications for a new generation of high temperature solar receivers. Renewable and Sustainable Energy Reviews, 2011. 15(9): p. 4855-4875.
19. Linde, A., Aluminium plate-fin heat exchangers. Catalogue. Cited on pages xiii, xix. 24.

20. Crawford, D.B. and G.P. Eschenbrenner, Heat transfer equipment for LNG projects. Journal Name: Chem. Eng. Prog.; (United States); Journal Volume: 68:9, 1972: p. Medium: X; Size: Pages: 62-70.
21. Finn, A., G. Johnson, and T. Tomlinson, Developments in natural gas liquefaction. Hydrocarbon processing, 1999. 78(4): p. 47-56.
22. London, A.L., Compact heat exchangers. Mechanical engineering, 1964. 86: p. 31-34.
23. Shah, R. and A. London, Laminar flow forced convection in ducts: a source book for compact heat exchanger analytical data, Supl. 1. Adv. Heat Transfer, 1978.
24. Kays, W.M., Description of Test Equipment and Method of Analysis for Basic Heat Transfer and Flow Friction Tests of High Rating Heat Exchanger Surfaces. Technical Report No. 2. 1948, Stanford University.
25. Lenfestey, A., Low temperature heat exchangers. Progress in Cryogenics, 1961. 3: p. 25-47.
26. Lenfestey, A.G., Compact Heat Exchangers for Gas Separation Plant Proc.: p. 47-49.
27. Manglik, R., O. Huzayyin, and M. Jog, Fin Effects in Flow Channels of Plate-Fin Compact Heat Exchanger Cores. Journal of Thermal Science and Engineering Applications, 2011. 3(4): p. 041004.
28. Fernández-Seara, J., R. Diz, and F.J. Uhía, Pressure drop and heat transfer characteristics of a titanium brazed plate-fin heat exchanger with offset strip fins. Applied Thermal Engineering, 2013. 51(1): p. 502-511.
29. Ceramatec. COMPACT MICROCHANNEL HEAT EXCHANGERS. Available from: <http://www.ceramatec.com/technology/top-ceramic-technologies/compact-microchannel-heat-exchangers-and-reactors.php>.
30. Taylor, M.A. and H. Transfer, Plate-Fin Heat Exchangers: Guide to Their Specification and Use. 1987: Heat Transfer and Fluid Flow Services.
31. Shah, R. and R. Webb, Compact and enhanced heat exchangers. Heat Exchangers: Theory and Practice, 1983: p. 440-444.
32. Haseler, L. and D. Butterworth, Boiling in Compact Heat Exchangers/Industrial Practice and Problems. Proceedings of Convective Flow Boiling, 1995: p. 57-70.
33. Achaichia, A. and T. Cowell, Heat transfer and pressure drop characteristics of flat tube and louvered plate fin surfaces. Experimental Thermal and Fluid Science, 1988. 1(2): p. 147-157.
34. Achaichia, A., et al. Numerical investigation of flow and friction in louvered fin arrays. in INSTITUTION OF CHEMICAL ENGINEERS SYMPOSIUM SERIES. 1994. HEMISPHERE PUBLISHING CORPORATION.
35. Atkinsona, K., et al., Two-and three-dimensional numerical models of flow and heat transfer over louvered fin arrays in compact heat exchangers. International Journal of Heat and Mass Transfer, 1998. 41(24): p. 4063-4080.
36. Ha, M.Y., et al., Fluid flow and heat transfer characteristics in multi-louvered fin heat exchanger. 1995, SAE Technical Paper.
37. Springer, M.E. and K.A. Thole, Experimental design for flowfield studies of louvered fins. Experimental Thermal and Fluid Science, 1998. 18(3): p. 258-269.

38. Tafti, D., Time-dependent calculation procedure for fully developed and developing flow and heat transfer in louvered fin geometries. *Numerical Heat Transfer: Part A: Applications*, 1999. 35(3): p. 225-249.
39. Tafti, D., G. Wang, and W. Lin, Flow transition in a multilouvered fin array. *International journal of heat and mass transfer*, 2000. 43(6): p. 901-919.
40. Patankar, S. and C. Prakash, An analysis of the effect of plate thickness on laminar flow and heat transfer in interrupted-plate passages. *International Journal of Heat and Mass Transfer*, 1981. 24(11): p. 1801-1810.
41. Suzuki, K., et al., Numerical and experimental studies on a two-dimensional model of an offset-strip-fin type compact heat exchanger used at low Reynolds number. *International journal of heat and mass transfer*, 1985. 28(4): p. 823-836.
42. Norris, R. and W. Spofford, High-performance fins for heat transfer. *Trans. ASME*, 1942. 64: p. 489-496.
43. Joyner, U.T., Experimental Investigation of Entrance-Region Heat-Transfer Coefficients. 1943, DTIC Document.
44. Manson, S., Correlations of heat-transfer data and of friction data for interrupted plane fins staggered in successive rows. 1950.
45. Kays, W. and A. London, Heat transfer and flow friction characteristics of some compact heat exchanger surfaces Part I. Test system and procedure. *Trans. ASME*, 1950. 72: p. 1075-1097.
46. Kays, W. and A. London, Heat transfer and flow friction characteristics of some compact heat exchanger surfaces Part II. Design data for thirteen surfaces. *Trans. ASME*, 1950. 72: p. 1075-1097.
47. Kays, W.M. and A.L. London, Compact heat exchangers: a summary of basic heat transfer and flow friction design data. 1955: National Press.
48. Kays, W., The basic heat transfer and flow friction characteristics of six compact high-performance heat transfer surfaces. *Journal of Engineering for Gas Turbines and Power*, 1960. 82(1): p. 27-34.
49. Briggs, D. and A.L. London, THE HEAT TRANSFER AND FLOW FRICTION CHARACTERISTICS OF FIVE OFFSET RECTANGULAR AND SIX PLAIN TRIANGULAR PLATE-FIN HEAT TRANSFER SURFACES. Technical Report No. 49. 1960, Stanford Univ., Calif.
50. Kays, W.M. and A.L. London, Compact heat exchangers. 1964.
51. London, A.L. and R.K. Shah, Offset rectangular plate-fin surfaces—heat transfer and flow friction characteristics. *Journal of Engineering for Gas Turbines and Power*, 1968. 90(3): p. 218-228.
52. Voronin, G. and E. Dubrovsky, Effective heat exchangers. *Mashinostroenie*, Moscow, 1973.
53. Wieting, A.R., Empirical correlations for heat transfer and flow friction characteristics of rectangular offset-fin plate-fin heat exchangers. *Journal of Heat transfer*, 1975. 97(3): p. 488-490.
54. Mochizuki, S. and Y. Yagi, Heat transfer and friction characteristics of strip fins. *Heat Transfer-Jpn. Res*, 1977. 6(3): p. 36-59.



55. Sparrow, E. and A. Hajiloo, Measurements of heat transfer and pressure drop for an array of staggered plates aligned parallel to an air flow. *Journal of Heat Transfer*, 1980. 102(3): p. 426-432.
56. Webb, R. and H. Joshi, Friction factor correlation for the offset strip-fin matrix. 1982, Pennsylvania State Univ., University Park (USA). Dept. of Mechanical Engineering.
57. Webb, R. and H. Joshi, Prediction of the friction factor for the offset strip-fin matrix. 1983, Pennsylvania State Univ., University Park (USA). Dept. of Mechanical Engineering.
58. Joshi, H.M. and R.L. Webb, Heat transfer and friction in the offset stripfin heat exchanger. *International Journal of Heat and Mass Transfer*, 1987. 30(1): p. 69-84.
59. Mochizuki, S., Y. Yagi, and W.-J. Yang, Transport phenomena in stacks of interrupted parallel-plate surfaces. *Experimental Heat Transfer An International Journal*, 1987. 1(2): p. 127-140.
60. Dubrovsky, E. and V.Y. Vasiliev, Enhancement of convective heat transfer in rectangular ducts of interrupted surfaces. *International journal of heat and mass transfer*, 1988. 31(4): p. 807-818.
61. Brockmeier, U., T. Guentermann, and M. Fiebig, Performance evaluation of a vortex generator heat transfer surface and comparison with different high performance surfaces. *International Journal of Heat and Mass Transfer*, 1993. 36(10): p. 2575-2587.
62. Dubrovsky, E. Highly Effective Plate-Fin "Heat Exchanger Surfaces: from Conception to Manufacturing,". in *Proceedings of the First International Conference on Aerospace Heat Exchanger Technology*, Palo Alto, CA, United States. 1993.
63. Dubrovsky, E., Experimental investigation of highly effective plate-fin heat exchanger surfaces. *Experimental thermal and fluid science*, 1995. 10(2): p. 200-220.
64. Manglik, R.M. and A.E. Bergles, Heat transfer and pressure drop correlations for the rectangular offset strip fin compact heat exchanger. *Experimental Thermal and Fluid Science*, 1995. 10(2): p. 171-180.
65. Waiters, F., Hypersonic Research Engine Project—Phase IIA, Category I Test Report on Fin Heat Transfer and Pressure Drop Testing. Data Item, 1969(63.02).
66. Youcef-Ali, S., Study and optimization of the thermal performances of the offset rectangular plate fin absorber plates, with various glazing. *Renewable Energy*, 2005. 30(2): p. 271-280.
67. Youcef-Ali, S. and J. Desmons, Numerical and experimental study of a solar equipped with offset rectangular plate fin absorber plate. *Renewable energy*, 2006. 31(13): p. 2063-2075.
68. Peng, H., X. Ling, and J. Li, Performance investigation of an innovative offset strip fin arrays in compact heat exchangers. *Energy Conversion and Management*, 2014. 80: p. 287-297.
69. Dong, J., et al., Air-side thermal hydraulic performance of offset strip fin aluminum heat exchangers. *Applied thermal engineering*, 2007. 27(2): p. 306-313.
70. Dong, J., J. Chen, and Z. Chen, Flow and heat transfer in compact offset strip fin surfaces. *Frontiers of Energy and Power Engineering in China*, 2008. 2(3): p. 291-297.
71. Robertson, J. Boiling heat transfer with liquid nitrogen in brazed-aluminum plate-fin heat exchangers. in *AIChE Symposium Series*. 1979.
72. Robertson, J. Boiling heat transfer with Freon-I 1 in brazed-aluminum plate-fin heat exchangers. in *AIChE Symposium Series*. 1980.

73. Roadman, R. and R. Loehrke, Low Reynolds number flow between interrupted flat plates. *Journal of Heat Transfer*, 1983. 105(1): p. 166-171.
74. Brinkmann, R., S. Ramadhyani, and F. Incropera, Enhancement of convective heat transfer from small heat sources to liquid coolants using strip fins. *Experimental Heat Transfer*, 1987. 1(4): p. 315-330.
75. Hou, K.S., Thermal performance of offset strip fins under unsymmetrical heating condition [s] for various fluids. 1988.
76. Marr, Y., CORRELATING DATA ON HEAT-TRANSFER IN PLATE-FIN HEAT-EXCHANGERS WITH SHORT OFFSET FINNS. *Thermal Engineering*, 1990. 37(5): p. 249-252.
77. Tinaut, F., A. Melgar, and A.R. Ali, Correlations for heat transfer and flow friction characteristics of compact plate-type heat exchangers. *International journal of heat and mass transfer*, 1992. 35(7): p. 1659-1665.
78. LeVasseur, R. Liquid cooled approaches for high density avionics. in *Digital Avionics Systems Conference*, 1991. Proceedings., IEEE/AIAA 10th. 1991. IEEE.
79. Hu, S. and K.E. Herold, Prandtl number effect on offset fin heat exchanger performance: experimental results. *International journal of heat and mass transfer*, 1995. 38(6): p. 1053-1061.
80. Herold, K.E., S. Sridhar, and S. Hu, Cooling of electronic boards using internal fluid flows. *ASME, NEW YORK, NY(USA)*. 1992. 1: p. 285-290.
81. DeJong, N.C. and A. Jacobi, An experimental study of flow and heat transfer in offset strip and louvered-fin heat exchangers. 1995, Air Conditioning and Refrigeration Center. College of Engineering. University of Illinois at Urbana-Champaign.
82. Peng, H. and X. Ling, Numerical modeling and experimental verification of flow and heat transfer over serrated fins at low Reynolds number. *Experimental thermal and fluid science*, 2008. 32(5): p. 1039-1048.
83. Peng, H. and X. Ling, Analysis of heat transfer and flow characteristics over serrated fins with different flow directions. *Energy Conversion and Management*, 2011. 52(2): p. 826-835.
84. Adarkar, D.B. and W. Kays, Heat transfer in wakes. 1963, DTIC Document.
85. Loehrke, R., R. Roadman, and G. Read. Low Reynolds number flow in plate wakes. in *ASME Numerical/Laboratory Computer Methods in Fluid Mechanics*. 1976.
86. Cur, N. and E. Sparrow, Experiments on heat transfer and pressure drop for a pair of colinear, interrupted plates aligned with the flow. *International Journal of Heat and Mass Transfer*, 1978. 21(8): p. 1069-1080.
87. Mochizuki, S. and Y. Yagi, Characteristics of vortex shedding in plate arrays. *Flow Visualization II*, 1982: p. 99-103.
88. Loehrke, R. and J. Lane, Flow through an array of interrupted, parallel plates. *Heat Transfer*, 1982. 3: p. 81-86.
89. Zelenka, R. and R. Loehrke, Heat transfer from interrupted plates. *Journal of Heat Transfer*, 1983. 105(1): p. 172-177.

90. Mullisen, R. and R. Loehrke, A study of the flow mechanisms responsible for heat transfer enhancement in interrupted-plate heat exchangers. *Journal of heat transfer*, 1986. 108(2): p. 377-385.
91. Mochizuki, S., Y. Yagi, and W.-J. Yang, Flow pattern and turbulence intensity in stacks of interrupted parallel-plate surfaces. *Experimental Thermal and Fluid Science*, 1988. 1(1): p. 51-57.
92. Kurosaki, Y., et al., Experimental study on heat transfer from parallel louvered fins by laser holographic interferometry. *Experimental Thermal and Fluid Science*, 1988. 1(1): p. 59-67.
93. Mayinger, F., et al., Visualization of high-frequency thermo-fluid phenomena using real-time holographic interferometry and numerical animation. *Topics in Heat Transfer*, 1992. 1: p. 206-1.
94. Y. Hagiwara, G.N.X., S. Futagami and K. Suzuki, An Experimental Study of Flow Characteristics of Offset Fin and In-Line Fin Arrays. Effects of Fin Thickness and Fin Pitches on Flow Instability. *Trans. JSME B*, 1993. 59(560): p. 1222-1227.
95. Brutz, J.M., J.C. Dutton, and A.M. Jacobi, Enhancement of Air-Side Heat Transfer in Offset-Strip Fin Arrays Using Unsteady Forcing. 2004.
96. Kays, W.M. and A.L. London, *Compact heat exchangers*. 1972.
97. Sparrow, E., B. Baliga, and S. Patankar, Heat transfer and fluid flow analysis of interrupted-wall channels, with application to heat exchangers. *Journal of Heat Transfer*, 1977. 99(1): p. 4-11.
98. Sparrow, E. and C. Liu, Heat-transfer, pressure-drop and performance relationships for in-line, staggered, and continuous plate heat exchangers. *International Journal of Heat and Mass Transfer*, 1979. 22(12): p. 1613-1625.
99. Suzuki, K., et al. Numerical study of heat transfer system with staggered array of vertical flat plates used at low Reynolds number. in *Heat Transfer 1982*, Volume 3. 1982.
100. Kelkar, K.M. and S.V. Patankar, Numerical prediction of heat transfer and fluid flow in rectangular offset-fin arrays. *Numerical Heat Transfer*, 1989. 15(2): p. 149-164.
101. Kelkar, K. and S. Patankar, Numerical prediction of flow and heat transfer in a parallel plate channel with staggered fins. *Journal of heat transfer*, 1987. 109(1): p. 25-30.
102. DeJong, N.C., et al., A Complementary Experimental and Numerical Study of the Flow and Heat Transfer in Offset Strip-Fin Heat Exchangers. *Journal of Heat Transfer*, 1998. 120(3): p. 690-698.
103. Saidi, A. and B. Sundén, A numerical investigation of heat transfer enhancement in offset strip fin heat exchangers in self-sustained oscillatory flows. *International Journal of Numerical Methods for Heat & Fluid Flow*, 2001. 11(7): p. 699-717.
104. Subramanian, S., *CFD modeling of compact offset strip-fin high temperature heat exchanger*. 2005, University of Nevada, Las Vegas.
105. Zhu, Y. and Y. Li, Three-dimensional numerical simulation on the laminar flow and heat transfer in four basic fins of plate-fin heat exchangers. *Journal of Heat Transfer*, 2008. 130(11): p. 111801.

106. Hao Peng, Xiang Ling and Juan Li "Performance investigation of an innovative offset strip fin arrays in compact heat exchangers" *Energy Conversion and Management* 80 ,pp. 287–297, (2014).
107. Ismail, L.S., C. Ranganayakulu, and R.K. Shah, Numerical study of flow patterns of compact plate-fin heat exchangers and generation of design data for offset and wavy fins. *International journal of heat and mass transfer*, 2009. 52(17): p. 3972-3983.
108. Wang, Y.Q., et al., Numerical Study on Plate-Fin Heat Exchangers with Plain Fins and Serrated Fins at Low Reynolds Number. *Chemical engineering & technology*, 2009. 32(8): p. 1219-1226.
109. Kim, M.-S., et al., Correlations and optimization of a heat exchanger with offset-strip fins. *International Journal of Heat and Mass Transfer*, 2011. 54(9): p. 2073-2079.
110. Saad, S.B., et al., Experimental distribution of phases and pressure drop in a two-phase offset strip fin type compact heat exchanger. *International Journal of Multiphase Flow*, 2011. 37(6): p. 576-584.
111. Saad, S.B., et al., Single phase pressure drop and two-phase distribution in an offset strip fin compact heat exchanger. *Applied Thermal Engineering*, 2012. 49: p. 99-105.
112. Khoshvaght-Aliabadi, M., F. Hormozi, and A. Zamzamian, Effects of geometrical parameters on performance of plate-fin heat exchanger: Vortex-generator as core surface and nanofluid as working media. *Applied Thermal Engineering*, 2014. 70(1): p. 565-579.
113. Reneaume, J. and N. Niclout, MINLP optimization of plate fin heat exchangers. *Chemical and biochemical engineering quarterly*, 2003. 17(1): p. 65-76.
114. Mishra, M., P.K. Das, and S. Sarangi, Optimum design of crossflow plate-fin heat exchangers through genetic algorithm. 2004.
115. Xie, G., B. Sundén, and Q. Wang, Optimization of compact heat exchangers by a genetic algorithm. *Applied Thermal Engineering*, 2008. 28(8): p. 895-906.
116. Peng, H. and X. Ling, Neural networks analysis of thermal characteristics on plate-fin heat exchangers with limited experimental data. *Applied Thermal Engineering*, 2009. 29(11): p. 2251-2256.
117. Mishra, M., P. Das, and S. Sarangi, Second law based optimisation of crossflow plate-fin heat exchanger design using genetic algorithm. *Applied Thermal Engineering*, 2009. 29(14): p. 2983-2989.
118. Sanaye, S. and H. Hajabdollahi, Thermal-economic multi-objective optimization of plate fin heat exchanger using genetic algorithm. *Applied Energy*, 2010. 87(6): p. 1893-1902.
119. Rao, R. and V. Patel, Thermodynamic optimization of cross flow plate-fin heat exchanger using a particle swarm optimization algorithm. *International Journal of Thermal Sciences*, 2010. 49(9): p. 1712-1721.
120. Rao, R.V. and V. Patel, Thermodynamic optimization of plate-fin heat exchanger using teaching-learning-based optimization (TLBO) algorithm. *optimization*, 2011. 10: p. 11.
121. Yousefi, M., A. Darus, and H. Mohammadi, An imperialist competitive algorithm for optimal design of plate-fin heat exchangers. *International Journal of Heat and Mass Transfer*, 2012. 55(11): p. 3178-3185.

122. London, A. and C. Ferguson, Test results of high-performance heat exchanger surfaces used in aircraft intercoolers and their significance for gas-turbine regenerator design. *Trans. ASME*, 1949. 71: p. 17-26.
123. Kalinin, E.K., G.A. Dreitser, and E.V. Dubrovsky, Compact tube and plate-finned heat exchangers. *Heat Transfer Engineering*, 1985. 6(1): p. 44-51.
124. Maiti, D.K., Heat transfer and flow friction characteristics of plate-fin heat exchanger surfaces—a numerical study. IIT Kharagpur, India, 2002.
125. Landau, H. and J. Hlinka, Steady state temperature distribution in a counterflow heat exchanger including longitudinal conduction in the wall. *ASME paper*, 1960(60-WA): p. 236.
126. Kroeger, P., Performance deterioration in high effectiveness heat exchangers due to axial heat conduction effects, in *Advances in cryogenic engineering*. 1967, Springer. p. 363-372.
127. Chowdhury, K. and S. Sarangi, Effect of finite thermal conductivity of the separating wall on the performance of counterflow heat exchangers. *Cryogenics*, 1983. 23(4): p. 212-216.
128. Hausen, H., M. Sayer, and A.J. Willmott, Heat transfer in counterflow, parallel flow and cross flow. 1983: McGraw-Hill New York.
129. Hahnemann, H., Approximate calculation of thermal ratios in heat exchangers including heat conduction in direction of flow. *National Gas Turbine Establishment Memorandum*, 1948. 36.
130. Bahnke, G. and C. Howard, The effect of longitudinal heat conduction on periodic-flow heat exchanger performance. *Journal of Engineering for Gas Turbines and Power*, 1964. 86(2): p. 105-117.
131. Chiou, J., The effect of longitudinal heat conduction on crossflow heat exchanger. *Journal of Heat Transfer*, 1978. 100(2): p. 346-351.
132. Chiou, J. The advancement of compact heat exchanger theory considering the effects of longitudinal heat conduction and flow nonuniformity. in *ASME-HTD Symposium on Compact Heat Exchangers*. 1980.
133. Narayanan, S.P. and G. Venkatarathnam, Performance degradation due to longitudinal heat conduction in very high NTU counterflow heat exchangers. *Cryogenics*, 1998. 38(9): p. 927-930.
134. Ranganayakulu, C., K. Seetharamu, and K. Sreevatsan, The effects of longitudinal heat conduction in compact plate-fin and tube-fin heat exchangers using a finite element method. *International journal of heat and mass transfer*, 1997. 40(6): p. 1261-1277.
135. Wood, B. and J. Kern. Design of heat exchangers with heat loss to the surroundings. in *Second National Meeting of the South African Institute of Chemical engineers Paper*. 1976.
136. Chowdhury, K. and S. Sarangi, Performance of cryogenic heat exchangers with heat leak from the surroundings, in *Advances in Cryogenic Engineering*. 1984, Springer. p. 273-280.
137. Barron, R.F., Effect of heat transfer from ambient on cryogenic heat exchanger performance, in *Advances in Cryogenic Engineering*. 1984, Springer. p. 265-272.
138. Gupta, P. and M. Atrey, Performance evaluation of counter flow heat exchangers considering the effect of heat in leak and longitudinal conduction for low-temperature applications. *Cryogenics*, 2000. 40(7): p. 469-474.

139. Mueller, A. and J. Chiou, Review of various types of flow maldistribution in heat exchangers. *Heat Transfer Engineering*, 1988. 9(2): p. 36-50.
140. Jiao, A., Y. Li, and R. Zhang. A study of the configuration and performance of distributor in plate-fin heat exchanger. in *Proceedings of the 18th International Cryogenic Engineering Conference*, Mumbai, India. 2000.
141. KITTO Jr, J.B. and J. Robertson, Effects of maldistribution of flow on heat transfer equipment performance. *Heat Transfer Engineering*, 1989. 10(1): p. 18-25.
142. Lalot, S., et al., Flow maldistribution in heat exchangers. *Applied thermal engineering*, 1999. 19(8): p. 847-863.
143. Zhang, Z., Y. Li, and A. Jiao, Numerical simulation of header construction of plate-fin heat exchanger. *JOURNAL OF CHEMICAL INDUSTRY AND ENGINEERING-CHINA-*, 2002. 53(11): p. 1182-1187.
144. Zhang, Z. and Y. Li, CFD simulation on inlet configuration of plate-fin heat exchangers. *Cryogenics*, 2003. 43(12): p. 673-678.
145. Wen, J. and Y. Li, Study of flow distribution and its improvement on the header of plate-fin heat exchanger. *Cryogenics*, 2004. 44(11): p. 823-831.
146. Wen, J., et al., PIV experimental investigation of entrance configuration on flow maldistribution in plate-fin heat exchanger. *Cryogenics*, 2006. 46(1): p. 37-48.
147. Jiao, A., R. Zhang, and S. Jeong, Experimental investigation of header configuration on flow maldistribution in plate-fin heat exchanger. *Applied Thermal Engineering*, 2003. 23(10): p. 1235-1246.
148. Wen, J., et al., An experimental and numerical investigation of flow patterns in the entrance of plate-fin heat exchanger. *International Journal of Heat and Mass Transfer*, 2006. 49(9): p. 1667-1678.
149. Shah, R.K.a.A.H., *Non Uniform Heat Transfer Coefficients for Heat Exchanger Thermal Design in Aerospace Heat Exchanger Technology*. 1993: p. 417-445.
150. Paffenbarger, J., *General computer analysis of multistream, plate-fin heat exchangers. Compact Heat Exchangers—A Festschrift for AL London*, 1990: p. 727-746.
151. Alur, S., *Experimental studies on plate fin heat exchangers*. 2012
152. Kline, Stephen J., and F. A. McClintock. "Describing uncertainties in single-sample experiments." *Mechanical engineering* 75.1 (1953): 3-8.
153. Marthinuss, James, George Hall, and N. Grumman. "Air cooled compact heat exchanger design for electronics cooling." *Electronics Cooling* 10.1 (2004): 28.

# Appendix

## I. Calculation for RTD

Thermometer	RTD1	RTD2	RTD3	RTD4	RTD5	Mean	Error
1	0.94	0.91	1.1	1	0.84	0.958	0.042
1.9	1.87	1.96	1.92	1.52	2.02	1.858	0.042
5	4.38	4.39	4.89	4.27	4.47	4.48	0.52
6	6	6.05	6.06	5.99	6.15	6.05	-0.05
8.4	8.52	8.34	8.16	8.16	8.36	8.308	0.092
11.1	11.22	10.9	11	11.38	11.42	11.184	-0.084
17	17.25	17.66	17.32	17.68	17.8	17.542	-0.542
24.1	24.05	24.22	24.44	23.92	24.17	24.16	-0.06
30.7	30.63	30.8	30.29	30.28	30.48	30.496	0.204
45.8	45.18	45.07	44.27	44.52	44.21	44.65	1.15
52.5	51.89	51.89	52.16	52.26	51.81	52.002	0.498
70.4	70.71	70.84	70.45	70.43	70.35	70.556	-0.156
81.4	81.76	81.48	81.86	81.95	81.85	81.78	-0.38
88.2	87.93	87.63	87.6	87.55	87.34	87.61	0.59
103.8	103.84	103.67	104	102.97	103.51	103.598	0.202
Total Error							0.137

## II. Heat leak Calculation

Muse	Thi	Tho	Tci	Tco	hot Eff.	Cold Eff.
6.029	307.5	124.21	107.6	285.54	0.916908	0.890145
8.201432	307.4	123.16	106.7	285.69	0.917987	0.891829
10.52912	307.4	121.33	106.1	285.55	0.924342	0.891456
11.68166	308.1	121.41	106.8	285.99	0.927422	0.890164
12.98	307.9	121.99	107.8	285.69	0.929085	0.889005
14.41906	308.2	121.82	108.1	285.61	0.931434	0.887106

Exp. lt/min	Thi	Tho	Tci	Tco	hot Eff.	Cold Eff.
6.029	307.5	128.221	107.8	281.5342	0.897742	0.869976
8.201432	307.4	127.0297	106.7	282.1773	0.898706	0.874327
10.52912	307.4	124.6144	106.1	282.5828	0.908026	0.876715
11.68166	308.1	124.8143	106.8	283.1027	0.91051	0.875821
12.98	307.9	125.2796	107.8	282.6864	0.912646	0.873995
14.41906	308.2	125.0969	108.1	282.6237	0.915058	0.872182